ABSTRACT

HAAS, SARAH ELIZABETH. Landscape Epidemiology of Sudden Oak Death: Spatial Analysis of Disease Dynamics in Natural Forest Ecosystems. (Under the direction of Ross K. Meentemeyer).

Plant diseases negatively impact human well-being through agricultural and economic loss, and can also have dire consequences for biodiversity conservation. Wildland pathosystems—defined as populations of plants and their pathogens that are not artificially planted, farmed, or intensively managed by humans—are particularly challenging to study because they occur in natural ecosystems that are characterized by complex spatial arrangements of host and environmental conditions across broad geographical extents. The burgeoning field of landscape epidemiology, which integrates concepts and approaches from disease ecology with the macroscale lens of landscape ecology, provides an analytical framework for examining wildland diseases across spatiotemporal scales in complex environmental settings. A unifying theme of my dissertation research is the application of landscape epidemiological approaches to the study of sudden oak death (SOD), an emerging forest disease caused by the oomycete plant pathogen *Phytophthora ramorum*. SOD is the latest in a growing number of exotic plant diseases that threaten the integrity and biodiversity of native forests in North America. In my first chapter, I examine the 'diversity-disease risk' hypothesis in the multihost *P. ramorum* pathosystem, in which I find evidence for pathogen "dilution" whereby disease risk is lower in forested stands with higher plant species diversity. These diversity-disease risk interactions remain even after accounting for the potentially confounding effects of host density and landscape heterogeneity, suggesting that although nearly all plants in the ecosystem are hosts, alternative hosts may dilute disease transmission by competent hosts, thereby buffering forest health from infectious disease. In my second

dissertation chapter I incorporate a temporal dimension to the study of *P. ramorum* epidemic dynamics, integrating data across multiple levels of host-pathogen-environment interactions to identity the principal drivers of SOD disease impacts over time. I implemented a survival analysis framework—incorporating multilevel, time-dependent properties of this complex multihost pathosystem—that revealed the collective importance of factors at the individual, community and landscape scale in mediating oak infection risk through space and time. These results demonstrate how multiscale environmental heterogeneity drives disease impacts in a wildland pathosystem, while providing an empirical basis for assessing the risk of extinction among co-occurring hosts in pathogen-invaded communities. In my third dissertation chapter, I perform data-driven spatial prediction analysis—integrating data from diverse sources with varying spatial and temporal coverage—to obtain quantitative assessments of disease-impacted trees across the entire geographic range of *P. ramorum*. This study, which is the first to provide estimates of the actual numbers of trees infected and dying from SOD across California and Oregon, can help guide management decisions regarding ecosystem impacts including the risk of carbon release following widespread tree mortality. Collectively, information gathered from my dissertation research has implications related to forest management of invasive diseases, biodiversity loss and forest health, and policy decisions concerning the regulation of emerging infectious diseases.

Landscape Epidemiology of Sudden Oak Death: Spatial Analysis of Disease Dynamics in Natural Forest Ecosystems

by
Sarah E. Haas

A dissertation submitted to the Graduate Faculty of
North Carolina State University
in partial fulfillment of the
requirements for the degree of
Doctor of Philosophy

Forestry and Environmental Resources

Raleigh, North Carolina

2014

APPROVED BY:

_____	_____
Ross K. Meentemeyer Committee Chair	Hugh Devine
_____	_____
Beth Gardner	Charles E. Mitchell

DEDICATION

I could never have gotten to where I am now if it were not for the unconditional love of my six siblings, parents and close friends. I have been blessed with an amazingly supportive doctoral graduate advisor, and above all friend—thank you Ross. My fellow graduate students in the lab have become family over the years and will never know just how important each one of them has been to me at times. I will be indebted to Monica forever for introducing me to IPA and Whalen for all those tasty dinners. Doug was instrumental in helping me become a hard-core mountain biker and provided support at the very end my graduate journey. There have been a few other incredibly special people in my life these past six years, whom shone for me when I could not. I am especially grateful for the unwavering support of David throughout the years. There are others that I do not mention by name, but were everyday champions to me in little ways. I dedicate this work to all of you.

BIOGRAPHY

I was born in Corpus Christi, Texas on June 25, 1981. After receiving my Bachelor of Science degree in Biology (minor in Chemistry) in May 2004 from Texas State University, I spent three years working towards a Master of Science degree in Zoology at the University of Florida. I then moved to Washington, D.C. for one year to explore environmental policy, in which I worked as a public policy intern at the National Audubon Society for six months and then as a research assistant in the Genetics Program at the Smithsonian National Zoological Park. In the summer of 2008 I moved to Charlotte, North Carolina to pursue my doctorate in the Department of Geography at the University of North Carolina at Charlotte. Following my advisor and his lab, I transferred to the Department of Forestry and Environmental Resources at North Carolina State University in the fall of 2013. Upon completion of degree requirements, I will begin a postdoctoral research position in Pieter Johnson's lab working on amphibian disease ecology in the Department of Ecology and Evolutionary Biology at the University of Colorado in Boulder.

ACKNOWLEDGMENTS

I am thankful for the support and guidance of my graduate committee members: Hugh Devine, Beth Gardner, Charles Mitchell and Ross Meentemeyer. I am deeply grateful to David Rizzo and his lab group at the University of California-Davis for their support along the years. My research was possible through financial support from the National Science Foundation (EF-0622770 and EF-0622677) as part of their joint NSF-NIH Ecology of Infectious Disease program, the USDA Forest Service – Pacific Southwest Research Station, and the USDA Forest Service – Forest Health Protection, State and Private Forestry. I thank the P.E.O. sisterhood for financial support through receipt of the P.E.O. Scholar Award and the NSF-sponsored RCN-FORECAST program for providing funds to receive training in data assimilation methods. Lastly, I thank the numerous field assistants and laboratory technicians that helped make this research possible.

TABLE OF CONTENTS

LIST OF TABLES

LIST OF FIGURES

CHAPTER 1. INTRODUCTION

The past two decades have witnessed an alarming rise in the number of emerging and re-emerging infectious diseases, such as West Nile virus and Lyme disease, which represent a substantial threat to wildlife and human health worldwide (Daszak et al. 2000, Crowl et al. 2008, Fisher et al. 2012). Although less well-studied but equally destructive, the emergence of plant diseases is also on the rise, driven mainly by the growing international trade in plants coupled with increases in human density and mobility (Anderson et al. 2004, Lovett et al. 2006, Jones 2009). Although the field of disease ecology has made critical strides in deepening our understanding of host-pathogen-environment interactions and disease dynamics, our knowledge of the factors driving the spread and impacts of wildland pathogens—defined as those inhabiting natural ecosystems that are not artificially created (i.e., planted, farmed, or intensively managed) by humans—remains limited due to the more complex spatial heterogeneity of biotic and abiotic conditions of natural ecosystems and often limited data (Kranz 1990, Alexander 2010, Dillon et al. 2014).

Over the past few decades, a growing number of wildland plant pathogens have invaded a variety of forest communities over landscape-to regional-scales (Aukema et al. 2010, Garnas et al. 2011, Meentemeyer et al. 2012). Although fine-scale studies have dominated forest pathology, it is now recognized that our understanding (and, ultimately, managing) of diseases on a regional scale requires a broader scope of investigation (Holdenrieder et al. 2004, Hatala et al. 2011, Chapman 2012). The burgeoning discipline of landscape epidemiology integrates concepts and approaches from disease ecology with the macroscale lens of landscape ecology, enabling examination of disease across spatiotemporal

scales in complex environmental settings (Holdenrieder et al. 2004, Ostfeld et al. 2005, Meentemeyer et al. 2012). To date however, the challenge of explicitly integrating landscape heterogeneity of the biophysical environment into epidemiological analyses of wildland pathosystems remains a frontier in disease ecology and spatial epidemiology.

One wildland forest pathogen of international concern is *Phytophthora ramorum*, a generalist pathogen (Oomycota) causing the emerging infectious forest disease known as sudden oak death (SOD) in North America (Rizzo et al. 2002), sudden larch death in Europe (Brasier and Webber 2010), and ramorum blight in nurseries worldwide (Grunwald et al. 2008). Since its introduction in North America in the mid-1990s near the San Francisco Bay Area, *P. ramorum* has reached epidemic levels in coastal forests of California and southwestern Oregon and continues to rapidly expand its range into uninvaded areas (Meentemeyer et al. 2008c, McPherson et al. 2010). Referred to as the 'bird flu' of trees, SOD poses a major threat to the ecological integrity of forests in the Pacific Northwest due to the pathogen's wide host range and concentration of mortality in a few dominant tree species of coastal forests in California and Oregon (Brown and Allen-Diaz 2009, Cobb et al. 2010, Metz et al. 2012).

Faced with the growing concern about the long-term impacts of tree mortality worldwide resulting from global change drivers (Dietze and Moorcroft 2011), it is imperative that we identify the environmental factors governing wildland forest disease epidemics in addition to obtaining reliable forecasts of ecosystem impacts following invasion. The overarching aim of my dissertation research is the application of landscape epidemiological approaches to examine disease processes across spatiotemporal scales in complex settings,

using the *P. ramorum* pathosystem as a model system. I approach this research in three distinct steps focusing on 1) the role of species diversity in moderating infectious disease risk in natural plant communities, 2) the influence of spatial-temporal heterogeneity on host mortality across multiple levels of host-pathogen-environment interactions, and 3) the challenges of data integration for mapping the impacts of a large-scale, spatially heterogeneous disease invasion. Each of these steps provided the framework for a single dissertation chapter and was designed to become its own publishable manuscript.

In chapter one, I tested an exciting research frontier called the 'diversity-disease risk' hypothesis, which predicts that increases in the species diversity of ecological communities can mediate epidemic dynamics and reduce infectious disease risk (Elton 1958, Keesing et al. 2006). Despite the importance of this topic, there remains a paucity of research on diversity-disease risk relationships in plant diseases in natural ecosystems (Kranz 1990, Haas et al. 2011). Building upon such "static" snapshots of host-pathogen-environment relationships, I then incorporated a temporal dimension into the epidemiological analysis of SOD in my second chapter, whereby I used a longitudinal data set spanning 8-years of survey data, combined with a survival analysis framework, to identify the influence of multiscale drivers (at the individual, community and landscape scale) on host mortality dynamics over time. Finally, in my third dissertation chapter I integrated SOD monitoring data from four different plot networks across California—encompassing diverse spatial and temporal coverage—to parameterize a large-scale spatial prediction model of host infection and mortality across the geographic ranges of *P. ramorum* and its wildland hosts in California and Oregon.

CHAPTER 2. FOREST SPECIES DIVERSITY REDUCES DISEASE RISK IN A GENERALIST PLANT PATHOGEN INVASION

Abstract

Empirical evidence suggests that biodiversity loss frequently increases disease transmission, yet our understanding of the 'diversity-disease hypothesis' in generalist plant pathogens in natural ecosystems is limited. We used a landscape epidemiological approach to examine two scenarios regarding diversity effects in the exotic plant pathogen *Phytophthora ramorum* across the Big Sur ecoregion: (1) an *amplification effect* exists where disease risk is greater in areas with higher plant diversity due to the pathogen's wide host range, or (2) higher diversity reduces risk due to a *dilution effect* on the two most competent host species. We found evidence for a dilution effect, where disease risk was lower in areas with higher plant species diversity, after accounting for host density and landscape context. Results suggest that although nearly all plants in the study were hosts, alternative hosts may hinder disease transmission by diluting effects of competent hosts, thereby buffering forest health from infectious disease.

Introduction

Emerging and re-emerging infectious diseases of plants and animals continue to pose threats to ecosystem services and public health worldwide (Daszak et al. 2000, Kilpatrick et al. 2010). The economic and ecological impacts they cause, coupled with accelerating anthropogenic environmental change, have stimulated increased interest in understanding the function of biodiversity in disease ecology (Mack et al. 2000, Pongsiri et al. 2009). Recent studies across a range of disease systems suggest that the species diversity of ecological

communities can moderate the prevalence of infectious disease through numerous biological mechanisms, referred to as *dilution* and *amplification effects* (Keesing et al. 2006). To date, the overwhelming majority of studies analyzing diversity-disease risk relationships have found evidence for dilution effects, whereby reduced diversity tends to increase pathogen transmission and disease incidence (Keesing et al. 2010). The specific mechanisms underlying these effects remain unclear in many cases, and concerns have been raised regarding the difficulty of separating out diversity effects from underlying host density effects and other less conspicuous habitat factors (Mitchell et al. 2002, McCallum 2008). In addition, empirical evidence remains scant and inconclusive for pathogen amplification, which is predicted to show the opposing effect of increased diversity leading to increased disease risk (Kranz 1990, Begon 2008). These uncertainties in our understanding of biodiversity and disease warrant the need for additional studies on this topic.

Although the effects of species diversity on disease risk have been well studied in a range of disease systems — including but not limited to zoonoses, aquatic systems, and experimental plant communities (Mitchell et al. 2002, Roscher et al. 2007, Raymundo et al. 2009) — there have not been any diversity-disease risk studies analyzing these relationships in emerging plant pathogens occurring within naturally-growing, non-experimental communities. Since the 'diversity-disease hypothesis' was first proposed by Elton (1958), which recognized that plant diseases could be ameliorated in 'complex' ecosystems if this complexity reduced host density, studies in agroecosystems, silviculture and experimental grassland communities have shown that high species diversity is often associated with lowered disease risk (Knops et al. 1999, Mitchell et al. 2002, Pautasso et al. 2005). However,

it remains uncertain whether these relationships will hold for plant pathogens in more complex natural ecosystems where non-cultivated plants and their pathogens are influenced by a multitude of interacting and often inconspicuous habitat factors (e.g., varying humidity, solar radiation) (Vila et al. 2005). Moreover, diversity effects may differ in emerging pathogens due to changing host-pathogen interactions throughout stages of the epidemiological process, including initial transmission of the pathogen and infection of a host, the production of transmission stages within the new host, and the establishment of the pathogen in the host population as a whole, including possible 'spillover' into additional host species (Keesing et al. 2010). Given these gaps in our knowledge and the growing threat plant diseases pose to forest health around the world (Anderson et al. 2004, Jones 2009), diversity-disease research on emerging plant pathogens within natural ecosystems is needed.

Here, we present results from a landscape-scale, observational study examining diversity-disease risk associations in an emerging plant pathogen, *Phytophthora ramorum*, across naturally growing forests of the Big Sur, California ecoregion (Figure 2.1). *P. ramorum* (Phylum *Oomycota*) is the causal agent of the emerging infectious disease sudden oak death and ramorum blight in North America and Europe (Rizzo et al. 2005, Brasier and Webber 2010). Since discovered in North America in the mid-1990s near San Francisco Bay, this environmentally transmitted pathogen has killed millions of oak (*Quercus* spp.) and tanoak (*Notholithocarpus densiflorus*) trees in coastal forests of California and Oregon (Rizzo et al. 2005). *P. ramorum* is a generalist, with over 100 species of plants (including ferns, gymnosperms and angiosperms) classified as hosts in native and horticultural settings (Rizzo et al. 2005). Over 40 host species are native to California and Oregon coastal forests.

The diseases the pathogen causes on its wide range of hosts are expressed in two ways: canker infections that often cause tree mortality in oaks and tanoak, and nonlethal foliar and twig infections in most non-oak host species and tanoak. Infections resulting in main-stem cankers (as on oaks and tanoak) have not been shown to transmit the pathogen in the field, whereas infections on foliage and small twigs may produce inoculum that is primarily transported via wind-driven rainsplash (Davidson et al. 2005). The two most competent foliar hosts in California forests, California bay laurel (*Umbellularia californica*) and tanoak, appear critical for natural spread of the pathogen between individual plants and across landscapes (Davidson et al. 2005, Davidson et al. 2008).

The *P. ramorum* pathosystem in Big Sur provides a unique model for studying diversity-disease risk relationships because the pathogen infects almost all woody plant species throughout the region, yet hosts exhibit asymmetric transmission and susceptibility (Davidson et al. 2005, Cobb et al. 2010). We examine two hypotheses regarding the effect of plant species diversity in this system: (1) an amplification effect where disease risk is greater in areas with higher diversity due to the generalist properties of *P. ramorum*, or in contrast, (2) higher diversity could lead to reduced disease risk due to a dilution effect on the competent hosts California bay laurel and tanoak. We use a landscape epidemiological approach, combining data on pathogen abundance with field-based and landscape context variables, to assess effects of host community structure and environmental conditions on diversity-disease associations. When studying emerging diseases at landscape to regional scales, data analytic complexities including zero-inflation and spatial autocorrelation may arise due to non-equilibrium dynamics of the invasion process (i.e., transient epidemic that

has not reached a steady state); failure to account for these issues can lead to biased parameter estimation and associated measures of uncertainty (Gschlobl and Czado 2008). To accommodate inherent spatial processes of the invasion process, we compare inference among a set of Bayesian hierarchical models with varying complexity: (1) a binomial generalized linear model (GLM), (2) a zero-inflated binomial GLM, and (3) a zero-inflated binomial generalized linear mixed model (GLMM) with a spatial random effect.

Materials and Methods

Study area

We established a long-term *P. ramorum* monitoring network consisting of 280 circular plots (500-m^2) throughout a 79,356-ha study area within the Big Sur region, extending 100-km along coastal, central California (Figure 2.1). Plots were randomly located across a broad range of ecological conditions stratified by host vegetation type (redwood-tanoak and mixed evergreen forests), elevation, latitude, and fire history, and were located in areas with and without the pathogen. Each plot was at least 200-m from its nearest neighbor. It is not known exactly when, nor how, *P. ramorum* initially invaded the study area, though impacts were first noted in Monterey County in the mid-1990s (Rizzo and Garbelotto 2003). The pathogen is patchily distributed at broad and fine spatial scales throughout the study area, with stands of uninfected hosts spatially juxtaposed to severely impacted stands, despite few apparent environmental differences between sites (Meentemeyer et al. 2008c). The region's topography is characterized by deeply dissected slopes and drainages, with elevation ranging from sea level to 1571-m within 5-km of the coast (Hensen and Usner 1996). A diversity of plant communities occurs throughout the study area, though plots were only established in

two dominant host forest community types: mixed evergreen forests occurring along moister slopes and redwood-tanoak forests at lower elevations (Figure 2.2).

Field Measurements

We collected data over a two-year period from June–October of 2006 and 2007. Plot coordinates were recorded using survey-grade global positioning system receivers. In each plot, we recorded the species identity and diameter at breast height (DBH) of all woody plant species that satisfied the following size requirements: trees and vines with a DBH ≥ 1-cm and shrubs that reached an area ≥ 1-m^2. Symptoms of *P. ramorum* were recorded for each host plant that satisfied size requirements, and symptomatic tissue from a subset of these individuals was removed and brought to the laboratory for pathogen isolation using a *Phytophthora*-selective media (PARP; Davidson et al. 2005). For analysis purposes, we considered symptomatic plants as 'infected' only if cultured samples confirmed the presence of *P. ramorum* in the respective plot. We derived the following variables for each plot: species richness (the number of host and non-host species), Shannon-Wiener diversity index H′ (takes into account the number of species and the evenness of the species), density of bay laurel and density of tanoak, and forest community type (mixed evergreen or redwood-tanoak forest).

Landscape context

We accounted for the effects of landscape context on disease risk by including three GIS-derived variables for each plot: average precipitation over the wet season, potential solar insolation (PSI), and amount of host habitat within a 200-m radius from plot center. We used the parameter elevation regression on independent slopes model (PRISM; Daly et al. 1994) to

map the 30-year (1971–2000) monthly average precipitation (800-m spatial grain) between December–May, which corresponds to the rainy season when conditions are favorable to *P. ramorum* infection (Davidson et al. 2005, Rizzo et al. 2005). To account for topographic variation in solar energy, we derived average PSI over the wet season from a U.S. Geological Survey 30-m digital elevation model. PSI uses the cosine of illumination on slope equation to measure the amount of potential solar energy incident at a location on the Earth's surface (Dubayah 1994). Lastly, we obtained the amount of host habitat surrounding each plot by summing the area of mixed evergreen and redwood-tanoak forest within 200-m (12.5-ha) of plot center, using vegetation maps described in Meentemeyer *et al.* (2008c; see Figure 2.1-C inset). A 200-m radius landscape boundary had been previously found as the scale at which *P. ramorum* responds most strongly to forest heterogeneity (Condeso and Meentemeyer 2007).

Data analysis

All statistical analyses were conducted using R version 2.12.1 (R Development Core Team 2010). We use a new method for fitting Bayesian Markov random field models called INLA (integrated nested Laplace approximations) (Rue et al. 2009), which substantially reduced computational time compared to Markov chain Monte Carlo (MCMC) methods for our dataset. The INLA algorithm is not an iterative stochastic method like MCMC, but rather a sequence of approximation techniques to find the marginal posterior distributions for well-posed latent Gaussian Markov random field models. It has been shown to be an accurate and efficient alternative to MCMC in terms of computational time for large datasets with correlated spatial effects (Rue et al. 2009). We used the R package INLA (Rue and Martino

2009) to construct models with varying complexity: (1) a binomial generalized linear model (GLM), (2) a zero-inflated binomial GLM, and (3) a zero-inflated binomial GLMM with a spatial random effect. The proportional response variable was disease incidence, calculated by grouping the number of symptomatic hosts with the number of non-symptomatic hosts per plot.

In what follows, we describe the third and most sophisticated model only (i.e., GLMM), as the remainder of models are simplifications of it. For the total number of plants (n_i) at each plot i, for m total plots, we record each individual plant as a binary variable (i.e., symptomatic/non-symptomatic) and let the sum of these be binomial distributed with probability θ_i if the pathogen has reached plot i and zero if the pathogen has not yet reached the plot. Since pathogen absence is difficult to observe perfectly, a zero-inflated binomial model for the data could help account for this source of uncertainty (as well as the transient nature of this ongoing epidemic).

In constructing the process portion of the models, we used the traditional 'logit' function to link the probabilities θ_i to a set of covariates:

$$logit\,(\theta_i) = \beta_0 + \beta_1 x_{1,i} + \ldots + \beta_q x_{q,i} + \varepsilon_i,$$

where the x variables represent plot-level characteristics. The errors, ε_i, were allowed to be spatially correlated, so that they could absorb any latent autocorrelation beyond that described by the model covariates. Specifically, we specified an intrinsic conditional autoregressive model (ICAR) for the errors, where in order to create the necessary spatial proximity matrix, we obtained 'pseudo-residuals' by fitting a preliminary model with i.i.d. errors and then computing the Moran's I spatial statistic to assess potential autocorrelation in

these pseudo-residuals. The spatial proximity matrix was based on the inter-plot neighborhood distance (in km) that had the lowest p-value for Moran's I, and we assumed that this distance was the scale in which the dominant latent spatial structure should be accounted for by our model (see Figure S2.1, S2.2 in supplementary materials). Lastly, to specify the parameter portion of this hierarchical model, the regression coefficients were given a Gaussian prior, $\boldsymbol{\beta} \sim N(0, 1000 \cdot \mathbf{I})$, the precision parameter for the latent errors was given a gamma prior, $\tau \sim \text{Gamma}(1, 5e\text{-}05)$, and the logit of the zero-inflation probability for the likelihood was given a standard normal prior distribution, N(0,1).

We fit separate models for species richness and the Shannon-Wiener diversity index H′ due to collinearity between these variables. Because the time of field data collection varied across plots, we added sampling year as an indicator covariate with year 2006 being zero and year 2007 being one. All variables were tested for multicollinearity and continuous variables were scaled prior to model implementation. Marginal posterior distributions were summarized by 95% Bayesian credible intervals (i.e., BCI; the 0.025 and 0.975 quantiles of the posterior distribution) and deviance information criterion (DIC) statistics were used to compare models (Spiegelhalter et al. 2002).

Results

A total of 10,152 known host plants (out of 13,599 total plants) were assessed for *P. ramorum* symptoms across 278 plots. Of these, 23% of hosts from 151 plots were infected based on laboratory confirmation of *P. ramorum* in the respective plot. The mean proportion of symptomatic host plants within infected plots was 0.37 and exhibited positive skew (range = 0.01–0.95, skew=0.52). Zero-inflation was observed in the 127 plots (46%) that did not

contain infected hosts, with the majority of uninfected plots clustering towards the southern portion of the study area (Figure 2.1). Approximately 80% of all plots contained one or more bay laurel host, 61% had at least one tanoak host, and 49% of plots contained both competent host species. Tanoak was the most abundant host and had higher prevalence of infection than all other host species, followed by bay laurel (Figure 2.3; see Table S2.1). Bay laurel density and species diversity exhibited weak correlations for both species richness (SR) and Shannon-Weiner diversity (H′) ($r_{SR, BAY} = 0.05$; $r_{H', BAY} = -0.02$), as did tanoak density and species diversity ($r_{SR, TOAK} = -0.17$; $r_{H', TOAK} = -0.32$). Species richness (of hosts and non-hosts) ranged from 1–12 species per plot (mean=5), while species richness of host species only ranged from 1–9 (mean=4). The Shannon-Wiener diversity index ranged from 0.00–2.10 (mean 1.01). The plot network spanned a wide degree of landscape heterogeneity: average precipitation (range: 71–192 mm), PSI (range: 0.2–1.00 watts/m^2), and amount of host habitat within 200-m (range: 0.27–12.56 ha). See Table S2.1 and S2.2 for a list of all host species assessed and descriptive statistics of all model covariates.

All three Bayesian hierarchical models indicated a negative relationship between species diversity (measured as species richness and H′) and disease incidence, after accounting for host density and landscape context effects. The zero-inflated binomial GLMMs with the ICAR spatial effect had better model fit based on DIC criterion (DIC_{SR} = 1050, $DIC_{H'}$ = 1061) compared to the simpler zero-inflated binomial GLMs (DIC_{SR} = 2194, $DIC_{H'}$ = 2312) and the standard binomial GLMs (DIC_{SR} = 3598, $DIC_{H'}$ = 3727). As such, we present further results for the spatial models only (see Table S2.3 for all results). Based on the graph of Moran's I p-values as a function of inter-plot distance, we chose a neighborhood

distance of 5150-m to calculate our spatial proximity matrix for the species richness (SR) model and 6201-m for the Shannon-Wiener diversity (H′) model. Table 2.1 compares parameter estimates for the two spatial models when host density of the competent hosts (bay laurel and tanoak) were included and excluded. The negative diversity effects remained and model fit substantially improved after incorporating host density effects (Δ DIC_{SR} = 2055; Δ $DIC_{H'}$ = 1947). Covariate relationships were considered statistically significant if the 95% Bayesian credible intervals did not overlap zero. For spatial models that included both diversity and density effects, the probability of *P. ramorum* infection was negatively associated with species richness ($\hat{\beta}_{SR}$ = -0.83, BCI = -1.14 – -0.54) and the Shannon-Wiener diversity index ($\hat{\beta}_{H'}$ = -0.49, BCI = -0.79 – -0.19), and was positively associated with the density of bay laurel and tanoak: species richness model ($\hat{\beta}_{BAY}$ = 1.21, BCI = 0.89 –1.57; $\hat{\beta}_{TOAK}$ = 0.95, BCI = 0.61 –1.31), and Shannon-Wiener diversity model ($\hat{\beta}_{BAY}$ = 1.16, BCI = 0.82 –1.53; $\hat{\beta}_{TOAK}$ = 0.91, BCI = 0.53 –1.30) (the beta hat corresponds to the posterior mean). In both diversity models, we found negative effects for average precipitation, forest community type (regression parameter estimated for redwood-tanoak forests) and sampling year (regression parameter estimated for 2007). We also found a positive effect for the amount of host habitat within a 200-m buffer around each plot. Neither model showed a significant effect for PSI.

Discussion

Despite a growing number of diversity-disease risk studies (Keesing et al. 2010), to our knowledge this study is the first to analyze these relationships in an emerging plant pathogen within the context of a natural community. We hypothesized that the *P. ramorum* system

would exhibit either an amplification effect due to the pathogen being able to infect multiple plant species in high diversity areas, or in contrast, higher diversity could lower disease risk due to a dilution effect on bay laurel and tanoak, the two principal reservoirs of inoculum. We found consistent negative relationships between disease incidence and plant species diversity, quantified as species richness and the Shannon-Wiener diversity index, suggesting that a dilution effect is operating in the Big Sur *P. ramorum* system. These relationships held after accounting for the potentially confounding effects of bay laurel and tanoak density, and after incorporating landscape context effects capturing biotic and abiotic environmental variation across the highly heterogeneous study area. Our findings suggest that although nearly all plant species in our plots are hosts, there is little evidence they play a strong role in facilitating disease transmission. As a result, many plants surrounding an oak may be alternate hosts yet protect the oak by diluting the impact of highly competent, inoculum-producing hosts like bay laurel and tanoak. Concerns have been raised regarding the difficulty of separating a dilution effect from a host density effect, as both can lead to similar outcomes (i.e., reduced pathogen abundance with greater host diversity), yet the underlying biological mechanisms are distinct (Mitchell et al. 2002, Keesing et al. 2006, Begon 2008). The negative diversity effects we found remained after including host density of both competent hosts in the model, suggesting that alternative mechanisms in addition to underlying host density effects account for the dilution effect reported in this study.

Although the effects of diversity on disease transmission have been described for multiple disease systems over the past decade, our understanding of the specific mechanisms governing these effects is still rudimentary. However, this information is needed for

predicting net effects and for evaluating the generality of patterns found in specific disease systems (Keesing et al. 2006). For plant pathogens, reduced host density is often the most important mechanism by which diversity reduces disease severity, particularly for fungal diseases in agricultural systems (Burdon and Chilvers 1982). In experimental grassland systems, Knops *et al.* (1999) and Mitchell *et al.*(2002, 2003) found that plots with high species richness had lower disease severity of specialist fungal diseases, but statistical analyses revealed that it was low host density that reduced disease severity rather than species diversity per se. More complicated mechanisms may arise in disease systems involving a multiplicity of hosts. In the *P. ramorum* system in Big Sur, the roles of hosts are complex. Bay laurel and tanoak produce copious amounts of inoculum spread primarily via wind-driven rain splash, but of these two host species only tanoak experiences mortality from sudden oak death. Less is known regarding the susceptibility and transmission potential of other less competent foliar hosts (e.g., redwood, madrone, toyon), and it remains unknown how important of a role these species play in the epidemiological process. Oak (*Quercus* spp.) canker hosts have not been shown to transmit inoculum in the field (i.e., they are pathogen sinks) but undergo disease-induced mortality. The wide host range of *P. ramorum*, coupled with vastly differing competency among host species, may facilitate a suite of non-mutually exclusive mechanisms that underlie a relationship between diversity and disease risk.

Density-dependent models of transmission are generally used to characterize diseases that are spread through environmental propagules or though random contact among individuals (Keesing et al. 2006). One density-dependent mechanism that may be occurring

in the *P. ramorum* system is 'encounter reduction' (Keesing et al. 2006, Begon 2008), whereby the addition of less competent hosts may, through effects on transmission pathways, make the pathogen less abundant, or less likely to persist, than in the presence of bay laurel or tanoak alone. This could occur, for example, if the added species intercept inoculum transmitted through space, or increase the distances which spatially-dispersed inoculum must traverse in order to spread between competent host plants. Another mechanism that may be operating in the *P. ramorum* system is 'susceptible host regulation' (Keesing et al. 2006), in which interspecific competition for limiting resources constrains the abundance of susceptible competent hosts. A decreased number of competing plant species may allow the abundance of bay laurel and tanoak to increase locally, facilitating the spread of *P. ramorum*. It could also be that diversity-dependent variations in microenvironmental conditions affect pathogen dynamics. Changes in light levels, temperature differentials, wind velocities, and relative humidities within forest stands have been shown to affect disease risk in other fungal pathogens (Kranz 1990), and may also be occurring in the *P. ramorum* system.

In this study, we analyzed diversity-disease associations in a broader ecological context in which we accounted for multiple sources of abiotic and biotic heterogeneity across a large region in addition to species diversity and host density. We found that mixed evergreen forests were associated with higher prevalence of disease compared to redwood-tanoak forests. Davidson et al. (2011) compared *P. ramorum* transmission in bay laurel between these forest community types and also found lower probability of infection in redwood-tanoak forest than in mixed evergreen forests in 2001–02, yet no significant difference in 2002–03. In contrast, in a follow-up study from 2003–05 they found higher

infection levels in the redwood forests. This suggests that *P. ramorum* transmission in coastal California forests represents a complex ecological process dependent on a number of factors including but not limited to forest type, invasion history, and variation in biotic (e.g., host species composition) and abiotic influences (e.g., moisture and light availability). Regarding the landscape distribution of host habitat surrounding each plot, we found that disease risk was positively associated with the amount of host habitat within a 200-m buffer around each plot, a finding which adds to the growing body of literature that highlights the importance of landscape connectivity of host habitat for influencing tree pathogen spread (Holdenrieder et al. 2004, Ellis et al. 2010). Contrary to expectations, the negative relationship between average precipitation during the rainy season and disease incidence that we found could be attributed to lower host densities at high elevations, or may be an artifact of the spatial grain of precipitation data (800-m) not corresponding to the scale of disease dynamics.

Over the past few decades, many forest pathogen outbreaks have occurred over landscape to regional scales (Castello et al. 1995, Holdenrieder et al. 2004, Meentemeyer et al. 2011). Despite the strong influence that landscape context may have on the spread of forest pathogens, landscape epidemiology has received little attention from plant pathologists (Holdenrieder et al. 2004, Plantegenest et al. 2007). When studying emerging pathogens across broad geographic scales, disease dynamics are often not in geographic equilibrium (i.e., the pathogen's distribution is patchy and stochastic in space and time), and as such, diversity-disease relationships may vary across spatial scales (Ostfeld et al. 2005). We found that models that accounted for the spatial structure inherent to our disease incidence data (i.e., zero-inflation and spatial autocorrelation) had better fit compared to non-spatially

structured models, and we therefore place more confidence in the observed negative effect of diversity on sudden oak death disease incidence knowing that we accounted for these potentially confounding effects. Studying diversity-disease associations across large geographic scales requires observation driven approaches because such studies are conducted on spatial and temporal scales untenable in manipulative experiments (Sagarin and Pauchard 2010). However, it can be difficult to draw firm conclusions from 'natural experiments', such as disease invasion into novel habitat, because of the complexity of natural environments in any given place and across gradients, and because it is not possible to hold all habitat conditions constant with only diversity varying. Due to the correlative nature of our study, it is challenging to assign particular causal mechanisms to the patterns we found or to disentangle the dilution mechanisms of encounter reduction from susceptible host regulation. Despite these concerns, our analyses did account for multiple sources of biotic and abiotic variation across the landscape, and are an important first step towards illustrating how a dilution effect may manifest in generalist plant pathogens emerging across vast, heterogeneous natural ecosystems.

In contrast to re-emerging diseases, exotic pathogens have not coevolved with the host or ecosystem in which they emerge and, as such, are more likely than endemic diseases to pose a threat to biodiversity through biomass loss and changes in species composition through the extinction of host species (Anderson et al. 2004, Burdon et al. 2006). When the pathogen is a generalist, infecting multiple host species including asymptomatic reservoirs, remedial action is more challenging and outbreaks may be followed by poorly contained spread, often with devastating consequences (Pautasso et al. 2005). For example, the

introduction of *Phytophthora cinnamomi*, a generalist and aggressive root pathogen, had severe consequences for the Jarrah forest of Western Australia, in which most native eucalypts had little if any resistance (Shearer and Dillon 1995). Despite high plant diversity Jarrah forests were very susceptible to this generalist pathogen, illustrating a case where the insurance hypothesis fails for a non-specific pathogen (Weste et al. 2002). Similarly, *P. ramorum* has already begun changing forest ecosystems along coastal California (Rizzo and Garbelotto 2003, Metz et al. 2011). The low cost of infection in some hosts, including bay laurel and redwood, is likely to initiate a shift to greater dominance of these species in the future (Cobb et al. 2010). Our results suggest that retaining plant diversity for management purposes could lower disease risk. Although this could be accomplished in theory by manipulating the abundance of certain host species, in natural systems sufficient resources will likely not be available for such a highly targeted strategy (Rizzo et al. 2005), and broader measures to foster species diversity will be needed. Conservation of coastal forests in the Pacific Northwest may ultimately hinge on better understanding the community epidemiology of the *P. ramorum* system. Additional studies are warranted to see if dilution effects occur in other infected forests in California, and whether similar ecological mechanisms operate in forests with varying epidemiological and community attributes. This information is needed for managing coastal forests against this highly destructive pathogen and for generalizing diversity-disease relationships to a wider range of disease systems, especially emerging plant pathogens in forest ecosystems.

CHAPTER 3. MULTILEVEL EFFECTS OF INDIVIDUAL, COMMUNITY AND LANDSCAPE DRIVERS IN A WILDLAND FOREST EPIDEMIC

Abstract

The dynamic and spatial nature of epidemiological processes presents unique challenges for managing the spread of infectious diseases in natural communities. Long-term ecological studies that combine data across multiple scales of host-pathogen-environment interactions are needed to identity the principal drivers of wildland epidemics. We designed a longitudinal study to evaluate the spatial and temporal dynamics of a wildland disease across multiple levels of host-pathogen-environment interactions (i.e., at the individual, community and landscape scale). Using the emerging forest disease sudden oak death as a case study, we applied a multi-level survival analysis framework that incorporates time-varying properties of the system to address the following questions: 1) which hierarchical scale of disease-environment interactions most strongly predicts time to infection in susceptible oaks, and 2) is their evidence for multi-year effects of climate variability on epidemic dynamics? We monitored 1125 oaks across 200 15 x 15 m plots in a natural coastal forest ecosystem in northern California for infection and disease-induced mortality annually over an 8-year period. Coast live oak exhibited a steady increase in the number of trees becoming infected and dying following infection, signaling the potential for sudden oak death to dramatically change oak woodlands through selective removal of this foundation species. To a lesser extent, the number of black oak becoming infected and dying from disease also increased over time. After accounting for unobserved heterogeneity using a frailty term (i.e., random effect) for oaks nested within the same plot, the survival analyses revealed the collective

importance of factors at the individual, community and landscape scale in mediating oak infection risk through space and time. Overall, we found that larger oaks of both species are more susceptible to infection than smaller stems, and that warmer and wetter average climate conditions over a two-year period increase infection risk, while increased plant species diversity lowered disease risk (i.e., a dilution effect). Plot density of the most competent foliar host species (California bay laurel) was positively associated with increased oak disease risk, yet became only marginally significant in global models containing variables collected at the individual, community and landscape scale. Our results demonstrate how multi-scale heterogeneity in the environment modulates disease dynamics in a wildland system, and provide an empirical basis for assessing the risk of population declines among co-occurring hosts in pathogen-invaded communities.

Introduction

Exotic plant pathogens pose a significant and growing threat to forest ecosystems throughout the world, often functioning as important disturbance agents that affect biodiversity, productivity, nutrient cycling, and consumer food webs (Castello *et al.* 1995, Lovett *et al.* 2006, Aukema *et al.* 2010). In extreme cases, exotic diseases such as chestnut blight, beech bark disease and white pine blister rust have caused epidemics associated with widespread tree mortality and extensive changes to forest communities (Houston 1994, Diskin et al. 2006, Smith et al. 2012). The economic and ecological impacts of these epidemics (Anderson *et al.* 2004, Kovacs *et al.* 2011), coupled with predictions of continual increase in the number of plant pathogens emerging over the coming decade (Jones 2009, Fisher *et al.* 2012), gives urgency to identifying the factors driving forest disease dynamics in wildland settings.

However, this is a challenging task because wildland ecosystems, in contrast to intensively-managed systems such as agriculture and tree plantations, are characterized by complex spatial arrangements of hosts and environmental conditions across broad geographical regions (Alexander 2010, Hatala *et al.* 2010, Meentemeyer *et al.* 2012). Moreover, the numerous sources of heterogeneity mediating wildland epidemics operate across multiple levels of host-pathogen-environment interactions (e.g., from the individual to the community and entire landscape). Given the logistical challenges of conducting longitudinal field surveys of host populations with measurements of corresponding (and surrounding) biotic and abiotic conditions at large spatial scales, there remains little empirical support for the importance of such sources of heterogeneity and the generality of their influence on disease dynamics in natural ecosystems (Meentemeyer *et al.* 2012, Dillon *et al.* 2014).

At the individual host level, variation in susceptibility is a principal source of heterogeneity controlling the trajectory of plant-disease invasions. Among host attributes influencing susceptibility are genetic variation for resistance and physical factors including host morphology and size/age class (Thrall and Burdon 2000, Kauffman and Jules 2006, McPherson *et al.* 2010). A growing number of studies on emerging forest diseases has reported significantly higher infection rates for larger trees compared to smaller conspecifics, which may result from size-related changes in host surface area, bark texture and chemistry, or other life-history traits correlated with size and age (Kauffman and Jules 2006; citations, Cobb *et al.* 2012). In multi-host systems, where pathogens can infect and be transmitted among various species, repeated surveys of the entire host species pool are needed to capture interspecific variability in infection and transmission dynamics, rates and patterns of disease-

induced mortality, and potential recovery from infection. Despite the importance of accounting for individual heterogeneity when studying epidemic dynamics, there remains a paucity of studies on pathogens in wildland systems that have quantified individual-level effects while simultaneously examining the influence of multi-scale variability in the surrounding environment (Kauffman and Jules 2006; citations). This knowledge gap likely results from the difficulties associated with monitoring individual hosts over large geographic regions and across meaningful temporal scales (Holdenrieder *et al.* 2004, Ostfeld *et al.* 2005, Meentemeyer *et al.* 2012, Dillon *et al.* 2014).

At the community level, complex relationships between host density and species diversity can also influence disease outcomes (Mitchell *et al.* 2002, Fenton and Pedersen 2005, Haas *et al.* 2011). In most plant-pathogen systems, disease development is regulated by density-dependent processes, which may arise through direct effects (e.g., increased pathogen transmission mediated by decreasing distance between hosts), or via indirect effects such as intraspecific competition or altered understory microclimate (Burdon and Chilvers 1982, Gilbert 2002, Parker and Gilbert 2004). In multi-host systems, generalist pathogens may be decoupled from the density of any single host species and instead respond to the joint population densities of several species, and/or be regulated by competition between tolerant and susceptible hosts (i.e., "pathogen spillover"; Power and Mitchell 2004). A growing body of evidence suggests that the species richness of ecological communities can mitigate infectious disease risk, through mechanisms collectively referred to as amplification and dilution effects (Keesing *et al.* 2006, Ostfeld and Keesing 2012). To date, the overwhelming majority of diversity-disease risk studies in plants has occurred in experimentally-

manipulated systems (Mitchell *et al.* 2002, Roscher *et al.* 2007, Pagan *et al.* 2012), resulting in uncertainty as to the relative roles of species identity, host density and species diversity in governing epidemic dynamics in natural forest ecosystems (though see Pautasso *et al.* 2005, Haas *et al.* 2011).

Although the field of disease ecology continues to deepen our understanding of plant-pathogen interactions in natural communities (Gilbert 2002, Alexander 2010, Burdon and Thrall 2013), a 'real world' perspective of epidemic dynamics necessitates that, in addition to local biotic effects, broader-scale influences of landscape heterogeneity are also examined (Ostfeld *et al.* 2005, Eastburn *et al.* 2011, Meentemeyer *et al.* 2012). Epidemiological processes vary among systems and environments, for example, depending on whether climate is favorable to epidemic development (Sturrock *et al.* 2011) or whether epidemics are driven by inoculum from distant populations (Ellis *et al.* 2010). Recent work has illustrated how landscape features can mediate disease processes by functioning as either conduits or barriers to pathogen dispersal (Condeso and Meentemeyer 2007, Meentemeyer et al. 2008b, Mundt et al. 2011). For example, Johnson and Haddad (2011) conducted a large-scale corridor experiment to examine the movement of a wind-dispersed fungal pathogen through a fragmented landscape, finding that edge effects were the key drivers of pathogen movement and disease development. Regarding the role of climatic variability on forest diseases, a growing body of evidence is revealing how many pathogens are expected to respond favorably to warmer and drier conditions, mainly through mechanisms involving heightened host stress and susceptibility during unfavorable environmental conditions (Dukes *et al.* 2009, Kliejunas *et al.* 2009, Eastburn *et al.* 2011). In contrast, other pathogens are expected

to thrive under warmer and wetter conditions, which are conducive to the processes of propagule production and germination (Kliejunas *et al.* 2009; citations).

Due to the inherently transient nature of epidemics, long-term studies capturing variability in host and environmental conditions through time are needed to better understand plant-pathogen systems in wildland environments (Meentemeyer *et al.* 2012; citations). Temporal drivers of epidemics may be regular and deterministic such as seasonal weather patterns (Altizer *et al.* 2006) or may be stochastic in nature such as disturbance events (e.g., drought, wildfire) (Birdsey and Pan 2011, Metz *et al.* 2011). In turn, host-pathogen responses to changing environmental conditions can range from simple annual cycles to more complex multiyear fluctuations (Smith *et al.* 2003). For instance, favorable weather conditions during a single season may facilitate pathogen reproduction, yet not instantly increase disease transmission because inoculum build-up and dispersal may require more than a single season of optimal conditions (Davidson *et al.* 2008). Despite recognition of the importance of longitudinal studies in disease ecology research, most studies on emerging forest pathogens have focused on single 'static' snapshots in time or occurred over relatively limited time periods, thereby limiting our understanding of the complex spatial and temporal patterns that are likely to predominate in natural settings. Improved forecasts of wildland epidemics will require well-parameterized systems that combine longitudinal data from detailed, fine-scale field studies with epidemiologically-relevant data collected over local to landscape extents (Meentemeyer *et al.* 2012).

Here, we designed a long-term study to capture temporal and spatial heterogeneity of wildland disease dynamics across multiple levels of host-pathogen-environment interactions

(i.e., from the individual to the community and entire landscape). Our study focuses on the spread of *Phytophthora ramorum*, an exotic and invasive water mold (Oomycota) that causes sudden oak death in North America (Rizzo *et al.* 2002), sudden larch death in Europe (Brasier and Webber 2010), and ramorum blight in nurseries worldwide (Grunwald *et al.* 2008). The inherent complexities of this multi-host disease system present an ideal opportunity to examine the roles that host and environmental heterogeneity play in the dynamics of a wildland forest epidemic. In this paper, we ask two interrelated questions. First, which hierarchical scale of disease-environment interactions most strongly predicts time to infection in susceptible oaks? For example, do individual host and community attributes matter more than broad-scale effects of landscape heterogeneity and climatic variability? Second, is their evidence for multi-year effects of climatic conditions over time on epidemic dynamics? That is, does the progression of host infection synchronize with spatial and temporal patterns of temperature and precipitation variability? Research addressing such questions is urgently needed to provide deeper insight into how natural forest ecosystems will respond to ongoing pest and pathogen introductions and help identify which environmental variables drive disease dynamics in wildland settings.

Methods

Study system

Sudden oak death impacts were first noted in North America during the mid-1990s in the San Francisco Bay area of northern California (citation). *P. ramorum* was later identified as the causal agent in 2000 (Rizzo et al. 2002). Since then, this exotic pathogen has spread rapidly across coastal forests of California and Oregon, causing extensive mortality of tanoak

(*Neolithocarpus densiflorus*) and oak (*Quercus* spp.) populations (Figure 1; Meentemeyer et al. 2008c). Although *P. ramorum* has an incredibly broad host range— infecting over 130 species across disparate plant taxa (Grunwald *et al.* 2008, APHIS 2013)— the pathogen exhibits substantial variation in its ability to infect, sporulate on, and kill different host species. The diseases that *P. ramorum* causes on this range of hosts are expressed in two ways: canker infections on the main stem that may be lethal to oaks and tanoak, and non-lethal foliar and twig infections on non-oak hosts (Rizzo 2005). Tanoak is the only known host that exhibits lethal canker infections while also producing inoculum on infected leaves and twigs, whereas the oak hosts have not been shown to produce inoculum on stem cankers in the field (Davidson *et al.* 2005). The two most competent, inoculum-producing foliar hosts in California forests, bay laurel (*Umbellularia californica*) and tanoak, appear critical for natural spread of the pathogen between individual plants and across landscapes (Davidson *et al.* 2005, 2008, 2011). The remaining foliar hosts are thought to play a lesser role in pathogen transmission, with little to no direct fitness consequences from infection, and have been shown to 'dilute' infection risk in biologically diverse forest stands (Haas *et al.* 2011).

Study area

Between 2004–2011, we collected field data from 200 geospatially-referenced plots (15 x 15 m) distributed across a 275 km^2 heterogeneous forested region in Sonoma County, California, USA, consisting of a mixture of public and privately owned land (Figure 1). The impacts of *P. ramorum* were first observed in the region in 2000, and the pathogen is now widely distributed across the landscape (Cushman and Meentemeyer 2008, Ellis *et al.* 2010). Upon plot establishment, detailed vegetation surveys were conducted to determine the

species identity of all woody plants in the understory and overstory. Plot locations were randomly distributed across the study area in a manner that enabled us to capture landscape-scale variability of environmental conditions and disease spread throughout the region. Elevation ranged from 55–800 m and vegetation cover included distinct patches of mixed evergreen forest dominated by bay laurel and oak species, interspersed with annual grassland as well as areas of chaparral and stands dominated by redwood. Tanoak prevalence was low across the study area, found in only nine of the 200 plots. The region's Mediterranean climate is characterized by generally moderate temperatures year round, with cool temperatures and rain in the winter and spring months followed by long periods of dry and warm weather during the summer months. During the 8-year study period, the region experienced interannual drought conditions as well as above-average precipitation in some years, providing an ideal situation to examine effects of climatic variability on disease dynamics in a wildland forest system.

Host assessment

Beginning in 2004 and continuing annually thereafter, we tagged and measured tree stems in each plot measuring ≥ 2 cm diameter at breast height (DBH; 1.4 m). Stems were defined as either the main trunk or as individual branches separating from the main trunk below breast height. We focused on the five important host species in this system: two foliar hosts – California bay laurel (*Umbellularia californica*) and tanoak (*Neolithocarpus densiflorus*) – and three oak canker hosts: coast live oak (*Quercus agrifolia*), black oak (*Q. kelloggii*) and canyon live oak (*Q. chrysolepis*). Only oaks rooted within plots were included in our study, whereas the foliar hosts could be located outside of a plot so long as a portion of their canopy

fell within the plot. This practice was implemented because wind-driven rain splash can shed inoculum from nearby foliar hosts into the plot (Davidson *et al.* 2008). Each year of our study, we assessed tagged stems in all plots for health status (alive/dead) and the presence of *P. ramorum* symptoms during peak symptom expression (March-May). Stem mortality (defined as the death of all aboveground tissue) was assessed based on an examination of cambial damage to the basal tree trunk and the drying and abscission of foliage. Assessment of *P. ramorum* infection on oaks was performed by looking for "bleeding" canker lesions (i.e., dark red exudates and discoloration of bark surface) on the main stem. To relocate cankers across years, we recorded canker dimensions and location (i.e., aspect and height from ground) for each stem. A stem's transition from an uninfected (i.e., non-symptomatic) to an infected (i.e., symptomatic) status required that one or more canker lesions be found for at least two (not necessarily consecutive) years. Oak stems that died following *P. ramorum* infection were classified as dead from SOD.

Environmental drivers of oak infection

We examined the influence of ten variables on oak disease progression, spanning the individual, community and landscape scale. At the individual level, we included the size (measured as DBH) and species identity of each stem. At the community level, we calculated woody tree species richness and density of bay laurel in each plot. Species richness was calculated as the total number of woody plant species that were rooted within or overhanging into each plot. We included overhanging species (i.e., those detected in the canopy overstory) in order to obtain a more realistic perspective of community effects on disease risk. Bay

laurel density was calculated anew each year to account for bay stems entering the study once satisfying size requirements.

To examine the influence of landscape heterogeneity on infection risk, we used GIS software to obtain three variables aimed at capturing topographic variability across the region: host habitat connectivity, topographic moisture index (TMI), and potential solar irradiation (PSI). We used a detailed map of host and non-host land-cover classes—derived from ADAR multispectral imagery (Condeso and Meentemeyer 2007)—to calculate the amount of host habitat occurring within a 200 m radius of plot center to examine the role of habitat contiguity on infection risk. We chose this distance based on previous findings that *P. ramorum* disease severity was greatest in plots surrounded by a high proportion of contiguous forest with increasing scale from 50–200 m (Condeso and Meentemeyer 2007). TMI was included to examine effects of variability in potential soil moisture across the landscape resulting from variations in terrain topography, derived as the natural logarithm of the upslope flow accumulation area divided by the tangent of the local slope (Moore *et al.* 1991). We calculated PSI to account for variation in solar energy incident dependent on the slope and aspect of each plot (during the spring and fall seasons), using the cosine of illumination on slope equation (Dubayah 1994). We included this variable because laboratory trials have shown that *P. ramorum* is sensitive to UV-radiation (Englander et al. 2006).

To examine the influence of climatic variability on disease, we included three down-scaled climatological variables derived from the parameter elevation regression on independent slopes model (PRISM; Daly *et al.* 2001). Mean monthly values of maximum temperature, minimum temperature and precipitation from the 30-yr period 1981–2010 (at a

2 x 2 km cell size) were converted to a 100 m spatial resolution following the statistical down-scaling methods described in Flint and Flint (2012). From these finer-scale data, we calculated three variables corresponding to the rainy season (November 1-May 31) for each year of the study: 1) average minimum monthly temperature (°C), 2) average maximum monthly temperature (°C), and 3) cumulative average monthly precipitation (mm). To assess multi-year effects of climatic conditions over time on oak infection, we composed these variables across four time steps: 1) current year only, 2) current and previous year average, 3) current and previous two years average, and 4) current and previous three years average. For current year calculations, we included monthly data from November to April only because many plots were sampled prior to May. Measurements for all previous years included the month of May.

Survival analysis

We used survival analysis— a collection of statistical procedures for data analysis in which the outcome variable of interest is time until an "event" occurs (Kleinbaum and Klein 2012)— to identify the multi-level drivers influencing time-to-infection in oaks. Here, time refers to the number of years elapsing since an individual oak stem entered the study and then either experienced the event or was censored. Here, an "event" refers to a field-based diagnosis of *P. ramorum* infection status (following the two-year classification criterion), whereas "censoring" refers to situations in which an oak never experienced the event during the study period or was removed from the study prematurely (e.g., mortality from causes other than SOD) (Kleinbaum and Klein 2012). Survival data are most often analyzed using the Cox proportional hazards regression model in which time-to-infection is treated as a

continuous variable (Cox 1972), yet correct inference based on these models requires independent and identically distributed samples, which is rarely obtained with observational disease data. Alternatively, the shared frailty model is an extension of the Cox model that can be used when observations are clustered into groups. As such, the survival and hazard functions used to quantify the probability distribution of events are dependent on an observable random quantity, the so-called "frailty" (i.e., random effect) that accounts for excess risk of distinct groups (Wienke 2010). Here, we analyze time to infection using a shared gamma frailty model with a frailty term for field plot, as oaks in the same plot share underlying risk factors that vary spatially yet are difficult or impossible to measure (e.g., invasion history). Models are partitioned into four levels: 1) individual effects, 2) community effects, 3) landscape effects, and 4) full models parameterized with significant covariates from each hierarchical scale.

We performed all analyses using the R program (version 3.0.1; R Development Core Team 2010), using the R-package 'frailtypack' (Rondeau *et al.* 2012). Shared gamma frailty models consisted of three components: a frailty with a gamma probability distribution, a baseline hazard function, and a term modeling the influence of observed covariates that are conditionally independent given the frailty. Following Rondeau *et al.* (2012), we let T_{ij} denote the grouped event times under study, with the j-th ($j = 1, \ldots, n_i$) individual stem belonging to the i-th plot ($i = 1,\ldots, G$). The hazard function, which is the instantaneous risk of mortality at time t conditional on surviving until t or longer, for the shared frailty model is,

$$\lambda_{ij}(t|\nu_i) = \nu_i \lambda_0(t) \exp\left(\beta^T X_{ij}\right) = \nu_i \lambda_{ij}(t),$$

where $\lambda_0(t)$ is the baseline hazard function, X_{ij} is the covariate vector associated with the vector of regression parameters β, and v_i is the random effect associated with the i-th group. The model assumes that the v_i are independently and identically distributed (i.i.d.) from a gamma distribution with $\mathbf{E}(v_i) = 1$ and $\mathbf{Var}(v_i) = \theta$, i.e., $v_i \sim \Gamma\left(\frac{1}{\theta}, \frac{1}{\theta}\right)$. To incorporate time-dependent covariates in our analyses (i.e., bay laurel density and the three climate variables), we used the "counting process" data format (Kleinbaum and Klein 2012), whereby multiple observations correspond to the same stem monitored through time. Using this method, an individual stem's total at-risk follow-up time is subdivided into smaller time intervals providing a way for values of variables to change from year to year for the same individual.

The method of estimation used to obtain the parameter coefficients in the R-package "frailtypack" is the maximization of the penalized loglikelihood, which entails a smooth estimation of the baseline hazard function using an approximation by splines (controlling the trade-off between the data fit and function smoothness) (Rondeau *et al.* 2003, 2012). An approximate version of likelihood cross-validation criterion (LCV_a) is used to guide selection among a set of candidate models, specifically in regards to the best predictive performance of estimating the hazard function. In semi-parametric models, such as the shared gamma frailty model, LCV_a is approximately equivalent to the AIC criterion, whereby lower values indicate better predictive ability of time to an event (Joly *et al.* 1998, Rondeau *et al.* 2012).

We used a modified Wald test to deduce frailty significance (Rondeau *et al.* 2012), which entails dividing the variance of the frailty term by the corresponding standard error and comparing this value to the critical value for a normal one-sided test. To minimize potential estimation problems arising from multicollinearity, we used a correlation

coefficient threshold of $|r| > 0.60$ for variable inclusion in the model. All numerical variables were standardized to a mean of zero and standard deviation of one in order to eliminate effects from differences in measurement scales on model outcomes.

Results

We monitored 1,201 oak stems distributed across 172 plots for signs of *P. ramorum* infection and mortality. The other 28 randomly located plots were excluded because they did not contain oak hosts. A total of 76 stems were dead upon plot establishment in 2004. Because we could not assess infection status (or species identity in most cases), we excluded these stems from our analysis. Of the remaining 1,125 stems, 732 (65%) were coast live oak, 271 (24%) were black oak, and 122 (11%) were canyon live oak. In addition to being the most abundant oak across the plot network, coast live oak was the third most prevalent species overall (including non-hosts), found within 124 plots. Black oak occurred in 75 plots while canyon live oak occurred in only 19 plots. As of 2011, 151 (21%) coast live oak stems and 35 (13%) black oak stems had been infected by *P. ramorum*. In contrast, infection was not detected for canyon live oak. Background mortality (i.e., stems dying for reasons other than SOD) was similar in coast live oak (n=58) and black oak (n=56). Coast live oak, however, had a significantly greater number of SOD-dead stems (n=49; mean = 0.07) compared to black oak (n=8; mean=0.03) ($t = 2.704$, $p = 0.007$). When analyzing infection and mortality through time, coast live oak exhibited a continual increase in the number of stems becoming infected by *P. ramorum* as well as those dying following infection, whereas both disease metrics were less pronounced in black oak (Figure 2). Coast live oak had a greater number of

large stems (in terms of DBH) compared to black oak, and in both species larger stems were more prone to infection than smaller stems (Figure 3).

Nine plots were omitted from the survival analyses because they did not contain coast live oak or black oak (i.e., they only included canyon live oak). Within the remaining plots (n=163), the number of coast live oak and black oak stems per plot ranged from 1–29 (mean=6.2, median=5), and the number of infected stems ranged from 1–16 (mean=2.4, median=2). A total of 54 woody plant species was found across the entire plot network during the 2004 vegetation survey; Figure S1). In oak plots, the average number of woody plant species was 7.6 (median=7) and ranged from 2–17. The two least biologically diverse plots, in terms of species richness, each contained only coast live oak and bay laurel. California bay laurel was the most prevalent species across the entire plot network, distributed across 180 plots, of which 141 contained coast live oak or black oak. The number of bay laurel stems in the oak host plots ranged from 0–68 (mean=12, median=8); 22 plots did not contain this highly competent host.

Average cumulative rainfall during the rainy seasons of 2004–2011 ranged between 84.12 and 329.48 mm per year, while average minimum temperature ranged between 3.51 and 7.39°C (Figure 3.4). Interannual patterns revealed that the study region experienced above average precipitation levels in 2003–05, with an especially wet rainy season in 2006. In contrast, 2007–09 marked a significant drought period, with precipitation levels for 2010 returning to average conditions. Average maximum temperature was omitted from the survival analysis models due to high correlation with precipitation across years.

Shared gamma frailty models

Survival analysis models were partitioned into four levels: 1) individual effects, 2) community effects, 3) landscape effects, and 4) full models parameterized with significant covariates from each nested scale of disease-environment interactions (Table 1). Because climate data were not available for 2011 (i.e., the PRISM data covered 1981–2010), we only included data from 2004–10 in our models, resulting in the omission of four oak infection events from the spring of 2011 (out of 186 in total). When multi-year effects of climate conditions (i.e., average rainy season precipitation and minimum temperature) on oak infection risk were examined across the four temporal extents, average conditions during the current and previous year had the greatest predictive power of oak infection risk across the 7-year study period (results not shown), and as such, these covariates were included in further analysis. Across all models, the variance of the frailty term was significant, implying greater unobserved heterogeneity in infection risk between plots and higher correlation of hazard risks for oaks within the same plot.

In Table 1, the estimated coefficients give the linear additive effects of covariates on the log-hazard scale, and are interpreted as a relative infection risk at the plot-level conditional on the frailty. Although the signs of the coefficients are simple to interpret (e.g., larger DBH increases infection risk), the magnitudes of the effects are not easily translated. In contrast, the exponentiated coefficients, referred to as hazard ratios, are more intuitive in that they are interpreted as a proportional shift in the hazard function due to a unit change in the associated covariate (noting that we standardized all numerical variables and thus coefficients are expressed in units of standard deviation). Similar to an odds ratio in logistic

regression, a hazard ratio of 1 (or a 95% confidence interval containing 1) indicates that there is no measurable effect on infection risk from the covariate (Kleinbaum and Klein 2012). In survival analysis models without a random effect, the parameters describe the population level relative risk. In our frailty models, however, the parameters have a plot-level relative risk interpretation, in which the hazard ratio refers to comparisons within plots where individual stems share the same frailty (Wienke 2010).

The full model, constructed using only significant covariates from the three nested models, had the best predictive performance of estimating the hazard risk of oak infection, based on having the smallest LCV_a score (Table 1 a-d). Two significant predictors ($p \leq 0.05$) occurred at the individual level, one at the community level and two at the landscape level. Specifically, we found that species identity, stem size, species richness, and the two climate variables were strong indicators of oak infection risk. After accounting for unobserved heterogeneity at the plot-level, the model revealed that coast live oak is at greater risk of infection compared to black oak, and that larger stems of both species are particularly susceptible to disease. Specifically, black oak had a reduced hazard risk compared to coast live oak by a factor 0.52, that is, by 100(1-0.52) =48 percent. Likewise, for every one standard deviation unit increase in the stem size of both species, an individual's risk of infection increases by 83%, i.e., 100(1.83-1). In regards to community-level influences, the model revealed a negative relationship between disease risk and plant species richness (i.e., a dilution effect), in which a one unit standard deviation increase in the richness of a plot reduces an individual stem's hazard by 32%. Despite interannual fluctuations in temperature and rainfall across the study region, our models revealed that warmer than average minimum

temperatures and wetter than average conditions during the current and previous rainy season play a strong role in increasing the hazard rate of susceptible oak hosts. Specifically, a one unit standard deviation increase in average precipitation and minimum temperature across this time period corresponds to more than a doubling in infection risk. Although bay laurel density and potential solar irradiation were significant predictors of infection risk in their respective nested model, these two covariates were only marginally significant in the full model.

Discussion

Non-indigenous forest pathogens continue to increase in number with growing recognition of their ability to act as important disturbance agents and determinants of complex ecosystem trajectories (Holdenrieder et al. 2004, Loo 2009, Aukema et al. 2010). Despite the often detrimental consequences exotic diseases can have on native communities (Shearer et al. 2009), there remains a critical lack of information concerning the relative importance and generality of the diverse factors affecting wildland epidemics. Long-term ecological research—conducted across spatial extents likely to capture forest disease processes—is needed to identify the factors that influence whether or not disease will cause extinctions, and which populations or species will persist (Cobb et al. 2012). Diseases of widespread temperate trees such as chestnut blight, Dutch elm disease and beech bark disease have precipitated regional population declines by altering canopy distribution and biomass rather than causing extinction of their hosts (Swinton and Gilligan 1996, Garnas et al. 2011). This pattern suggests that understanding pathogen-caused reductions in host population size and biomass, and subsequent changes in community structure of widespread forest trees are more

essential than forecasting host extinction risk per se, especially for pathogens that cause broad-scale shifts in size-class distributions (Cobb et al. 2012).

In oak woodlands of coastal California, coast live oak is often the dominant tree (defined by highest proportions of basal area and canopy cover compared to co-occurring species), reaching upwards of 10–25 m in height and commonly living up to 250 years (Davidson et al. 2005, Brown and Allen-Diaz 2009). We found that coast live oak—the third most prevalent species across the study area—is highly susceptible to *P. ramorum* infection and disease-induced mortality. Across the 8-year study period, we observed a steady increase in the number of coast live oak becoming infected and dying following infection, signaling the potential for this emerging forest disease to dramatically change oak woodlands through selective removal of this keystone species. Previous studies documenting SOD impacts in coast live oak reported infection rates as high as $5.0\%^{-1}$ for coast live oak, with annual mortality rates approximating $3\text{-}6\%^{-1}$ in highly impacted stands (Brown and Allen-Diaz 2009, McPherson et al. 2010). We found that the number of infected black oak and those dying following infection also increased over time, albeit to a lesser degree. In contrast, we did not detect *P. ramorum* symptoms on canyon live oak. Unlike coast live oak and black oak, which develop obvious infection symptoms characterized by bleeding cankers, canyon live oak exhibits a different pattern of symptom expression, making it difficult to identify and document *P. ramorum* cankers in this species (Murphy and Rizzo 2003, Aram et al. 2011). Symptom information gleaned from inoculation studies have successfully isolated *P. ramorum* from several naturally infected canyon live oak, but isolation efficiency has remained very low, suggesting that many infected canyon live oak do not bleed and cankers

in these cryptically infected trees cannot be seen until they are colonized by secondary organisms (Murphy and Rizzo 2003, Aram et al. 2011).

Given the potential impacts of SOD on coast live oak and black oak populations, it is critical that we obtain a deeper understanding of the factors mediating epidemic dynamics in this wildland pathogen invasion. This information is needed for improved forecasts of population decline and changes in host biomass, and for management efforts aimed at controlling the overall impact of this pathogen invasion. However, when dealing with natural ecosystems, it is usually the case that not all variables affecting epidemic processes can be measured or even observed (e.g., demographic stochasticity). In survival analysis, failing to account for such latent heterogeneity can lead to biased estimates of the underlying hazard and survival functions (Wienke 2010). In all shared gamma frailty models we found that the variance of the plot-level frailty term was significantly different from zero, indicating that oaks occurring within the same plot share underlying, yet unknown, risk factors. This unobserved heterogeneity could arise from many sources, including differences in invasion history or land-use practices (Meentemeyer et al. 2008b). After adjusting for frailties, our models revealed the collective importance of factors at the individual, community and landscape scale in mediating oak infection risk. We found that larger coast live oak are particularly susceptible to SOD, and that warmer and wetter conditions increase infection risk, while species diversity has a buffering effect against disease.

Ecosystems may be fundamentally altered when abundant tree species are functionally eliminated, as occurred with American chestnut and chestnut blight, in which cycles of re-sprouting following death of the main stem followed by subsequent blight-

related death of sprouts have caused regional population declines of this once dominant tree species in eastern North American forests (Davelos and Jarosz 2004). In contrast, pathogen impacts may be more subtle but still significant and long lasting when pathogens cause broad-scale shifts in size-class distributions (Loo 2009, Cobb et al. 2012). Previous studies on SOD have shown that only larger oaks exhibit symptoms, whereas infection of smaller oak trees has not been documented in nature (Davidson et al. 2005, McPherson et al. 2010). We found a significant and strong positive relationship between tree size and infection risk for both coast live oak and black oak. McPherson et al. (2010) also reported that larger coast live oaks were more likely to become infected with *P. ramorum*, yet they did not find a significant relationship in black oak. Positive correlations between tree size and susceptibility to infection have been documented in other forest diseases, including comandra blister rust (*Cronartium comandrae*) on lodgepole pine (Jacobi et al. 1993) and white pine blister rust (*Cronartium ribicola*) on white pine species (Smith and Hoffman 2001). The mechanisms underlying these relationships likely vary among pathosystems and across site conditions. Nonetheless, they could potentially arise from direct effects whereby larger-sized hosts support more pathogens through effects of size per se, or indirectly through traits correlated with plant size, such as the diversity of habitats embodied by the host or the longevity of individuals and their tissues (Smith and Hoffman 2001, Miller 2012). Across the geographic distribution of *P. ramorum* in California and Oregon, regional-scale declines of large coast live oak and black oak will likely result in substantial structural and functional changes to coastal forest ecosystems (Brown and Allen-Diaz 2009, Metz et al. 2012). For instance, Cobb et al. (2012) analyzed structural changes to redwood-tanoak forests following *P. ramorum*

invasion and found that pathogen-invaded stands had smaller average tanoak tree size and higher proportions of large dead tanoak trees compared to uninvaded stands.

Species are embedded within community assemblages, and as such, between-species interactions likely play a key role in disease dynamics of multihost systems. Theoretically, the level of biodiversity in a community might amplify or dilute disease risk by changing the relative abundance of competent hosts (Keesing et al. 2006, Ostfeld and Keesing 2012). Our current understanding of diversity-disease risk relationships in plant pathosystems hinges primarily on experimentally-manipulated communities (Mitchell et al. 2002, Roscher et al. 2007, Pagan et al. 2012), with surprisingly little attention given to wildland forest pathogens (Pautasso et al. 2005, Haas et al. 2011). Due to the incredibly broad host range of *P. ramorum*, the SOD pathosystem could potentially exhibit an amplification effect, whereby biologically diverse forests experience 'amplified' disease risk due to greater host species diversity, or in contrast, a dilution effect in which greater species diversity reduces disease risk by 'diluting' the impact of highly-competent hosts (i.e., bay laurel and tanoak). Based on a large-scale field survey of coastal forests in California, Haas et al. (2011) found a negative relationship between SOD disease incidence and plant species diversity (i.e., a dilution effect), which held after accounting for the potentially confounding effects of host density and landscape heterogeneity. Yet, the study used a static snapshot of disease distribution and environmental conditions, preventing an examination of how diversity-disease relationships change through future stages of disease progression. In our paper, we examined the role of species diversity on oak infection risk across a 7-year period, while accounting for

unobserved heterogeneity and fluctuating environmental conditions through time, and again found a dilution effect occurring in the *P. ramorum* pathosystem.

Density-dependent models of transmission are often used to describe pathogens spread through environmentally transmitted propagules (Burdon and Chilvers 1982). One density-dependent mechanism that may be underlying diversity-disease relationships in the *P. ramorum* pathosystem is 'encounter reduction' (Keesing et al. 2006), whereby the inclusion of less competent hosts in the community interfere with transmission pathways between competent hosts and oak hosts (Haas et al. 2011). For example, less competent hosts may function as physical barriers to pathogen dispersal by intercepting inoculum transmitted through space, or by increasing the distance inoculum must traverse between competent hosts. A second mechanism that may be occurring in the *P. ramorum* pathosystem is 'susceptible host regulation' (Keesing et al. 2006), through which interspecific competition for limiting resources constrains the abundance of competent hosts in biologically diverse forests. In communities with a single highly-competent host that is also the community dominant, pathogen transmission may be closely tied to population fluctuations of this species (Ostfeld and Keesing 2000). In the SOD pathosystem, many previous studies have found that the density, abundance and/or dominance of bay laurel is positively correlated with the overall disease intensity in a region (Cushman and Meentemeyer 2008, Cobb et al. 2010, Haas et al. 2011). In our study, although bay laurel was the most abundant and widespread species across the study area, we did not find a strong relationship (i.e., $p \leq 0.05$) between bay density and oak infection risk, after accounting for other environmental covariates and the frailty term. The transmission biology of *P. ramorum* is complex—

characterized by over 130 host species in over 75 genera exhibiting vastly asymmetric competency—and it may be that the infection dynamics governing oaks are not tightly coupled to the numerical dynamics of a single competent host, but rather respond to the joint population densities of several host species. Another research area to explore is "infectiousness" versus "contagiousness" of *P. ramorum*, in which oaks may be more likely to become infected only under strict environmental conditions, such as rain-splashed inoculum hitting the right spot (e.g., bark fissure) on a large oak trees during ideal weather conditions (e.g., prolonged rain, cool temperatures).

Because natural plant communities are nested within heterogeneous landscapes, we should expect that processes occurring at these broader spatial extents play a key role in disease dynamics at local scales (Ostfeld et al. 2005, Johnson and Haddad 2011, Meentemeyer et al. 2012). In the SOD pathosystem, the area, density and host composition of woodlands may be important sources of landscape heterogeneity capable of mediating epidemic dynamics, as greater amounts of pathogen inoculum have been shown to occur in forests with high landscape connectivity and high abundance of foliar host vegetation (Meentemeyer et al. 2008b, Ellis et al. 2010). For instance, Condeso and Meentemeyer (2007) used high resolution maps of host habitat across a 20 km^2 region of California and found that bay laurel disease severity was greater in plots surrounded by a higher area of contiguous host habitat within increasing spatial extent from 50-200 m. In our study, however, we did not find evidence that progression of oak infection was influenced by the amount of host habitat surrounding field plots. We used Euclidean distance in our measurements of host habitat connectivity, and it may be that more biologically accurate

measurements (e.g., using least-cost path analysis; Ellis et al. 2010) have better predictive power of the role of landscape connectivity in governing infection dynamics of wildland *P. ramorum* pathosystems.

Although we are making critical strides in obtaining a better understanding of natural plant-pathogen interactions (Gilbert 2002, Alexander 2010, Burdon and Thrall 2013), deeper insight into real-world disease dynamics under actual field conditions will require that we simultaneously examine the role of extrinsic abiotic drivers on the invasion process. Moisture and temperature strongly affect plant disease development by regulating pathogen survival, growth and reproductive rate, and in many cases the probability of spread at regional or larger scales (Davidson et al. 2011, Garrett et al. 2011, Kliejunas 2011). Moreover, altered precipitation and temperature regimes resulting from climate change are predicted to directly affect plant disease development, as well as multiple host plant attributes including growth, survival, susceptibility and host defense mechanisms, as these phenomena are all closely tied to these parameters (e.g. chronic leaf wetness, relative humidity) (Davidson et al. 2008, Alexander 2010, Eastburn et al. 2011). In areas where cold seasons become warmer and shorter with less frequent and extreme cold spells, we might expect this to enhance the ability of pathogens to survive the winter, altering both their annual cycles of transmission intensity and their latitudinal and altitudinal distributions (Marcais et al. 2004, Kliejunas 2011, Rodo et al. 2013). For example, in Central Europe increased mean winter temperatures, seasonal precipitation shifts from summer into winter, and heavier rainfall events have amplified the risk and impact from several species of *Phytophthora* root rot diseases, increasing the instability and vulnerability of forest ecosystems throughout the region (Sturrock et al. 2011).

For much of California, regional climate change models reach consensus in that temperatures will increase substantially, although models differ considerably in their projections of precipitation (Kliejunas 2011). There is, however, no evidence that the Mediterranean pattern of precipitation will change and all models indicate that the vast majority of precipitation will continue to fall during the winter months (Kliejunas 2011). In our study, we found that warmer and wetter average conditions during the current and previous year's rainy season substantially increased infection risk in oaks. The 1-yr lag effect we found supports findings from other studies on the SOD pathosystem that suggest that two wet years in succession lead to more significant outbreaks of disease in bay laurel because of cumulative effects linked to higher inoculum levels at the end of the first year's wet season followed by a higher rate of pathogen survival during a shorter dry season in between the two wet years (Davidson et al. 2008, 2011). Sporangia production in bay laurel leaves has been shown to substantially decrease during hot, dry summer months, via abscission of infected leaves and/or death and deep dormancy of the pathogen in the remaining leaves (Davidson et al. 2011). These findings are consistent with other studies documenting that *Phytophthora* species generally require very high moisture levels nearing 100% humidity for sporangia production (Erwin and Ribeiro 1996, Marcais et al. 2004). Although our results suggest that climate change will affect forest health in locations with *P. ramorum*, there is much uncertainty regarding the degree of climate change that will occur, pathogen biology under changing climate, the effects of changing climate directly on the host, and the interactions between the pathogen, host and climate.

Our study is one of a growing number that documents the destructive impacts of emerging forest diseases to native community structure, function and services (Ellison et al. 2005, Lovett et al. 2006, Aukema et al. 2010). In the past century, North American forests have suffered devastating effects from introduced diseases including chestnut blight, Dutch elm disease, pitch canker of Monterey pine, beech bark disease, white pine blister rust, and now more recently, sudden oak death (Gilbert 2002, Holdenrieder et al. 2004, Aukema et al. 2010). The increasing introduction of non-native plant pathogens around the world will likely trigger destabilizing effects in forest ecosystems through the selective mortality of abundant tree species or species that play a foundational role in ecosystem functioning (Ellison et al. 2005, Lovett et al. 2006). Since the discovery of *P. ramorum* in central California in the mid-1990s, potentially millions of trees have died throughout the pathogens range (Meentemeyer et al. 2008c), with further increases in disease-induced mortality likely to occur as the pathogen expands its geographic range locally within infested regions and beyond into previously uninfested areas of natural ecosystems in California and Oregon (Meentemeyer et al. 2011). The low cost of infection in some host, such as bay laurel and redwood may facilitate long-term pathogen persistence in space and time and prevent periodic pathogen fade-outs based on the density of susceptible hosts, initiating a shift to greater dominance of these species in the future through parasite-mediated competition (Cobb et al. 2010).

As with the case of chestnut blight, it may be that coast live oak and black oak are capable of persisting in disease-impacted forests via vegetative reproduction, but overstory trees may be eliminated or greatly reduced in abundance (Davelos and Jarosz 2004, Cobb et al. 2012). As the *P. ramorum* epidemic continues, the effects are likely to ramify throughout

impacted forests and have consequences for the numerous biota with which they are associated. This is particularly significant because mixed evergreen forests and oak woodlands provide some of the most ecologically diverse habitats in California. Moreover, coast live oak is dominant in many forests and loss of this keystone species will result in the diminishment of habitat and food resources for wildlife, increased fire danger, accelerated runoff and associated soil erosion, and changes to the structure and composition of plant, animal, and microbial communities (Rizzo and Garbelotto 2003, Rizzo et al. 2005, Monahan and Koenig 2006). Our study provides insight into key environmental factors that can determine the impact of a plant pathogen on a community of co-occurring hosts, and provides an empirical basis for assessing risk of extinction from disease. Comparative long-term ecological studies across disease systems are needed to better understand how forests will respond to ongoing pest and pathogen introductions, in conjunction with additional stressors resulting from global change drivers.

CHAPTER 4. DATA-INTEGRATION FOR SPATIAL ESTIMATION OF A LARGE-SCALE, ENVIRONMENTALLY HETEROGENEOUS DISEASE INVASION

Abstract

Over the past few decades, a growing number of nonnative pathogens have invaded forest ecosystems worldwide, substantially altering ecosystem structure and function. Although spatially-explicit probabilistic risk models have provided valuable insight into the drivers of pathogen spread and establishment, fewer studies on emerging forest pathogens have provided large-scale quantitative estimates of the actual number of disease-impacted trees. Analytical complications arising from geographic disequilibrium of emerging pathogens challenge our ability to spatially estimate disease impacts over large-scale, heterogeneous landscapes. Sudden oak death, caused by the nonnative pathogen *Phytophthora ramorum*, is an emerging forest disease that has reached epidemic levels in coastal forests of California and Oregon, killing large but unknown numbers of oak and tanoak trees. In response to the urgent need to examine regional to continental impacts from sudden oak death, we conducted the first study to quantify the number of diseased trees of key host species over the entire geographic distribution of *P. ramorum*, integrating data from diverse sources including long-term disease monitoring networks, published findings from previous sudden oak death research, remotely-derived geospatial data and government and citizen science monitoring data. Spatial estimates of the abundance of disease-impacted trees varied by ecoregion and state, reflecting geographical differences in host distribution. After examining detection bias in disease surveys, we estimated 29.4–44.5 million (1.6–2.5%) disease-impacted tanoak trees, 1.9–3.3 million (0.4–0.7%) coast live oak, and 0.27–1.1 million (0.04–0.17%) black

oak trees across each species geographic range. For bay laurel, the most competent host species largely responsible for driving disease spread, we estimated 91.4 million (21%) infected trees, occurring in regions that overlap oak and tanoak populations. These results can inform landscape- to regional-scale models of sudden oak death disease dynamics and guide regulatory policy decisions regarding ecosystem impacts due to widespread tree mortality.

Introduction

Humans are causing unprecedented alterations to forest ecosystems around the globe through habitat conversion, over-consumption of resources, and introductions of pests and pathogens (Ellison et al. 2005, Lovett et al. 2006). Over the last century, the forests of North America have undergone repeated introductions of exotic pathogens (Rizzo et al. 2002, Garnas et al. 2011, Hatala et al. 2011), while more continue to invade with unknown long-term impacts on forest ecosystems (Lovett et al. 2006, Loo 2009). As such, the economic and ecological consequences of the introduction of nonnative forest pathogens has presented a tremendous challenge for resource managers (Pimentel et al. 2005, Metz et al. 2011). Spatially-explicit quantitative predictions of host infection and mortality are needed to identify where in the landscape and to what extent emerging diseases are impacting ecosystem function and community structure (Swinton and Gilligan 1996, Cobb et al. 2012). To date, large-scale models of forest disease have relied mostly on predicting impacts based on risk, using probabilistic modeling of pathogen occurrence (i.e., presence/absence) (Meentemeyer et al. 2004, Ellis et al. 2010), rather than providing quantitative estimates of the actual number of disease-impacted trees (Meentemeyer et al. 2008c, Lamsal et al. 2011). Obtaining such

estimates for wildland forest pathogens, defined as those inhabiting natural forests that are not artificially created (i.e., planted, farmed, or intensively managed), creates additional challenges due to the multiple time scales of epidemic invasion occurring across expansive, and often remote, geographic areas (Holdenrieder et al. 2004, Meentemeyer et al. 2012). Nonetheless, accurate predictions of the 'when and where' of large-scale tree mortality from emerging diseases are urgently needed to inform forest management and policy decisions (Gilligan 2002, Holmes et al. 2009).

The emerging infectious disease sudden oak death, caused by the exotic plant pathogen *Phytophthora ramorum*, is an example of a destructive biological invasion that threatens regional-scale mortality of several ecologically important tree species including tanoak (*Neolithocarpus densiflorus*), California black oak (*Quercus kelloggii*), canyon live oak (*Quercus chrysolepis*), coast live oak (*Quercus agrifolia*) and Shreve's oak (*Quercus parvula var. shrevei*) in western North American forests (Rizzo et al. 2005, Meentemeyer et al. 2011). Extensive tree mortality of tanoak was first noticed in the mid-1990s in the San Francisco Bay Area and *P. ramorum* was later identified as the causal agent in 2000 (Rizzo et al. 2002). Since then, sudden oak death has reached epidemic levels in coastal forests of California and Oregon, killing large but unknown numbers of oak and tanoak trees (Meentemeyer et al. 2008c, Brown and Allen-Diaz 2009, McPherson et al. 2010). The geographic range of *P. ramorum* in natural ecosystems extends approximately 800 km from a southern extent in coastal forests of the Big Sur ecoregion in California to an isolated northern outbreak in southwestern Oregon (Meentemeyer et al. 2011). The disease is thought to be primarily transported via infective spores formed on the leaves of California bay laurel

(*Umbellularia californica*) and tanoak (Davidson et al. 2005, 2008). The potential for wide-ranging and long-lasting impacts to forest ecosystems of western North America from this epidemic is high given that *P. ramorum* can infect over 130 species of trees, shrubs, herbs, and ferns throughout several coastal forest habitat types (Rizzo et al. 2005, Metz et al. 2012).

Regional spread risk models predict that *P. ramorum* could undergo considerable range expansion over the next 20 years due to high host contagion and suitable weather conditions in California and Oregon (Meentemeyer et al. 2004, 2011, Vaclavik and Meentemeyer 2009, Filipe et al. 2012). Collectively, these risk-based studies—focusing on pathogen presence/absence—have predicted the actual and potential distribution of *P. ramorum* by relating geo-located observations of pathogen occurrence to environmental variables thought to contribute to pathogen survival and propagation. Other studies have quantified the impact of sudden oak death on actual mortality estimates of oak and tanoak populations at spatial scales ranging from local (Brown and Allen-Diaz 2009, Cobb et al. 2010, McPherson et al. 2010, Ramage et al. 2011) to regional (Meentemeyer et al. 2008c, Davis et al. 2010). Although these quantitative estimates have provided insight into the spatial distribution of mortality over defined ecological regions, there has been no quantification of host mortality across the entire geographic range of *P. ramorum*. To date, our ability to forecast large-scale numbers of disease-impacted hosts has been impeded by a lack of spatially-explicit data on the abundance of host populations. Recently, Lamsal et al. (2011) quantified and mapped the spatial distribution of the five key *P. ramorum* host species (tanoak, coast live oak, canyon live oak, California black oak and bay laurel) across California and Oregon by integrating multiple sources of vegetation data, assembled from

sparsely distributed forest inventory and analysis (FIA) plots and more densely distributed plots for monitoring sudden oak death. These spatially-explicit estimates of host density (trees ha^{-1}) provide the opportunity to predict the actual numbers of infected and dead trees impacted by sudden oak death across the geographic range of *P. ramorum*. This information is critically needed to prioritize landscape- to regional-scale management strategies for prevention and control of this emerging forest disease.

Obtaining reliable estimates of the number of disease-impacted trees across broad spatial extents is challenged by the presence of geographic disequilibrium inherent in the distribution of emerging disease at different stages of invasion (Sutherst and Bourne 2009, Meentemeyer et al. 2012, Rodriguez-Rey et al. 2013). In the sudden oak death pathosystem, Haas et al. (2011) analyzed diversity-disease risk relationships in the Big Sur ecoregion (the southernmost range of the pathogen's distribution) and had to accommodate zero-inflation and spatial autocorrelation in the observational data (280 plots spanning 100-km), arising from the pathogen's patchy distribution across the landscape. Despite growing impacts of emerging pathogens on forest ecosystems, financial and logistical restraints continue to limit our ability to intensively monitor hosts over large geographic regions and across meaningful temporal scales (Holdenrieder et al. 2004, Hanks et al. 2011, Meentemeyer et al. 2012, Dillon et al. 2014). As such, the spatial distribution of observations, extent of the study area, sample size, evenness of the sample (species prevalence), disease detectability, and temporal resolution of the observations are often compromised and should be carefully examined when conducting large-scale spatial predictions (Stockwell and Peterson 2002, Peters et al. 2004, Franklin 2010). Analyses that integrate data from diverse sources—including published

studies, long-term observatory sites, freely-accessible geospatial data, and publicly available government and citizen science data—may help mitigate some of these data limitations.

Here, we predict the spatial distribution and magnitude of sudden oak death impacts using data from four long-term disease monitoring networks in conjunction with spatially-explicit estimates of host density from Lamsal et al. (2011), remotely-derived geospatial data capturing landscape heterogeneity and climatic variability, and government and citizen science disease monitoring data. Specifically, we examine (1) the number and prevalence of disease-impacted trees across the entire range of *P. ramorum*, and (2) the distribution of disease impacts by state and ecoregion. We also examine the influence of detection bias in attributing tree mortality to sudden oak death on our spatial predictions of disease impacts. This is the first study to provide realistic estimates of the number of trees infected or dead from sudden oak death across California and Oregon. This information is critically needed to manage disease spread and minimize the impacts of tree mortality on biodiversity, nutrient cycling, and fire risk.

Materials and methods

Study system

Our study focuses on five key *P. ramorum* host species including three oak hosts (*Quercus* spp.) that can develop lethal stem cankers upon infection (coast live oak, California black oak, and canyon live oak), California bay laurel which develops nonlethal sporulation-supporting foliar infections, and tanoak which can develop both lethal main-stem and twig cankers while sustaining inoculum-producing leaf infections (Rizzo et al. 2002). Although Shreve's oak (*Q. parvula*) is an additional canker host found in California, this recently

recognized species is not as geographically widespread as the other hosts and is difficult to distinguish from coast live oak (Lamsal et al. 2011). For these reasons, we have treated coast live oak and Shreve's oak as a single host. Collectively, these species cover a broad region of tremendous physiographic variability across California and Oregon with diverse topoclimatic conditions and complex disturbance regimes (Ohmann et al. 2007). Forested landscapes containing *P. ramorum* hosts occur from sea level to 3862 m in elevation. The region has Mediterranean-type climatic conditions with cool wet-winters and warm dry summers that exhibit substantial variability in average annual precipitation (17–458 cm) and average temperature (minimum = -5.7 to 12.7 °C; maximum = 5.1 to 29.8 °C) depending on elevation, latitude, and proximity to the coast (Daly et al. 2001).

Although numerous species can develop *P. ramorum* foliar infections, bay laurel and tanoak are the two most competent, inoculum-producing hosts, considered critical for natural spread of the pathogen between hosts and across the landscape (Davidson et al. 2005, 2008). In contrast, infections resulting in main-stem cankers on oaks and tanoak have not been shown to transmit the pathogen in the field (Davidson et al. 2005). *P. ramorum* inoculum produced on host tissue may be spread or dispersed by various means. Local dispersal occurs primarily through rain splash of sporangia, intermediate dispersal is thought to occur via turbulent air during storm events, and rare long-distance dispersal occurs primarily through the movement of infected plant material moved in trade; movement of contaminated soil or spread in watercourses can also result in long-distance dispersal (see Kliejunas 2010 for a review). Sporulation is most active during warm, wet springs (Davidson et al. 2005, 2008), whereby epidemic dynamics reflect distinct signatures of climatic variation on multiple time

scales (Huberli et al. 2012, Haas et al. *in prep*). Host species distribution across California and Oregon is spatially variable and highly heterogeneous at local scales (Meentemeyer et al. 2011). Bay laurel is a common component of redwood, oak, and mixed evergreen forests in coastal habitats stretching from southern California to southwestern Oregon. Tanoak ranges from southern California to southwestern Oregon with a disjunct population in the northern foothills of the Sierra Nevada, reaching its greatest density and contagion in Del Norte and Humboldt counties in northern California (Meentemeyer et al. 2004, Rizzo et al. 2005). Bay laurel and tanoak tend to be more abundant within the coastal fog belt although bay laurel often also occurs in dryer, hotter inland forests. Coast live oak and California black oak have a high degree of overlap with bay laurel, resulting in considerable decline of these two species in infected regions (Kelly and Meentemeyer 2002, Rizzo et al. 2005, Brown and Allen-Diaz 2009).

Plot network surveys

We integrated plot data from four long-term monitoring networks (n=815 plots) along coastal California—from Monterey Co. in the south to Del Norte, Co. in the north—that were established between 2000 and 2007 to monitor the spread and impacts of sudden oak death at local to landscape scales (Figure 4.1). The "North Coast" network consisted of 318 plots (500 m^2 each), spanning 677 km southwards from Monterey Co. northwards to Del Norte Co. (Figure 4.1-A; Maloney et al. 2005). The "Big Sur" network, consisting of 264 plots (500 m^2 each), is distributed across an approximately 80,000 ha region spanning 100 km along the Pacific slope of the Santa Lucia range (Figure 4.1-B; Haas et al. 2011). The "Sonoma" plot network encompasses 198 plots (225 m^2 each) within a 275 km^2 region in eastern Sonoma

Co. (Figure 4.1-C; Haas et al., *in prep*). Finally, we used a subset of 35 plots (200 m^2 each) from the "Phytosphere" research network to obtain sampling coverage in the San Francisco Bay area, ensuring that all plots were a minimum distance of 50 m from their nearest neighbor. The Phytosphere plot survey protocol does not entail monitoring individual bay laurel trees for disease status. As such, bay laurel models only include data from the other three plot networks.

The frequency of follow-up plot surveys varied both within and among networks. The most recent sampling dates for the North Coast plots ranged from 2004-2012, in which 147 plots (46%) were last sampled in 2004. In the Big Sur network, plots were last surveyed between 2006 and 2011, whereas all Sonoma plots were last sampled in 2011 and Phytosphere plots in 2012. Preliminary analyses revealed improved predictive performance when the oldest 2004 survey were omitted (results now shown). As such, we only include data from 2005-12 in our analyses (n=668 plots), using survey information from the most recent plot visit dates across the four networks. We refrained from omitting additional data from later years (e.g., 2005-06) due to sample size limitations. During plot visits, stems $\geq$ 1 cm were tagged and measured for diameter at breast height (1.35 m; dbh), identified to species, and assessed for health status (alive/dead) and *P. ramorum* infection (symptomatic/non-symptomatic). The presence of *P. ramorum* symptoms on a given host led to a "disease-impacted" status only if the pathogen had been previously confirmed to occur in the plot based on standard laboratory testing (Vettraino et al. 2009). Tree mortality (defined as the death of all aboveground tissue) was assessed based on an examination of cambial damage to the basal tree trunk and the drying and abscission of foliage. Trees were

considered dead due to sudden oak death if they died following a previously documented *P. ramorum* infection.

Environmental heterogeneity

Six spatial covariates at a resolution of 1 ha (100 m cell) were selected on the basis of their potential predictive power in driving disease patterns across the landscape, grouped into three categories: climate, topography, and biotic interactions (Table 4.1). A 1 ha cell size was chosen to match the spatial resolution of host density estimates mapped in Lamsal et al. (2011), and was considered a trade-off between finer-scale spatial resolution and computational feasibility. Within a geographic information system (GIS), we used a 30 m USGS National Elevation Dataset (DEM) to derive the elevation of each gridded hectare via cubic convolution resampling. Using this up-scaled DEM, we calculated two topographic variables: (i) topographic moisture index (TMI)—computed as the natural log of the ratio between upslope drainage area and local slope gradient of a given grid cell (Moore et al. 1991)—was used to characterize topographic effects of potential soil moisture distribution, and (ii) potential solar insolation (PSI) as the mean incoming solar irradiation at the spring equinox based upon the cosine of illumination on slope algorithm (Dubayah 1994). Climate variation from 1990-2010 was described using rainy season (Dec-May) average precipitation and minimum and maximum temperature, based on 30-year average annual values (1981–2010) downscaled to 1 ha resolution from the PRISM model (Daly et al. 2001, Flint and Flint 2012). Finally, we included competent host density (trees ha^{-1}) as a covariate, obtained by summing the spatially-aligned bay laurel and tanoak density estimates produced by Lamsal et al. (2011).

Dispersal constraints

To incorporate effects of pathogen dispersal constraints on the spatial distribution of diseased hosts, which can have important analytical repercussions in the presence of geographic disequilibrium, we quantified the potential "force of infection" for each hectare across our predictive domain (Meentemeyer et al. 2008a). Force of infection (F_i) was calculated as a negative exponential dispersal kernel:

$$F_i = \sum_{k=1}^{N} \exp\left(\frac{-d_{ik}}{a}\right)$$

where d_{ik} is the Euclidean distance between each potential source of infection k and target cell i (N is the total number of target cells across the study extent). The parameter a modifies the form of the dispersal kernel where low values of a indicate high dispersal limitation and high values of a indicate low dispersal limitation (Havel et al. 2002, Meentemeyer et al. 2008a). The optimal value of a was selected based upon Akaike Information Criterion separately for each host species. Specifically, we iteratively added a force of infection variable constructed using varied values of a to a generalized linear model that included all six environmental variables, choosing the final a value based on the model with the lowest AIC (Meentemeyer et al. 2008a). We used a negative exponential dispersal kernel because previous research has shown that this kernel adequately describes dispersal characteristics of rain splash dispersed plant pathogens (McCartney and Fitt 1985, Fitt et al. 1989). Geographically-referenced data of all known sites infested with *P. ramorum* as of 2012 (n=3120 ha) were used to create the force of infection covariate. Data came from numerous sources in California including the SOD Blitz program (Kelly and Tuxen 2003), the

California Department of Food and Agriculture, research groups from the University of California at Davis and Berkeley, and from the four sudden oak death monitoring networks. All known positive *P. ramorum* sites in Oregon were provided from the Oregon Department of Forestry. In all cases, *P. ramorum* infection was confirmed using standard laboratory methods (Vettraino et al. 2009).

Modeling the density of disease-impacted hosts

The response variable for all models, "disease prevalence", was defined as the number of trees in a plot that are either alive and infected with *P. ramorum* or dead following previous infection, $y(s)$, divided by the total number of trees for each focal species, $n(s)$, per plot. Because we are modeling binomial proportions, $y(s)/n(s)$, we fit generalized linear models (GLM) with a binomial distribution and logit link function. With this method, the binomial denominators, $n(s)$, are used as weights in the regression. We specified a quasibinomial error distribution to account for overdispersion in the data (i.e., when the observed variance is greater than that of the theoretical model being used to fit the data), which incorporates an empirical scale parameter that causes the model to use standard error estimates that account for the amount of overdispersion (Barton 2013). The cause of tree mortality within infected plots was attributed to sudden oak death only if *P. ramorum* infection was observed on that tree during a previous plot visit. As such, our estimates of disease-induced tree mortality for oak and tanoak are likely conservative (i.e., underestimated). To examine potential detection bias in disease designation of dead trees, we calculated disease prevalence two ways for canker hosts (i.e., all hosts except bay laurel), referred to as the "conservative" and "liberal" methods. In the conservative method, disease prevalence was calculated using the number of

alive, infected trees and those dead following previously-confirmed *P. ramorum* infection during one or more plot surveys. For the liberal approach, we applied a heuristic rule to all dead trees from plots with known *P. ramorum* occurrence, whereby an annual 1% background mortality rate of oak and tanoak (Hunter 1997, Brown and Allen-Diaz 2009, McPherson et al. 2010) across a 5-year period (the time we assumed it would take for dead trees to remain standing following death) was assigned to all trees, resulting in a 5% chance of background mortality and a 95% chance of mortality due to sudden oak death.

To mitigate bias in parameter estimation resulting from geographic disequilibrium of *P. ramorum*, in which plots with suitable environmental conditions for disease are uninvaded due solely to pathogen dispersal constraints and colonization time-lags, we implemented an "exposure" distance-based rule in which plots that were more than 3 km away from a known 'force of infection' site were excluded from analysis. This rule, based on previous sudden oak death research showing that the majority of rare long-distance pathogen dispersal events occur within 3-4 km (Davidson et al. 2005, Hansen et al. 2008, Kliejunas 2010), led to the omission of 145 plots (18%) located in areas in which the pathogen is believed to have not yet colonized (n= 523 remaining plots). The vast majority of these omitted plots occurred in the three northernmost California counties (Mendocino, Humboldt, and Del Norte), south of isolated infection sites in southwestern Oregon.

For all binomial regression models, we used a correlation coefficient threshold of $|r| > 0.60$ for predictor variable inclusion to minimize potential estimation problems arising from multicollinearity. Because rainy season average maximum temperature and precipitation were strongly collinear ($r = -0.71$), we included only rainy season average minimum

temperature and precipitation as the climatic variables in our models. We used the R-package "MuMIn" (Barton 2013) to (i) generate a set of models with all possible combinations of the terms in the 'full' model (i.e., TMI, PSI, rainy season average precipitation and minimum temperature and competent host density), (ii) select the subset of models with delta QAIC < 2 (the quasi-likelihood AIC is a modification of Akaike's Information Criterion for overdispersed data), and (iii) create a final averaged model based on QAIC criterion to use in spatial prediction. Model averaging was implemented in an attempt to avoid selecting a spurious "best" model, as individual model weights (i.e., the relative likelihood of a given model) exhibited small differences. We used the R-package "raster" (Hijmans 2014) to predict the probability of disease prevalence for each hectare across the prediction domain. Each probability raster was then multiplied by host density estimates '*n*' from Lamsal et al. (2011) to produce a final map of the number of disease-impacted trees ha^{-1} ("*np*") across California and Oregon for each of the five host species. Prediction maps were masked to a 4 km buffer around force of infection sites to prevent prediction of disease impacts in areas in which the pathogen has not yet been found. Finally, estimates of disease impacts were summarized by range-wide, state, and ecoregion levels. We used ecoregion boundaries from the US-EPA "Level III Ecoregions" mapping (i.e., the Coast Range, Klamath Mountains, and California Chaparral and Oak Woodlands ecoregions) to match host density estimates reported in Lamsal et al. (2011).

Model performance

For each species, model performance was evaluated using two diagnostic metrics on the response residuals (i.e., the actual minus predicted number of disease-impacted trees per

plot): (i) the root mean squared error (RMSE) as a measure of overall prediction quality based on differences between true and predicted values, and (ii) scatterplots of the true versus predicted values of disease-impacted trees per plot, with Pearson's 'r' used as a measure of the linear correlation between these two values. A limitation of these residual-based calibration statistics (i.e., "apparent validation") is that the same data is being used to both fit and test the model, which may result in optimistic performance estimates. One rigorous method of prediction accuracy is "external validation", in which some data are left out when fitting the model and used later during the model testing phase (e.g., cross validation techniques; Arlot 2010). We did not choose the latter option because (i) we are dealing with an emerging pathogen in a relatively early stage of invasion and do not want to "throw out" any data, and (ii) our focus is on getting the most accurate inferential results through model averaging and AIC criterion, as we are unable to directly validate our predictive models at the hectare level.

Spatial and temporal autocorrelation

Geographical pattern in model residuals can lead to important insights, yet also to potentially serious violations of assumptions by presence of autocorrelation (i.e., an effective reduction in sample size and increased type I error) if not properly accounted for in the modeling process (Legendre 1993). Diagnostic tests for spatial non-randomness of response residuals was performed using semivariance analyses (Bailey and Gatrell 1995). Because there are several shapes that a variogram might follow, we compared fit among spherical, exponential and Gaussian models. We also examined temporal autocorrelation in disease prevalence by running separate binomial GLMs for the Sonoma plot network data—the only network in

which hosts were monitored each year of the study period (i.e., 2004–11)—including "sampling year" as a covariate. Statistical significance of this 'year' effect was decided based on p-value assessment.

Results

The total number of trees monitored, as well as those impacted by *P. ramorum*, varied greatly within and among networks (Figure 4.2). A total of 10,346 trees were monitored across the four networks, in which 4676 (45%) were tanoak (n=213 plots), 2586 (25%) were bay laurel (n=352 plots), 2410 (23%) were coast live oak (n=307 plots), 385 (4%) were canyon live oak (n=75 plots), and 289 (3%) trees were black oak (n=102 plots). However, only 11 canyon live oak trees from three Big Sur plots exhibited *P. ramorum* symptoms; therefore, we excluded this species from further analysis. Notably, almost 100% of bay laurel trees were classified as infected in the Sonoma network, whereas only approximately half of monitored individuals in the North Coast and Big Sur networks were recorded as infected (Figure 4.2-A). Tanoak abundance was much lower in the Sonoma and Phytosphere networks, yet these areas still exhibited high disease prevalence in this host species (Figure 4.2-B). In contrast, tanoak disease prevalence was much lower in the North Coast (conservative to liberal range: 15-18%) and Big Sur (30-36%) plot networks. Coast live oak and black oak exhibited higher disease prevalence in the Sonoma (coast live oak: 20-28%; black oak: 13-37%) and Phytosphere (28-39%; 60%) networks as compared to the North Coast (9-14%; 9-19%) and Big Sur (3-9%; 3%) plot networks (Figure 4.2-C,D).

Spatial prediction models

Overall, we found modest improvement between the actual versus predicted number of disease impacted trees based on Pearson's 'r' and visual examination of scatterplots when the liberal method of calculating disease prevalence was used, although differences in RMSE were relatively negligible (e.g., a RMSE change of 0.46 trees between the conservative and liberal coast live oak global models) (Table 4.2). We report estimates of the number of disease-impacted trees using both methods, yet show spatial prediction maps constructed using the liberal method of disease diagnosis (Figure 4.3). The number of disease-impacted trees varied by state and ecoregion, reflecting geographical differences in host distribution of each host (Table 4.3). Bay laurel exhibited the highest disease prevalence overall, in which the number of infected trees ranged from 0–2424 trees per ha^{-1} (mean = 127), spanning Monterey Co., California to Curry Co., Oregon. The Coast Range and California Chaparral and Oak Woodland ecoregions had similarly high levels of disease prevalence (~30%), whereas the Klamath Mountains ecoregion exhibited only 2% of infection in bay laurel trees. The number of diseased tanoak ranged from 0–3319 per ha^{-1} (mean = 75), ranging from Monterey Co., California to Curry Co., Oregon. The number of diseased tanoak increased from south to north reaching the highest numbers in the Coast Range ecoregion, although disease prevalence was the most severe in the California Chaparral and Oak Woodland ecoregion. In coast live oak, the number of diseased trees varied from 0–273 per ha^{-1} (mean = 5). In contrast to bay laurel and tanoak, the geographic range of disease-impacted trees was confined to a smaller area encompassing Monterey Co., California in the south to Mendocino Co., California in the north, with a small, isolated outbreak of low numbers of infected trees

in southern Humboldt County. Coast live oak reached its highest number of disease-impacted trees in the California Chaparral and Oak Woodlands ecoregion, yet the percentage of sudden oak death impacted trees was most severe in the Coast Range, reaching 3.8% prevalence. Overall, black oak exhibited substantially fewer diseased trees than the other hosts, in which the number of impacted trees ranged from 0-163 trees per ha^{-1} (mean = 7). The patchy distribution of diseased black oaks ranged from Monterey Co, California in the south to an isolated outbreak in the southern part of Humboldt, Co., California.

Model averaged parameter estimates are shown in Table 4.4 for the liberal estimate of disease prevalence. Force of infection was significant and positive across host species, and was especially important in driving disease patterns in tanoak and coast live oak. Rainy season average minimum temperature was positively associated with disease prevalence in all hosts, with stronger effects in bay laurel and tanoak. Competent host density was positive and significant in the bay laurel and coast live oak models. TMI and SRI were important predictors of disease prevalence in the bay laurel model only. Rainy season average precipitation was not associated with disease prevalence in any host.

Spatial and temporal autocorrelation

Across species, all semivariance models (exponential, spherical or Gaussian) revealed weak spatial patterning in response residuals, rendering us unable to adequately characterize spatial autocorrelation structure across the spatial domain (Figure S4.1). In regards to temporal autocorrelation, we found a steady increase in plot-level disease prevalence (n=164 plots) across years (2004-11) in coast live oak and black oak in the Sonoma network (Figure 4.4). Regression models for both canker hosts revealed a significant “year” effect after accounting

for all other covariates in the model. Specifically, for every year increase the logit (logged odds) of disease prevalence increased by 0.21 ($p < 0.001$) in coast live oak and 0.19 ($p < 0.001$) in black oak. Average disease prevalence in coast live oak went from 0.17 to 0.20 (a change of 3% per year) and from 0.30 to 0.35 (a change of 5% per year) for black oak. When applied to our range-wide estimates of sudden oak death impacted trees, the results suggest that the number of newly infected coast live oak increases by approximately 99,000 trees yr^{-1} compared to 55,000 trees yr^{-1} for black oak.

Discussion

Spatially-explicit information on the distribution and ecological impacts of emerging forest diseases is needed for large-scale analyses of disease dynamics and development of targeted management actions (Holdenrieder et al. 2004; Meentemeyer et al. 2012). In this study we provide the first range-wide estimates of the number of trees that are infected and dead due to sudden oak death across California and Oregon. We assimilated plot survey data on host conditions encompassing a seven year period (2005-12), as limited financial resources prevented the re-measurement of many older plots and thereby the use of more recent plot disease conditions. However, our temporal autocorrelation models—parameterized using annually collected longitudinal data (2004-11) from 164 Sonoma network plots—detected serial dependence in disease prevalence in coast live oak and black oak. As such, it is likely that our spatial predictions underestimate the impacts of sudden oak death on host infection and mortality. Preliminary data analysis (results not shown) revealed that many 'North Coast' plots (46%) were last surveyed in 2004 and exhibited little to no *P. ramorum* infection

at that time, yet are located in areas currently known to harbor *P. ramorum* (i.e., the 'force of infection' sites).

Detection bias in disease diagnosis can occur through the inability to detect cryptic and/or latent infection (Leclerc et al. 2014). Across networks, we were able to assign the cause of individual tree mortality to sudden oak death only if *P. ramorum* infection had been confirmed during a previous plot survey. As such, our conservative method of calculating plot-level disease prevalence is prone to underestimation of disease impacts in cases where, for example, cryptically infected trees at plot establishment died shortly thereafter or trees that became infected and subsequently died in between plot surveys. Using stand reconstruction techniques, Brown and Allen-Diaz (2009) found that *P. ramorum* infected sites had already lost 44–55% of coast live oak basal area when their monitoring efforts began. Moreover, counts based only on standing dead stems during plot establishment underestimated the degree of coast live oak mortality by one-half to two-thirds. The small difference between conservative and liberal estimates of disease prevalence in tanoak may result from dual symptom expression in this species—characterized by inoculum-producing foliar and twig infections and lethal canker lesions on the main stem and twigs—leading to increased probability of detecting symptoms of *P. ramorum* infection. Tanoak is considered the most susceptible host due to an apparent lack of host resistance and sporulation of inoculum on leaf and twig infections that are sufficient to cause disease locally and spread the pathogen regionally (Rizzo and Garbelotto 2003, Cobb et al. 2010, Hayden et al. 2011). Our results show that tanoak had the greatest number of diseased trees out of all canker hosts, further supporting these findings. Although the actual impact of sudden oak death on this

native tree species is not fully understood, our analyses provide a starting point for choosing areas to prioritize for tanoak disease management (e.g., susceptible stands).

Spatial prediction models of *P. ramorum* spread risk have unanimously suggested heightened infection probability along coastal forest ecosystems from southern-central California northwards to isolated outbreaks in southwestern Oregon, with the most severe impacts spreading outwards from the presumed points of pathogen introduction near the San Francisco Bay Area. Meentemeyer et al. (2004) predicted the risk of *P. ramorum* spread and establishment in California based on plant host susceptibility and weather variables, reporting that the rainy season climate of coastal California from Del Norte Co. in the north to San Luis Obispo Co. in the south, and the western slopes of the northern Sierra Nevada in Butte and Yuba Counties, as moderately to highly suitable for establishment and spread. Guo et al. (2005) predicted similar results except they did not include the northernmost California county (Del Norte) as a high risk area for sudden oak death. Because our goal was to quantify a realistic number of disease-impacted trees, as opposed to predicting the "potential" distribution of *P. ramorum* (i.e., pathogen presence/absence), we confined our predictions to 4 km of known sites harboring the pathogen, in an attempt to account for dispersal limitation and colonization time lags. We did not predict any disease-impacted hosts further south than Monterrey Co., California, or in locations further than 70 km from the Pacific Coast. Our models predicted large areas of uninvaded yet suitable habitat between isolated outbreaks in southern Humboldt Co., California and southwestern Oregon. Yet, Lamsal et al. (2011) predicted high host density and biomass in these regions, making it likely that *P. ramorum* will soon expand its range into these areas. Moreover, Vaclavik and Meentemeyer (2009)

predicted the "actual" distribution of *P. ramorum* across California, explicitly incorporating pathogen dispersal constraints in their models, and forecasted an extremely patchy and variable distribution of pathogen presence in northern California.

In Oregon, Vaclavik et al. (2010) developed predictive models of the potential and actual distribution of *P. ramorum* establishment and spread risk (whereby the latter contained dispersal constraints in the model). The predicted actual distribution revealed that forests at greatest risk of sudden oak death are concentrated in southwestern Oregon where the highest densities of susceptible host species exist, in particular tanoak. Our results support these findings, in which we found evidence for epidemic "hotspots" in tanoak and bay laurel in this area. However, spatial prediction estimates of *P. ramorum* impacts in Oregon, in our study and others, should be interpreted with an important caveat in mind. Upon discovery of *P. ramorum* in Curry Co., Oregon in 2001, an aggressive eradication campaign was launched that continued until 2010, in which recently killed host trees were located annually in systematic aerial surveys and then cut and burned in a treatment area extending at least 100 m beyond symptomatic plants (Peterson et al. 2014). Although these management actions slowed down the intensification of local spread of *P. ramorum*, new geographically isolated sites were detected every year of the eradication program (Hansen et al. 2008, Peterson et al. 2014). As such, the estimates of disease impacts we report in southwestern Oregon may be higher than actual levels in locations that underwent eradiation attempts.

Although our study on sudden oak death is the first to obtain quantitative estimates of diseased trees across all of California and Oregon, previous studies on the *P. ramorum* pathosystem have provided smaller-scale, regional estimates of host mortality. Using a

combination of high-resolution imagery and field data, Meentemeyer et al. (2008c) quantified the impact of *P. ramorum* invasion on oak and tanoak tree mortality across the Big Sur ecoregion (~ 80,000 ha). They estimated 235,678 trees killed by disease across the Big Sur plot network (~ 20% of all available host trees in impacted forest stands according to their predictions), whereby mortality was concentrated in the northern portion of the ecoregion. The authors were not able to distinguish between dead coast live oak, Shreve's oak and black oak via remote sensing, which prevented a species-specific comparison of *Quercus* mortality estimates. Davis et al. (2010) also analyzed sudden oak death host mortality in the Big Sur ecoregion, reporting severe plot-level mortality estimates in tanoak in which dieback ranged from 0–100% of surveyed trees. In a smaller study extent consisting of 20 plots located in Marin Co., California, McPherson et al. (2010) reported that by 2008, 80% of the tanoaks that were asymptomatic in 2000 had developed *P. ramorum* disease symptoms. Collectively, our study in conjunction with these others indicates that *P. ramorum* has substantially impacted forest ecosystems across coastal forest ecosystems of California and Oregon through direct mortality of canker host species.

The patchy distribution of *P. ramorum* on the landscape creates challenges for spatial prediction models (Vaclavik and Meentemeyer 2009, Haas et al. 2011). Invasive species, by definition, are not in geographic equilibrium with their environment and as such, do not occur at all locations where the environmental conditions are favorable due to dispersal limitation and colonization time-lags (Sutherst and Bourne 2009, Franklin 2010). In wildland pathogen invasions, spatial autocorrelation can arise from contagious processes of dispersal that lead to patchy disease distributions clustered around introductory foci (Kelly and

Meentemeyer 2002, Meentemeyer et al. 2012). The incorporation of distance constraints can be considered as a means of dealing with these issues (Allouche et al. 2008). We mapped the "force of infection" with an auto-covariate as an index of the potential for a location to receive propagules from surrounding inoculum sources in the landscape (Kot et al. 1996, Havel et al. 2002, Meentemeyer et al. 2008a). Force of infection was a strong predictor of heightened disease prevalence in all host species models, suggesting that pathogen dispersal plays a dominant role in limiting the spread of the invasion and that the cumulative proximity of a focal site to disease spreading hosts is a strong predictor of disease severity. Previous studies on the *P. ramorum* pathosystem also reported that inclusion of dispersal constraints resulted in model improvement (Vaclavik and Meentemeyer 2009, Ellis et al. 2010, Meentemeyer et al. 2011). Similar findings have been reported in other plant and animal pathosystems exhibiting passive pathogen dispersal, whereby dispersal gradients favor new infections closer to the source of inoculum introduction (Carlsson and Thrall 2002, Hasting et al. 2005).

Clearly, in order to invade new habitats, a species must both arrive there by dispersal and proliferate in the local environment. In addition to distance metrics, we found that disease prevalence was also influenced by biotic and abiotic landscape features. Model averaged parameter estimates revealed that warmer minimum temperatures during the rainy season were associated with heightened disease risk in all hosts species. Previous studies have shown that *P. ramorum* is commonly recovered from rain traps from December into the spring months, peaking during warm rains in May (Davidson et al. 2005). In contrast to expectations based on plot-level studies documenting the importance of bay laurel and tanoak

in increasing disease risk (Davidson et al. 2005; Rizzo et al. 2005), we found a significant effect of competent host density in the bay laurel and coast live oak models only. It may be that the force of infection covariate was sufficient in capturing inoculum pressure effects, and that observations of competent host density at the hectare level are too coarse to capture underlying community epidemiology relationships.

A take-home message of our analyses is that we are likely underestimating the magnitude of disease impacted hosts across California and Oregon. The Sonoma network models suggest that many, if not all, older plot surveys (those more than 5 years old) cause an under-reporting of current disease conditions in those areas. Yet, the temporal autocorrelation results we report are rough approximations of the "true" serial dependence of disease prevalence, as we did not account for the fact that different locations across California and Oregon are undergoing different stages of pathogen invasion. Here, as a baseline estimate of change we assumed a single epidemic wave occurring homogeneously in space and time. We advocate that future analyses should seek to formally incorporate temporal autocorrelation in dynamic epidemiological models (Meentemeyer et al. 2011). Previous studies on the *P. ramorum* pathosystem documented rapid increase in disease prevalence of tanoak and oak populations. For example, Waring and O'Hara (2008) observed basal area and tree density reductions of over 50% in monitored tanoak stands within 8 years of initial infestation. Moreover, annual mortality rates of 4.5–5.5% (over an order of magnitude higher than background rates) have also been reported in coast live oak in infested areas (Brown and Allen-Diaz, 2009). Such pulses of downed wood have also been documented in other forests hit by nonnative pathogens such as in former chestnut (*Castanea*

dentata) dominated communities due to chestnut blight fungus (McCarthy and Bailey 1994), eastern hemlock (*Tsuga canadensis*) dominated forests due to the hemlock woody adelgid (Benzinger 1994), and in American beech (*Fagus grandifolia*) dominated forests due to beech bark disease (McGee 2000, Ellison et al. 2005, Lovett et al. 2006).

Although much remains to be learned about the long-term ecosystem impacts of the sudden oak death epidemic to coastal forest ecosystems of the western USA, our results estimate levels of landscape-scale mortality that are likely to result in substantial alterations to carbon sequestration, biodiversity, and possibly even ecosystem resilience to subsequent disturbances (Ellison et al. 2005, Monahan and Koenig 2006, Metz et al. 2011). This information is required for many aspects of environmental research, resource management and conservation planning. For example, Lamsal et al. (2011) estimated that *P. ramorum* susceptible forests account for about 29% and 2.2% (respectively) of total above ground forest carbon in California and nationwide forests. Extensive tree mortality from sudden oak death has the potential to compromise the role of coastal forests ecosystems in regulating carbon balance dynamics (Lamsal et al. 2011, Cobb et al. 2012). Ideally, future analyses will incorporate finer-scale covariates, such as disturbance history, microclimate and community interactions (Cushman and Meentemeyer 2008, Meentemeyer et al. 2008b, Metz et al. 2011), although it is currently not feasible to reliably map these variables across vast spatial extents.

CHAPTER 5. CONCLUSION

Forests are among the best-studied and globally important terrestrial ecosystems, owing to their extensive distribution, socio-economic and aesthetic value, importance to biodiversity, and also for their essential role as regulators of hydrologic, energetic and elemental cycles affecting many of Earth's systems, including climate (Bonan 2008, Garnas et al. 2011). The fate of forests is of particular interest because these highly productive ecosystems cover almost 4 billion ha worldwide and provide important ecosystems services (FAO 2007). Yet, the simultaneous impacts of climate change, elevated CO_2, acid rain, nitrogen deposition, ozone pollution, land-use change and invasive species are creating substantial uncertainty about what future forest ecosystems will look like and how they will function (Dietze and Moorcroft 2011).

Predictions of continual increases in the number of plant pathogens emerging over the coming decade (Jones 2009, Fisher et al. 2012) gives urgency to identifying high-risk areas undergoing large-scale die-off events in natural forest ecosystems. Analyses are also needed that elucidate the cross-scale spatial and temporal factors driving invasion patterns and processes (Garnas et al. 2011, Hatala et al. 2011, Metz et al. 2012). This is not a trivial task, however, given that the landscapes of wildland forest pathosystems exhibit substantial environmental heterogeneity compared to intensively managed ecosystems, such as agroecosystems and tree plantations. The nascent field of landscape epidemiology, which integrates concepts and approaches from disease ecology with the macroscale lens of landscape ecology, holds promise for examining epidemic dynamics of wildland forest pathogens across space and time in complex environmental settings (Holdenrieder et al.

2004, Ostfeld et al. 2005, Meentemeyer et al. 2012). To date however, the challenge of explicitly integrating landscape heterogeneity of the biophysical environment into epidemiological analyses of wildland pathosystems remains a frontier in disease ecology and spatial epidemiology.

Sudden oak death is one of the latest emerging forest diseases causing high levels of mortality in forests of the western United States. Potentially millions of trees have died throughout *P. ramorum*'s geographic range since its discovery in the mid-1990s near San Francisco Bay. As this generalist pathogen becomes established throughout coastal forests of California and Oregon—where host biomass and densities are relatively high (Lamsal et al. 2011)—the cumulative biomass and number of hosts killed by this disease is likely to increase substantially (Meentemeyer et al. 2008c, Cobb et al. 2012, Metz et al. 2012). In my first dissertation chapter, I found that forest stands with higher plant species diversity had, on average, reduced disease risk compared to stands with low biodiversity. This finding supports the hypothesis that in generalist pathosystems—where multiple host species vary in competency—host community composition and diversity can moderate disease outcomes. If more diverse plant assemblages support a greater fraction of low-competency hosts, biodiversity losses have the potential to increase disease risk ("dilution effect"). Obtaining deeper insight into host-pathogen-environment interactions requires that we understand the importance of drivers that operate at different spatial scales and across time. In my second chapter I conducted a longitudinal analysis, finding that heterogeneity at the individual, community and landscape scale influenced the rate of tree mortality events. These results provide valuable information on regional-scale variability in disease-induced mortality that

can be used to guide management efforts and policy decisions. Understanding regional to sub-continental scale dynamics of emerging pathogens is challenging because reliable ecological data can be difficult and costly to obtain, especially over large landscapes (Hanks et al. 2011; Dillon et al. 2014). In my third chapter I integrated diverse data sets from long-term sudden oak death monitoring plots with remotely-derived geospatial data capturing landscape features, results from previous studies on the *P. ramorum* pathosystem, and publicly-available citizen science data, to obtain spatial estimates of the number of infected trees of the four key *P. ramorum* host across each species geographic range in California and Oregon. These results illustrate how data integration approaches can facilitate the spatial estimation of the impacts of large-scale, spatially heterogeneous disease invasions.

REFERENCES CITED

Alexander, H. 2010. Disease in natural plant populations, communities, and ecosystems: insights into ecological and evolutionary processes. Plant Disease **94**:492-503.

Allouche, O., O. Steinitz , D. Rotem, A. Rosenfeld, and R. Kadmon. 2008. Incorporating distance constraints into species distribution models. Journal of Applied Ecology **45**:599-609.

Anderson, P. K., A. A. Cunningham, N. G. Patel, F. J. Morales, P. R. Epstein, and P. Daszak. 2004. Emerging infectious diseases of plants: pathogen pollution, climate change and agrotechnology drivers. Trends in Ecology and Evolution **19**:535-544.

APHIS. 2013. Plant health: *Phytophthora ramorum*/sudden oak death. USDA Animal and Plant Health Inspection Service, Washington D.C. Retrieved January 17, 2014, from http://www.aphis.usda.gov/plant_health/plant_pest_info/pram/index.shtml.

Aram, K., T. Swiecki, E. Berhhardt, and D. M. Rizzo. 2011. Canyon live oak (*Quercus chrysolepis*) is susceptible to bole infection by *Phytophthora ramorum*. Phytopathology **101**:S8.

Arlot, S. 2010. A survey of cross-validation procedures for model selection. Statistics Surveys **4**:40-79.

Aukema, J. E., D. G. McCullough, B. Von Holle, A. M. Liebhold, K. Britton, and S. J. Frankel. 2010. Historical accumulation of nonindigenous forest pests in the continental United States. BioScience **60**:886-897.

Bailey, T., and A. Gatrell. 1995. Interactive spatial data analysis. Longman Scientific & Technical.

Barton, K. 2013. MuMIn: multi-model inference, R package version 1.9.13.

Begon, M. 2008. Effects of host diversity on disease dynamics.*in* R. S. Ostfeld, F. Keesing, and V. T. Eviner, editors. Infectious Disease Ecology: Effects of Ecosystems on Disease and of Disease on Ecosystems. Princeton University Press, Princeton.

Birdsey, R., and Y. Pan. 2011. Drought and dead trees. Nature Climate Change **1**:444-445.

Bonan, G. 2008. Forest and climate change: forcings, feedbacks, and the climate benefits of forests. Science **320**:1444-1449.

Brasier, C. M., and J. Webber. 2010. Sudden larch death. Nature **466**:824-825.

Brown, L., and B. Allen-Diaz. 2009. Forest stand dynamics and sudden oak death: mortality in mixed-evergreen forests dominated by coast live oak. Forest Ecology and Management **257**.

Burdon, J. J., and G. A. Chilvers. 1982. Host density as a factor in plant disease ecology. Annual Review of Phytopathology **20**:143-166.

Burdon, J. J., and P. H. Thrall. 2013. What have we learned from studies of wild plant-pathogen associations? -- the dynamic interplay of time, space and life-history. European Journal of Plant Pathology **138**:417-429.

Burdon, J. J., P. H. Thrall, and L. Ericson. 2006. The current and future dynamics of disease in plant communities. Annual Review of Phytopathology **44**:19-39.

Carlsson, U., and P. H. Thrall. 2002. The spatial distribution of plant populations, disease dynamics and evolution of resistance. Oikos **97**:97-110.

Castello, J. D., D. J. Leopold, and P. J. Smallidge. 1995. Pathogens, patterns, and processes in forest ecosystems. BioScience **45**:16-24.

Chapman, T. B., Veblen, T.T., Schoennagel, T. 2012. Spatiotemporal patterns of mountain pine beetle activity in the southern Rocky Mountains. Ecology **93**:2175-2185.

Cobb, R. C., J. A. N. Filipe, R. K. Meentemeyer, C. A. Gilligan, and D. M. Rizzo. 2012. Ecosystem transformation by emerging infectious disease: loss of large tanoak from California forests. Journal of Ecology **100**:712-722.

Cobb, R. C., R. K. Meentemeyer, and D. M. Rizzo. 2010. Apparent competition in canopy trees determined by pathogen transmission rather than susceptibility. Ecology **91**:327-333.

Condeso, T. E., and R. K. Meentemeyer. 2007. Effects of landscape heterogeneity on the emerging forest disease sudden oak death. Journal of Ecology **95**:364-375.

Cox, D. R. 1972. Regression models and life-tables. Journal of the Royal Statistical Society, Series B **34**:187-220.

Crowl, T., T. Crist, R. Parmenter, G. Belovsky, and A. Lugo. 2008. The spread of invasive species and infectious disease as drivers of ecosystem change. Frontiers in Ecology and the Environment **6**:238-246.

Cushman, J. H., and R. K. Meentemeyer. 2008. Multi-scale patterns of human activity and the incidence of an exotic forest pathogen. Journal of Ecology **96**:766-776.

Daly, C., R. P. Neilson, and D. L. Phillips. 1994. A statistical-topographic model for mapping climatological precipitation over mountainous terrain. Journal of Applied Meteorology **33**:140-158.

Daly, C., G. H. Taylor, W. P. Gibson, T. W. Parzybok, G. L. Johnson, and P. Pasteris. 2001. High-quality spatial climate data sets for the United States and beyond. Transactions of the American society of agricultural engineers **43**:1957-1962.

Daszak, P., A. A. Cunningham, and A. D. Hyatt. 2000. Emerging infectious diseases of wildlife-- threats to biodiversity and human health. Science **287**:443-449.

Davelos, A. L., and A. M. Jarosz. 2004. Demography of American chestnut populations: effects of a pathogen and a hyperparasite. Journal of Ecology **92**:675-685.

Davidson, J. M., H. A. Patterson, and D. M. Rizzo. 2008. Sources of inoculum for *Phytophthora ramorum* in a redwood forest. Phytopathology **98**:860-866.

Davidson, J. M., H. A. Patterson, A. C. Wickland, E. J. Fichtner, and D. M. Rizzo. 2011. Forest type influences transmission of *Phytophthora ramorum* in California oak woodlands. Phytopathology **101**:492-501.

Davidson, J. M., A. C. Wickland, H. A. Patterson, K. R. Falk, and D. M. Rizzo. 2005. Transmission of *Phytophthora ramorum* in mixed-evergreen forest in California. Phytopathology **95**:587-596.

Davis, F. W., M. Borchert, R. K. Meentemeyer, A. Flint, and D. M. Rizzo. 2010. Pre-impact forest composition and ongoing tree mortality associated with sudden oak death in the Big Sur region; California. Forest Ecology and Management **259**:2342-2354.

Dietze, M. C., and P. R. Moorcroft. 2011. Tree mortality in the eastern and central United States: patterns and drivers. Global Change Biology **17**:3312-3326.

Dillon, W., S. E. Haas, D. M. Rizzo, and R. K. Meentemeyer. 2014. Perspectives of spatial scale in a widland forest epidemic. European Journal of Plant Pathology **138**:449-465.

Diskin, M., K. C. Steiner, and F. V. Hebard. 2006. Recovery of American chestnut characteristics following hybridization and backcross breeding to restore blight-ravaged *Castanea dentate*. Forest Ecology and Management **223**:439-447.

Dubayah, R. C. 1994. Modeling a solar radiation topoclimatology for the Rio Grande River Basin. Journal of Vegetation Science **5**:627-640.

Dukes, J. S., J. Pontius, D. Orwig, J. R. Garnas, V. L. Rodgers, N. Brazee, B. Cooke, K. A. Theoharides, E. E. Stange, R. Harrington, J. Ehrenfeld, J. Gurevitch, M. Lerdau, K. Stinson, R. Wick, and M. Ayres. 2009. Responses of insect pests, pathogens, and invasive plant species to climate change in the forests of northeastern North America: what can we predict? Canadian journal of forest research **39**:231-248.

Eastburn, D. M., A. J. McElrone, and D. D. Bilgin. 2011. Influence of atmospheric and climatic change on plant-pathogen interactions. Plant Pathology **60**:54-69.

Ellis, A. M., T. Vaclavik, and R. K. Meentemeyer. 2010. When is connectivity important? A case study of the spatial pattern of sudden oak death. Oikos **119**:485-493.

Ellison, A. M., M. S. Bank, B. D. Clinton, E. A. Colburn, K. Elliot, C. R. Ford, D. R. Foster, B. D. Kloeppel, J. D. Knoepp, G. M. Lovett, J. Mohan, D. A. Orwig, N. L. Rodenhouse, W. V. Sobczak, K. A. Stinson, J. K. Stone, C. M. Swan, J. Thompson, B. Von Holle, and J. R. Webster. 2005. Loss of foundation species: consequences for the structure and dynamics of forested ecosystems. Frontiers in Ecology and the Environment **3**:479-486.

Elton, C. S. 1958. The ecology of invasions by animals and plants. John Wiley, New York, New York, USA.

Englander, L., M. Browning, and P. W. Tooley. 2006. Growth and sporulation of *Phytophthora ramorum* in vitro in response to temperature and light. Mycologica **98**:365-373.

Erwin, D. C., and O. K. Ribeiro. 1996. *Phytophthora* diseases worldwide. American Phytopathological Society, St. Paul, MN.

Fenton, A., and A. B. Pedersen. 2005. Community epidemiology framework for classifying disease threats. Emerging Infectious Diseases **11**:1815-1821.

Filipe, J. A. N., R. C. Cobb, R. Meentemeyer, C. A. Lee, Y. S. Valachovic, A. R. Cook, D. M. Rizzo, and C. A. Gilligan. 2012. Landscape epidemiology and control of pathogens with cryptic and long-distance dispersal: sudden oak death in northern California forests. PLoS Computational Biology **8**:e1002328.

Fisher, M. C., D. A. Henk, C. J. Briggs, J. Brownstein, L. Madoff, S. McCraw, and S. Gurr. 2012. Emerging fungal threats to animal, plant and ecosystem health. Nature **484**:186-194.

Fitt, B., H. McCartney, and P. Walklate. 1989. The role of rain in dispersal of pathogen inoculum. Annual Review of Phytopathology **27**:241-270.

Flint, L. E., and A. L. Flint. 2012. Downscaling future climate scenarios to fine scales for hydrological and ecological modelign and analysis. Ecological Processes **1**:1-15.

Franklin, J. F. 2010. Mapping species distributions: spatial inference and prediction. Cambridge University Press, Cambridge, UK.

Garnas, J. R., M. P. Ayres, A. M. Liebhold, and C. Evans. 2011. Subcontinental impacts of an invasive tree disease on forest structure and dynamics. Journal of Ecology **99**:532-541.

Garrett, K. A., G. A. Forbes, S. Savary, P. Skelsey, A. H. Sparks, C. Valdivia, A. H. C. van Bruggen, L. Willocquet, A. Djurle, E. Duveiller, H. Eckersten, S. Pande, C. Vera Cruz, and J. Yuen. 2011. Complexity in climate-change impacts: an analytical framework for effects mediated by plant disease. Plant Pathology **60**:15-30.

Gilbert, G. S. 2002. Evolutionary ecology of plant diseases in natural ecosystems. Annual Review of Phytopathology **40**:13-43.

Gilligan, C. A. 2002. An epidemiological framework for disease management. Advances in botanical research **38**:1-64.

Grunwald, N. J., E. M. Goss, and C. M. Press. 2008. *Phytophthora ramorum*: a pathogen with a remarkably wide host range causing sudden oak death on oaks and ramorum blight on woody ornamentals. Molecular Plant Pathology **9**:729-740.

Gschlobl, S., and C. Czado. 2008. Modelling count data with overdispersion and spatial effects. Statistical Papers **49**:531-552.

Guo, Q., M. Kelly, and C. H. Graham. 2005. Support vector machines for predicting distribution of sudden oak death in California. Ecological Modelling **182**:75-90.

Haas, S. E., W. W. Dillon, J. H. Cushman, N. E. Rank, D. M. Rizzo, and R. K. Meentemeyer. *in prep*. Spatial-temporal heterogeneity of a wildland forest epidemic: Multilevel effects of individual, community and landscape drivers.

Haas, S. E., M. B. Hooten, D. M. Rizzo, and R. K. Meentemyer. 2011. Forest species diversity reduces disease risk in a generalist plant pathogen invasion. Ecology Letters **14**:1108-1116.

Hanks, E. M., M. B. Hooten, and F. A. Baker. 2011. Reconciling multiple data sources to improve accuracy of large-scale prediction of forest disease incidence. Ecological Applications **21**:1173-1188.

Hansen, E., A. Kanaskie, S. Prospero, M. G. McWiliams, and D. J. Goheen. 2008. Epidemiology of *Phytophthora ramorum* in Oregon tanoak forests. Canadian Journal of Forest Research **38**:1133-1143.

Hasting, A., K. Cuddington, K. F. Davies, C. J. Dugaw, S. Elmendorf, A. Freestone, S. Harrison, M. Holland, J. Lambrinos, U. Malvadkar, B. Melbourne, K. Moore, C. Taylor, and D. Thomson. 2005. The spatial spread of invasions: new developments in theory and practice. Ecology Letters **8**:91-101.

Hatala, J. A., R. L. Crabtree, K. Halligan, and P. R. Moorcroft. 2010. Landscape-scale patterns of forest pest and pathogen damage in the Greater Yellowstone Ecosystem. Remote Sensing of the Environment **114**:375-384.

Hatala, J. A., M. C. Dietze, R. L. Crabtree, K. Kendall, D. Six, and P. R. Moorcroft. 2011. An ecosystem-scale model for the spread of a host-specific forest pathogen in the Greater Yellowstone Ecosystem. Ecological Applications **21**:1138-1153.

Havel, J., J. Shurin, and J. Jones. 2002. Estimating dispersal from patterns of spread: spatial and local control of lake invasions. Ecology **83**:3306-3318.

Hayden, K. J., A. Nettel, R. Dodd, and M. Garbelotto. 2011. Will all the trees fall? Variable resistance to an introduced forest disease in a highly susceptible host. Forest Ecology and Management **261**:1781-1791.

Hensen, P., and D. J. Usner. 1996. The natural history of Big Sur. University of California Press, Los Angeles, California.

Hijmans, R. 2014. Introduction to the 'raster' package, R package version version 2.2-31.

Holdenrieder, O., M. Pautasso, P. J. Weisberg, and D. Lonsdale. 2004. Tree diseases and landscape processes: the challenge of landscape pathology. Trends in Ecology and Evolution **19**:446-452.

Holmes, T. P., J. E. Aukema, B. Von Holle, A. M. Liebhold, and E. Sills. 2009. Economic impacts of invasive species in forests: past, present, and future. Annals of the New York Academy of Sciences **1162**:18-38.

Houston, D. R. 1994. Major new tree disease epidemics: beech bark disease. Annual Review of Phytopathology **32**:75-87.

Huberli, D., K. J. Hayden, M. Calver, and M. Garbelotto. 2012. Intraspecific variation in host susceptibility and climatic factors mediate epidemics of sudden oak death in western US forests. Plant Pathology **61**:579-592.

Hunter, J. 1997. Fourteen years of change in two old-growth *Pseudotsuga-Lithocarpus* forests in northern California. Journal of the Torrey Botanical Society **124**:273-279.

Jacobi, W., B. Geils, J. Taylor, and W. Zentz. 1993. Predicting the incidence of comandra blister rust on lodgepole pine: site, stand, and alternate host influences. Phytopathology **83**:630-637.

Johnson, B. L., and N. M. Haddad. 2011. Edge effects, not connectivity, determine the incidence and development of a foliar fungal plant disease. Ecology **92**:1551-1558.

Joly, P., D. Commenges, and L. Letenneur. 1998. A penalized likelihood approach for arbitrarily censored and truncated data: application to age-specific incidence of dementia. Biometrics **54**:185-194.

Jones, R. A. C. 2009. Plant virus emergence and evolution: Origins, new encounter scenarios, factors driving emergence, effects of changing world conditions, and prospects for control. Virus Research **141**:113-130.

Kauffman, M. J., and E. S. Jules. 2006. Heterogeneity shapes invasion: host size and environment influence susceptibility to a nonnative pathogen. Ecological Applications **16**:166-175.

Keesing, F., L. K. Belden, P. Daszak, A. Dobson, C. D. Harvell, R. D. Holt, P. Hudson, A. Jolles, K. E. Jones, C. E. Mitchell, S. S. Myers, T. Bogich, and R. S. Ostfeld. 2010. Impacts of biodiversity on the emergence and transmission of infectious diseases. Nature **468**:647-652.

Keesing, F., R. D. Holt, and R. S. Ostfeld. 2006. Effects of species diversity on disease risk. Ecology Letters **9**:485-498.

Kelly, M., and R. Meentemeyer. 2002. Landscape dynamics of the spread of sudden oak death. Photogrammetric Engineering & Remote Sensing **68**:1001-1009.

Kelly, N., and K. Tuxen. 2003. WebGIS for monitoring "sudden oak death" in coastal California. Computers, Environment and Urban Systems **27**:549-1549.

Kilpatrick, A. M., C. J. Briggs, and P. Daszak. 2010. The ecology and evolution of chytridiomycosis: an emerging disease of amphibians. Trends in Ecology and Evolution **25**:109-118.

Kleinbaum, D. G., and M. Klein. 2012. Survival analysis: a self-learning text. Third Edition edition. Springer, New York.

Kliejunas, J. T. 2010. Sudden oak death and *Phytophthora ramorum*: a summary of the literature. 2010 edition. Gen. Tech. Rep. PSW-GTR-234.*in* F. S. U.S. Department of Agriculture, Pacific Southwest Research Station, editor. U.S. Department of Agriculture, Forest Service, Pacific Southwest Research Station, Albany, CA.

Kliejunas, J. T. 2011. A risk assessment of climate change and the impact of forest diseases on forest ecosystems in the Western United States and Canada.*in* F. S. US Department of Agriculture, Pacific Southwest Research Station, editor. Gen. Tech. Rep. PSW-GTR-236., Albany, CA.

Kliejunas, J. T., B. W. Geils, J. Micales Glaeser, E. Michaels Gohenn, P. Hennon, M. Kim, H. Kope, J. Stone, R. Sturrock, and S. J. Frankel. 2009. Review of literature on climate change and forest diseases of western North America.*in* F. S. US Department of Agriculture, Pacific Southwest Research Station, editor. General Technical Report PSW-GTR-225, Albany, CA.

Knops, J. M. H., D. Tilman, N. M. Haddad, S. Naeem, C. E. Mitchell, J. Haarstad, M. E. Ritchie, K. M. Howe, P. B. Reich, E. Siemann, and J. Groth. 1999. Effects of plant species richness on invasion dynamics, disease outbreaks, insect abundances and diversity. Ecology Letters **2**:286-293.

Kot, M., M. A. Lewis, and P. van den Driessche. 1996. Dispersal data and the spread of invading organisms. Ecology **77**:2027-2042.

Kovacs, K., T. Vaclavik, R. G. Haight, A. Pang, N. J. Cunniffe, C. A. Gilligan, and R. K. Meentemyer. 2011. Predicting the economic costs and property value losses attributed to sudden oak death damage in California (2010-2020). Journal of Environmental Management **92**:1292-1302.

Kranz, J. 1990. Fungal diseases in multispecies plant communities. New Phytologist **116**:383-405.

Lamsal, S., R. C. Cobb, J. H. Cushman, Q. M. Meng, D. M. Rizzo, and R. Meentemeyer. 2011. Spatial estimation of the density and carbon content of host populations for *Phytophthora ramorum* in California and Oregon. Forest Ecology and Management **262**:989-998.

Leclerc, M., T. Dore, C. A. Gilligan, P. Lucas, and J. A. N. Filipe. 2014. Estimating the delay between host infection and disease (incubation period) and assessing its significance to the epidemiology of plant disease. PLoS ONE **9**:e86568.

Legendre, P. 1993. Spatial autocorrelation: trouble or new paradigm? Ecology **74**:1659-1673.

Loo, J. A. 2009. Ecological impacts of non-indigenous invasive fungi as forest pathogens. Biological Invasions **11**:81-96.

Lovett, G. M., C. D. Canham, M. A. Arthur, K. C. Weathers, and R. D. Fitzhugh. 2006. Forest ecosystem responses to exotic pests and pathogens in eastern North America. BioScience **56**:395-405.

Mack, R. N., D. Simberloff, W. M. Lonsdale, H. Evans, M. Clout, and F. A. Bazzaz. 2000. Biotic invasions: causes, epidemiology, global consequences, and control. Ecological Applications **10**:689-710.

Maloney, P. E., S. C. Lynch, S. F. Kane, C. E. Jensen, and D. M. Rizzo. 2005. Establishment of an emerging generalist pathogen in redwood forest communities. Journal of Ecology **93**:899-905.

Marcais, B., M. Bergot, V. Perarnaud, A. Levy, and M. Desprez-Loustau. 2004. Prediction and mapping of the impact of winter temperatures on the development of *P. cinnamomi* induced cankers on red and pedonculate oak. Phytopathology **94**:826-831.

McCallum, H. 2008. Landscape structure, disturbance, and disease dynamics.*in* R. S. Ostfeld, F. Keesing, and V. T. Eviner, editors. Infectious disease ecology: effects of ecosystems on disease and of disease on ecosystems. Princeton University Press, New Jersey.

McCartney, H., and B. Fitt. 1985. Construction of dispersal models. Pages 107-143 *in* D. Ingram, P. Williams, and C. A. Gilligan, editors. Advances in plant pathology, Vol. 3, Mathematical modeling of crop disease. Academic Press, London.

McGee, G. 2000. The contribution of beech bark disease-induced mortality to coarse woody debris loads in northern hardwood stands of Adirondack Park, New York, USA. Canadian journal of forest research **40**:1453-1462.

McPherson, B. A., S. R. Mori, D. L. Wood, M. Kelly, A. J. Storer, P. Svihra, and R. B. Standiford. 2010. Responses of oaks and tanoaks to the sudden oak death pathogen after 8 yr of monitoring in two coastal California forests. Forest Ecology and Management **259**:2248-2255.

Meentemeyer, R. K., B. L. Anacker, W. Mark, and D. M. Rizzo. 2008a. Early detection of emerging forest disease using dispersal estimation and ecological niche modeling. Ecological Applications **18**:377-390.

Meentemeyer, R. K., N. J. Cunniffe, A. R. Cook, J. A. N. Filipe, R. D. Hunter, D. M. Rizzo, and C. A. Gilligan. 2011. Epidemiological modeling of invasion in heterogeneous landscapes: spread of sudden oak death in California (1990-2030). Ecosphere **2**:art17.

Meentemeyer, R. K., S. E. Haas, and T. Vaclavik. 2012. Landscape epidemiology of emerging infectious diseases in natural and human-altered ecosystems. Annual Review of Phytopathology **50**:379-402.

Meentemeyer, R. K., N. E. Rank, B. L. Anacker, D. M. Rizzo, and J. H. Cushman. 2008b. Influence of land-cover change on the spread of an invasive forest pathogen. Ecological Applications **18**:159-171.

Meentemeyer, R. K., N. E. Rank, D. A. Shoemaker, C. B. Oneal, A. C. Wickland, K. M. Frangioso, and D. M. Rizzo. 2008c. Impact of sudden oak death on tree mortality in the Big Sur ecoregion of California. Biological Invasions **10**:1243-1255.

Meentemeyer, R. K., D. M. Rizzo, W. Mark, and E. Lotz. 2004. Mapping the risk of establishment and spread of sudden oak death in California. Forest Ecology and Management **200**:195-214.

Metz, M. R., K. M. Frangioso, R. K. Meentemeyer, and D. M. Rizzo. 2011. Interacting disturbances: wildfire severity affected by stage of forest disease invasion. Ecological Applications **21**:313-320.

Metz, M. R., K. M. Frangioso, A. C. Wickland, R. K. Meentemeyer, and D. M. Rizzo. 2012. An emergent disease causes directional changes in forest species composition in coastal California. Ecosphere **3**:1-16.

Miller, Z. J. 2012. Fungal pathogen species richness: why do some plant species have more pathogens than others? The American Naturalist **179**:282-292.

Mitchell, C. E., P. B. Reich, D. Tilman, and J. Groth. 2003. Effects of elevated CO_2, nitrogen deposition, and decreased species diversity on foliar fungal plant disease. Global Change Biology **9**:438-451.

Mitchell, C. E., D. Tilman, and J. V. Groth. 2002. Effects of grassland plant species diversity, abundance, and composition on foliar funal disease. Ecology **83**:1713-1726.

Monahan, W. B., and W. D. Koenig. 2006. Estimating the potential effects of sudden oak death on oak-dependent birds. Biological Conservation **127**:146-157.

Moore, I. D., R. B. Grayson, and A. R. Ladson. 1991. Digital terrain modeling: a review of hydrological, geomorphological, and biological applications. Hydrological Processes **5**:3-30.

Mundt, C. C., K. E. Sackett, and L. D. Wallace. 2011. Landscape heterogeneity and disease spread: experimental approaches with a plant pathogen. Ecological Applications **21**:321-328.

Murphy, S., and D. M. Rizzo. 2003. First report of *Phytophthora ramorum* on canyon live oak in California. Plant Disease **87**:315.

Nations, F. a. A. O. F. o. t. U. 2007. State of the World's Forests 2007. FAO, Rome.

Ohmann, J. L., M. J. Gregory, and T. A. Spies. 2007. Influence of environment, disturbance and ownership on forest vegetation of coastal Oregon. Ecological Applications **17**:18-33.

Ostfeld, R. S., G. E. Glass, and F. Keesing. 2005. Spatial epidemiology: an emerging (or re-emerging) discipline. Trends in Ecology and Evolution **20**:328-336.

Ostfeld, R. S., and F. Keesing. 2000. The function of biodiversity in the ecology of vector-borne zoonotic diseases. Canadian journal of zoology **78**:2061-2078.

Ostfeld, R. S., and F. Keesing. 2012. Effects of host diversity on infectious risk. Annual Review of Ecology and Systematics **43**:157-182.

Pagan, I., P. Gonzalez-Jara, A. Moreno-Letelier, M. Rodelo-Urrego, A. Fraile, D. Pinero, and F. Garcia-Arenal. 2012. Effect of biodiversity changes in disease risk: exploring disease emergence in a plant-virus system. PLOS pathogens **8**:1-12.

Parker, I., and G. S. Gilbert. 2004. The evolutionary ecology of novel plant-pathogen interactions. Annual Review of Ecology and Systematics **35**:675-700.

Pautasso, M., O. Holdenrieder, and J. Stenlid. 2005. Susceptibility to fungal pathogens of forests differing in tree diversity.*in* M. Scherer-Lorenzen, C. Korner, and M. Scherer-Lorenzen, editors. Forest diversity and function- temperate and boreal systems. Springer-Verlag, Berlin.

Peters, D., J. Herrick, D. Urban, R. Gardner, and D. Breshears. 2004. Strategies for ecological extrapolation. Oikos **106**:627-636.

Peterson, E., E. Hansen, and A. Kanaskie. 2014. Spatial relationship between *Phytophthora ramorum* and roads or streams in Oregon tanoak forests. Forest Ecology and Management **312**:216-224.

Pimentel, D., R. Zuniga, and D. Morrison. 2005. Update on the environmental and economic costs associated with alien-invasive species in the United States. Ecological Economics **52**:273-288.

Plantegenest, M., C. Le May, and F. Fabre. 2007. Landscape epidemiology of plant diseases. Journal of the Royal Society Interface **4**:963-972.

Pongsiri, M. J., J. Roman, V. O. Ezenwa, T. L. Goldberg, H. S. Koren, S. C. Newbold, R. S. Ostfeld, S. K. Pattanayak, and D. J. Salkeld. 2009. Biodiversity loss affects global disease ecology. BioScience **59**:945-954.

Power, A. G., and C. E. Mitchell. 2004. Pathogen spillover in disease epidemics. The American Naturalist **164**:S79-S89.

R Development Core Team. 2010. R: A language and environment for statistical computing. R Foundation for Statistical Computing, Vienna, Austria. R Foundation for Statistical Computing.

Ramage, B. S., A. B. Forrestel, M. A. Moritz, and K. L. O'Hara. 2011. Sudden oak death disease progression across two forest types and spatial scales. Journal of Vegetation Science.

Raymundo, L. J., A. R. Halford, A. P. Maypa, and A. M. Kerr. 2009. Functionally diverse reef-fish communities ameliorate coral disease. Proceedings of the National Academy of Sciences **106**:17067-17070.

Rizzo, D. M. 2005. Exotic species and fungi: Interactions with fungal, plant and animal communities. Pages 857-877 *in* J. Dighton, P. Oudemans, and J. White, editors. The fungal community. CRC Press, Boca Raton, FL.

Rizzo, D. M., and M. Garbelotto. 2003. Sudden oak death: endangering California and Oregon forest ecosystems. Frontiers in Ecology and the Environment **1**:197-204.

Rizzo, D. M., M. Garbelotto, J. M. Davidson, G. W. Slaughter, and S. T. Koike. 2002. *Phytophthora ramorum* as the cause of extensive mortality of *Quercus* spp. and *Lithocarpus densiflorus* in California. Plant Disease **86**:205-214.

Rizzo, D. M., M. Garbelotto, and E. M. Hansen. 2005. *Phytophthora ramorum*: integrative research and management of an emerging pathogen in California and Oregon forests. Annual Review of Phytopathology **43**:309-335.

Rodo, X., M. Pascual, F. J. Doblas-Reyes, A. Gershunov, D. A. Stone, F. Giorig, P. J. Hudson, J. Kinter, M. Rodriguez-Arias, N. C. Stenseth, D. Alonso, J. Garcia-Serrano, and A. P. Dobson. 2013. Climate change and infectious diseases: can we meet the needs for better prediction? Climatic Change **118**:625-640.

Rodriguez-Rey, M., A. Jimenez-Valverde, and P. Acevedo. 2013. Species distribution models predict range expansion better than chance but not better than a simple dispersal model. Ecological Modelling **256**:1-5.

Rondeau, V., L. Filleul, and P. Joly. 2003. Maximum penalized likelihood estimation in a gamma-frailty model. Lifetime Data Analysis **9**:139-153.

Rondeau, V., Y. Mazroui, and J. R. Gonzalez. 2012. frailtypack: An R package for the analysis of correlated survival data with frailty models using penalized likelihood estimation or parametrical estimation. Journal of statistical software **47**:1-28.

Roscher, C., J. Schumacher, O. Foitzik, and E. D. Schulze. 2007. Resistance to rust fungi in *Lolium perenne* depends on within-species variation and performance of the host species in grasslands of different plant diversity. Oecologia **153**:173-183.

Rue, H., and S. Martino. 2009. INLA: Functions which allow to perform a full Bayesian analysis of structured additive models using Integrated Nested Laplace Approximation. R package version 0.0.

Rue, H., S. Martino, and N. Chopin. 2009. Approximate Bayesian inference for latent Gaussian models by using integrated nested Laplace approximations. Journal of the Royal Statistical Society **71**:319-392.

Sagarin, R., and A. Pauchard. 2010. Observational approaches in ecology open new ground in a changing world. Frontiers in Ecology and the Environment **8**:379-386.

Shearer, B. L., C. Crane, and C. Dunne. 2009. Ecosystem dynamics altered by pathogen-mediated changes following invasion of *Banksia* woodland and *Eucalyptus marginata*

forest biomes of south-western Australia by *Phytopthora cinnamomi*. Australasian Plant Pathology **38**:417-436.

Shearer, B. L., and M. Dillon. 1995. Susceptibility of plant-species in *Eucalyptus marginata* forests to infection by *Phytophthora cinnamoni*. Australian Journal of Botany **43**:113-134.

Smith, C. M., B. Sheperd, C. Gillies, and J. Stuart-Smith. 2012. Changes in blister rust infection and mortality in whitebark pine over time. Canadian journal of forest research **43**:90-96.

Smith, D. L., L. Ericson, and J. J. Burdon. 2003. Epidemiological patterns at multiple spatial scales: an 11-year study of a *Triphragmium ulmariae- Filipendula ulmaria* metapopulation. Journal of Ecology **91**:890-903.

Smith, J., and J. Hoffman. 2001. Site and stand characteristics related to white pine blister rust in high-elevation forests of Southern Idaho and Western Wyoming. Western North American Naturalist **61**:409-416.

Spiegelhalter, D. J., N. G. Best, B. P. Carlin, and A. van der Linde. 2002. Bayesian measures of model complexity and fit. Journal of the Royal Statistical Society Series B **64**:583-639.

Stockwell, D., and A. T. Peterson. 2002. Effects of sample size on accuracy of species distribution models. Ecological Modelling **148**:1-13.

Sturrock, R. N., S. J. Frankel, A. V. Brown, P. E. Hennon, J. T. Kliejunas, K. J. Lewis, J. J. Worrall, and A. J. Woods. 2011. Climate change and forest disease. Plant Pathology **60**:133-149.

Sutherst, R. W., and A. S. Bourne. 2009. Modelling non-equilibrium distributions of invasive species: a tale of two modelling paradigms. Biological Invasions **11**:1231-1237.

Swinton, J., and C. A. Gilligan. 1996. Dutch elm disease and the future of the elm in the U.K., a quantitative analysis. Philosophical Transactions of the Royal Society B: Biological Sciences **351**:605-615.

Thrall, P. H., and J. J. Burdon. 2000. Effect of resistance variation in a natural plant host-pathogen metapopulation on disease dynamics. Plant Pathology **49**:767-773.

Vaclavik, T., A. Kanaskie, E. M. Hansen, J. L. Ohmann, and R. K. Meentemyer. 2010. Predicting potential and actual distribution of sudden oak death in Oregon: prioritizing landscape contexts for early detection and eradication of disease outbreaks. Pages 1026-1035 Forest Ecology and Management.

Vaclavik, T., and R. K. Meentemeyer. 2009. Invasive species distribution modeling (iSDM): are absence data and dispersal constraints needed to predict actual distributions? Ecological Modelling **220**:3248-3258.

Vettraino, A., S. Sukno, A. Vannini, and M. Garbelotto. 2009. Diagnostic sensitivity and specificity of different methods used by two laboratories for the detection of *Phytopthora ramorum* on multiple natural hosts. Plant Pathology **59**:289-300.

Vila, M., P. Inchausti, J. Vayreda, O. Barrantes, C. Gracia, J. J. Ibanez, and T. Mata. 2005. Confounding factors in the observational productivity-diversity relationship in forests.*in* M. Scherer-Lorenzen, C. Korner, and E. D. Schulze, editors. Forest diversity and function: temperate and boreal systems. Springer-Verlag, Berlin.

Waring, K. M., and K. L. O'Hara. 2008. Redwood/tanoak stand development and response to tanoak mortality caused by *Phytophthora ramorum*. Forest Ecology and Management **255**:2650-2658.

Weste, G., K. Brown, J. Kennedy, and T. Walshe. 2002. *Phytophthora cinnamoni* infestation-a 24-year study of vegetation change in forests and woodlands of the Grampians, Western Victoria. Australian Journal of Botany **50**:247-274.

Wienke, A. 2010. Frailty models in survival analysis. Chapman & Hall.

TABLES

Table 2.1. Parameter estimates (marginal posterior means) for species diversity and landscape context on *P. ramorum* disease risk, shown when excluding and including host density effects of the two most competent foliar hosts (bay laurel and tanoak). Estimates are from the zero-inflated binomial GLMM with a spatial random effect (ICAR) (see Table S3 for all model results). *Species Richness* and the *Shannon-Wiener diversity index* were fit separately due to collinearity between these diversity measurements. Covariates were obtained for all 278 field plots across the Big Sur study area. 95% Bayesian credible intervals (i.e., the 0.025 and 0.975 quantiles of the posterior distribution) are shown in parentheses‡

ICAR model	Species Diversity	Bay Laurel Density	Tanoak Density	Year	Forest Type	Precipitation	Host Habitat (200 m buffer)	DIC
				Species Richness				
Exclude Host density	-0.49 (-0.56 – -0.42)	--	--	-0.32 (-0.45 – -0.19)	-0.40 (-0.53 – -0.28)	-0.30 (-0.37 – -0.23)	0.25 (0.18 – 0.32)	3105
Include Host Density	-0.83 (-1.14 – -0.55)	1.22 (0.90 – 1.57)	0.96 (0.61 – 1.32)	-0.75 (-1.33 – -0.21)	-0.83 (-1.37 – -0.28)	-0.73 (-1.19 – -0.29)	0.41 (0.12 – 0.71)	1050
				Shannon-Wiener Index				
Exclude Host density	-0.57 (-0.65 – -0.51)	--	--	-0.39 (-0.52 – -0.26)	-0.45 (-0.58 – -0.32)	-0.43 (-0.51 – -0.36)	0.26 (0.19 – 0.33)	3008
Include Host Density	-0.48 (-0.79 – -0.19)	1.16 (0.82 – 1.53)	0.91 (0.53 – 1.30)	-0.73 (-1.33 – -0.15)	-0.72 (-1.31 – -0.14)	-0.74 (-1.18 – -0.32)	0.39 (0.07 – 0.73)	1061

‡ Only parameter estimates whose 95% Bayesian credible interval did not overlap zero are shown. Potential Solar Insolation (PSI) is the only covariate that was ommited based on this criterion.

Table 3.1. Shared gamma frailty models for time to *P. ramorum* infection in coast live oak and black oak from 2004–10 (n=163 plots): (a) individual effects, (b) community effects, (c) landscape effects, and (d) the full model containing only significant covariates ($p \leq 0.05$) from previous models. 'Coef'. is the penalized marginal log-likelihood estimate of each fixed regression coefficient (conditional on the frailty); 'Std. Err.' gives the standard errors of the estimated regression coefficients; 'p-value' is the two-sided p-value for the null hypothesis tests that each regression coefficient is 0 (or each hazard ratio is 1); 'Hazard Ratio' is the exponentiated coefficient for each covariate; and '95% CI' represents the 95% confidence interval of each hazard ratio. We used LCV_a, an approximate version of likelihood cross-validation criterion, to guide model selection, whereby lower values indicate better predictive performance of estimating the hazard function (i.e., time to infection) (Rondeau et al. 2012). θ is the variance of the frailty term and SE (θ) is the standard error of the frailty term. All numerical variables have been standardized to a mean of zero and standard deviation of one. * Although the values of the three time-dependent covariates fluctuate across years, survival models only provide one coefficient for each variable, representing the effect across the entire study period (Kleinbaum and Klein 2012); † parameter estimate is for black oak; "RS" is rainy season months.

(a) Individual Effects:

Covariate	Coef.	Std. Err.	p-value	Hazard Ratio	95% CI
Species identity†	-0.58	0.27	0.03	0.56	0.33-0.94
Diameter at breast height (cm)	0.61	0.08	<0.001	1.84	1.59-2.14

LCV_a: 0.106454, frailty parameter, θ: 1.84559, SE(θ): 0.391291

(b) Community Effects:

Covariate	Coef.	Std. Err.	p-value	Hazard Ratio	95% CI
Species richness	-0.59	0.14	<0.001	0.55	0.42-0.73
Bay laurel density*	0.29	0.12	0.02	1.33	1.05-1.69

LCV_a: 0.11004, frailty parameter, θ: 1.42383, SE(θ): 0.327788

Table 3.1. (continued)

(c) Landscape Effects:

Covariate	Coef.	Std. Err.	p-value	Hazard Ratio	95% CI
Host habitat connectivity	-0.17	0.16	0.29	0.84	0.61-1.16
Topographic Moisture Index	0.10	0.13	0.46	1.10	0.85-1.43
Potential solar irradiation	0.31	0.16	0.05	1.37	1.00-1.87
RS precipitation (2-yr avg.)*	1.57	0.13	<0.001	4.81	3.70-6.26
RS minimum temp. (2-yr avg.)*	0.34	0.17	0.04	1.40	1.01-1.94

LCV_a: 0.106652, frailty parameter, θ: 1.87761, SE(θ): 0.414002

(d) Full Model:

Covariate	Coef.	Std. Err.	p-value	Hazard Ratio	95% CI
Species identity†	-0.66	0.30	0.03	0.52	0.28-0.93
Diameter at breast height (cm)	0.60	0.08	<0.001	1.83	1.55-2.15
Species richness	-0.39	0.17	0.03	0.68	0.48-0.95
Bay laurel density*	0.24	0.15	0.10	1.27	0.95-1.69
Potential solar irradiation	0.27	0.18	0.13	1.31	0.93-1.84
RS precipitation (2-yr avg.)*	0.88	0.15	<0.001	2.42	1.79-3.26
RS minimum temp. (2-yr avg.)*	0.86	0.19	<0.001	2.36	1.62-3.45

LCV_a: 0.10218, frailty parameter, θ: 2.14921, SE(θ): 0.477456

Table 4.1. Ecological and physiographic covariates used to characterize environmental regimes and develop predictive models of *P. ramorum* host infection across California and Oregon. All covariates were scaled to a grid cell resolution of 1-ha (100-m x 100-m). 'RS' – rainy season (November 1st through May 31st of a given year).

CATEGORY	COVARIATE	DATA SOURCE
Topography	Topographic moisture index (TMI)	National Elevation Dataset
	Solar radiation intensity (SRI)†	
Climate	RS average precipitation (mm)	Parameter-elevation Regressions on Independent Slopes Model (PRISM)
	RS average minimum temperature (°C)	
	RS average maximum temperature (°C)	
Biotic interactions	Competent host density	Lamsal et al. (2011)
	Force of infection	CDFA, UC-Davis, UC-Berkeley, OR Dept. of Forestry, network survey data

† SRI calculated for the month of March.

Table 4.2. Residual diagnostics of models constructed using the conservative versus liberal method of calculating plot-level disease prevalence. Pearson's 'r' is a measure of the linear correlation between two values and is shown to the left of each vertical bar. The root mean squared error (RMSE), which quantifies the differences between true and predicted values, is shown to the right of each bar. Because bay laurel does not experience direct disease-induced mortality following *P. ramorum* infection, disease prevalence for this host species was calculated as the number of alive, infected trees out of the total number of trees in a plot.

	Tanoak	**Coast live oak**	**Black oak**
Conservative	0.68 | 9.36	0.47 | 1.23	0.31 | 0.56
Liberal	0.73 | 9.15	0.56 | 1.69	0.60 | 0.95

Table 4.3. Spatial prediction estimates of the number of disease-impacted trees (in millions) for the four main *P. ramorum* host species, categorized by range-wide, state and US-EPA Level III Ecoregions. Host density (trees per ha^{-1}), not accounting for disease status, was estimated by Lamsal et al. (2011) and is used to calculate the percentage of disease-impacted trees by zone (shown in parentheses). "NA" denotes instances where a species either does not occur (i.e., coast live oak is not found in Oregon) or was not present within the exposure buffer (i.e., black oak was not found within 4 km of known infection sites in southwestern Oregon). Estimates from the conservative method of calculating disease prevalence are shown above the corresponding liberal estimations of the number and percentage of disease-impacted trees.

	Bay laurel	**Tanoak**	**Coast live oak**	**Black oak**
Range-wide	91.4 (21%)	44.5 (2.5%) 29.4 (1.6%)	1.9 (0.4%) 3.3 (0.7%)	0.27 (0.04%) 1.1 (0.17%)
Estimation by state				
California	86.3 (21.9%)	27.7 (2%) 21.7 (1.5%)	1.9 (0.4%) 3.3 (0.7%)	0.27 (0.05%) 1.1 (0.19%)
Oregon	5.1 (12.3%)	16.8 (4.4%) 7.8 (2%)	NA	NA*
Estimation by ecoregion				
Coast range	23.5 (28%)	25.1 (2.9%) 18 (2.1%)	0.47 (2.6%) 0.7 (3.8)	0.06 (1.3%) 0.25 (5.6%)
Klamath Mountains	1.6 (2%)	13.4 (1.6%) 5.7 (0.7%)	NA	NA*
CA chaparral & oak woodlands	66.4 (29.9%)	5.9 (10.3%) 5.8 (9.9%)	1.4 (0.36%) 2.6 (0.66%)	0.21 (0.24%) 0.82 (0.93%)

Table 4.4. Model averaged parameter coefficients using the liberal method of disease prevalence in oak and tanoak models. Significance values are represented as follows: $p \leq 0.10$ = '▪', $p \leq 0.05$ = '*', $p \leq 0.01$ = '**', $p \leq 0.001$ = '***'. The number of models averaged based on the delta QAIC criterion varied among host species: bay laurel-2; tanoak-6; coast live oak-6; black oak-9. "TMI" =topographic moisture index; "SRI" = solar radiation intensity; "RS" = rainy season. An α-value of 25 provided the best model fit for the 'force of infection' covariate.

	Intercept	*Competent host density*	*Force of infection*	*TMI*	*SRI*	*RS avg. precipitation*	*RS avg. min. temperature*
Bay laurel	-7.25***	0.005***	9.16**	-0.15***	0.005***	0.007	0.75***
Tanoak	-7.06***	3e-04	25.64***	8e-04	5e-04	2e-05	0.89***
Coast live oak	-5.69***	0.002***	25.11***	-0.02	0.002	0.003	0.27*
Black oak	-5.06*	3e-04	11.08*	-0.007	3e-04	-0.002	0.65*

FIGURES

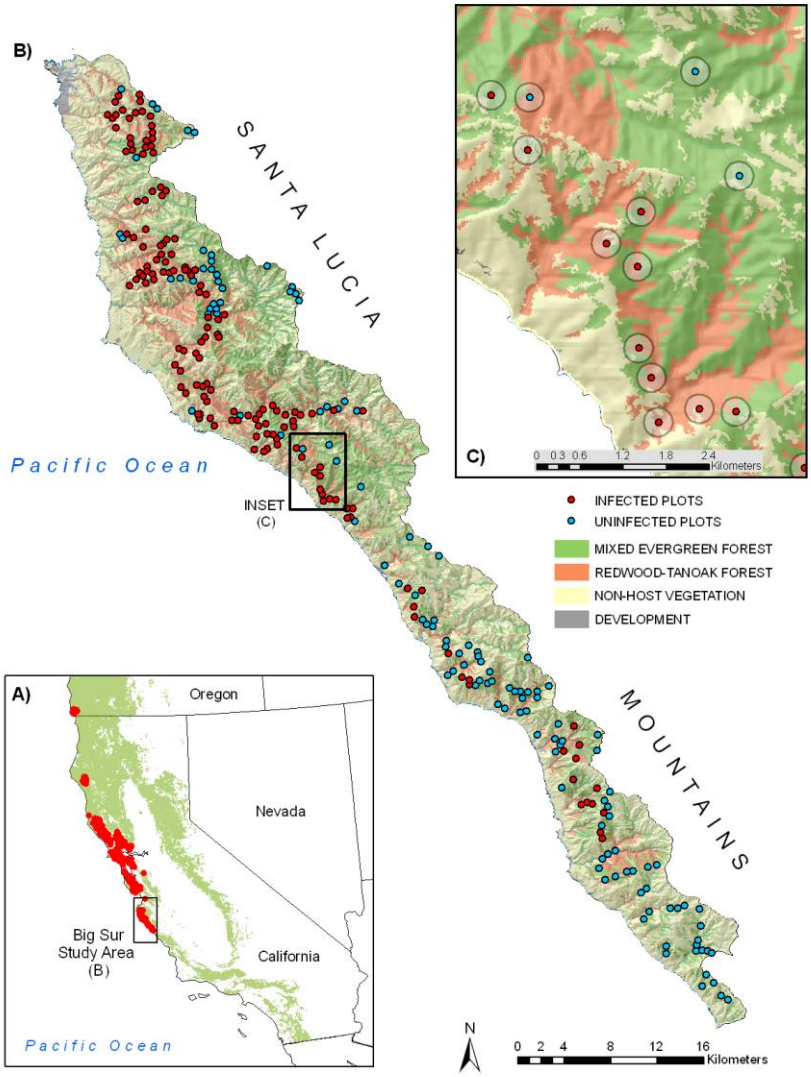

Figure 2.1 (A) Geographic distribution of *P. ramorum* in North America (shown in red), extending from Monterey County in central CA to Curry County, OR in the north. Host vegetation is shown in green. (B) The Big Sur study area (79,356-ha) extends 100-km along the Pacific slope of the Santa Lucia range. Host forest community types (mixed evergreen and redwood-tanoak forests) are mapped throughout the region. *P. ramorum* infected plots are shown in red (n=151) with uninfected plots shown in blue (n=127). (C) Inset map shows the high degree of spatial heterogeneity in forest community types. Circles represent the 200-radius buffers from plot center used to obtain the amount of host habitat surrounding each plot.

A)

B)

Figure 2.2 Examples of landscape heterogeneity in the Big Sur, California ecoregion showing mixed evergreen forest (A) and redwood-tanoak forest (B). These two forest community types are optimal habitat for *P. ramorum* throughout the study area. There were 162 plots located in mixed evergreen forest and 116 plots in redwood-tanoak forest. Photo credit: S. E. Haas.

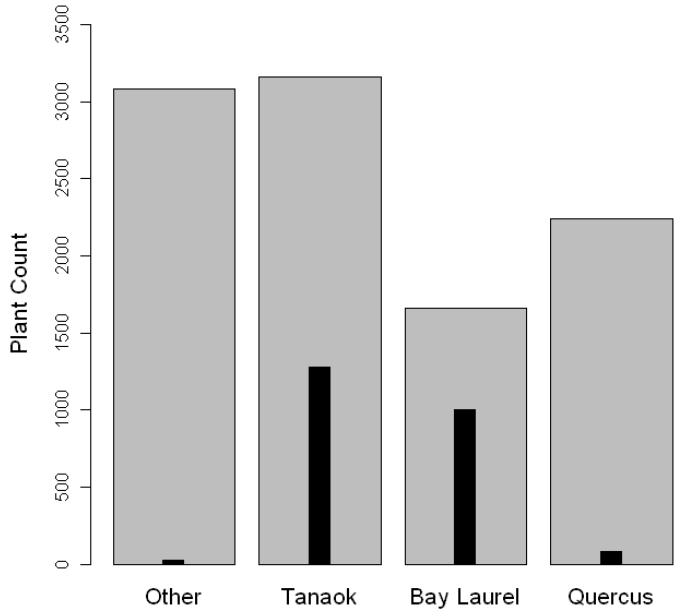

Figure 2.3 Total plant count shown in gray bars and infected count shown in black bars for four categories of host species sampled across the Big Sur, CA study area (18 host species total from 278 plots). The two most competent foliar hosts, tanoak and bay laurel, were the most abundant and also exhibited the highest infection levels (n_{Tanoak} = 1280 infected plants/3163 total plants; $n_{Bay\ Laurel}$ = 1000 infected plants/1660 total plants). 'Other' includes the additional 12 foliar host species (n_{Other} = 25 infected plants/3086 total plants); less is known about their potential to produce inoculum. 'Quercus' represents the canker hosts, which have not been shown to transmit inoculum in the field, and includes: coast live oak (*Quercus agrifolia*), California black oak (*Q. kelloggii*), Canyon live oak (*Q. chrysolepis*), and Shreve's oak (*Q. parvula* var. *shrevei*) ($n_{Quercus}$ = 80 infected plants/2243 total plants) (Rizzo et al. 2002). See Table S2 for a list of all host counts across the study area.

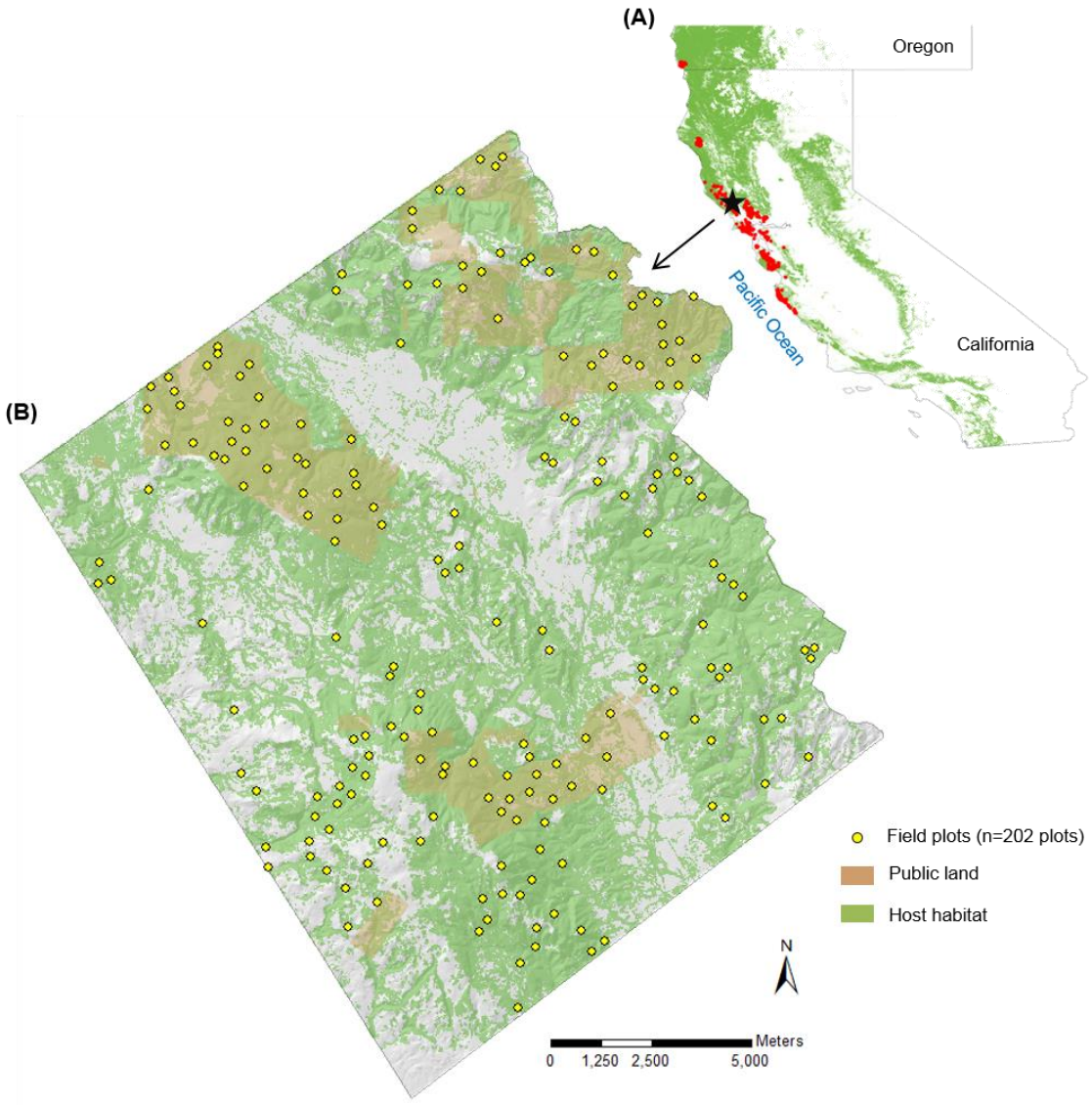

Figure 3.1. (a) First noticed in the San Francisco Bay Area in the mid-1990s, the geographic range of Phytophthora ramorum in North America (shown in red) extends over 700 km from Monterey County, California in the south to Curry County in southwestern OR. Host plant communities are shown in green and our study location is denoted by the star. (b) The study area consists of a long-term sudden oak death monitoring network composed of 200 randomly-stratified plots (15-m x 15-m) distributed across a 275 km^2 heterogeneous region of mixed oak woodland in Sonoma County, California, USA.

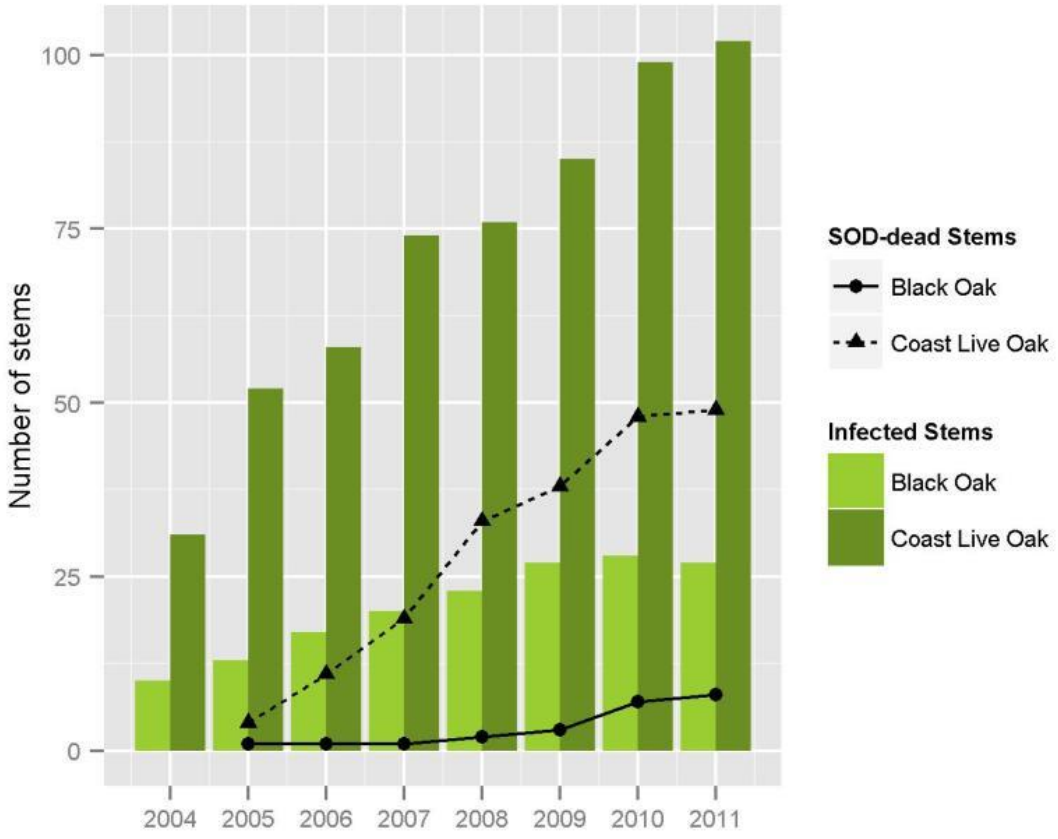

Figure 3.2. The number of stems infected with *P. ramorum* and those dying following infection (referred to as "SOD-dead stems") for coast live oak and black oak across the 8-yr study period. The number of SOD-dead stems is a cumulative measure over time, whereas the number of infected stems changes when a stem transitions from an "infected" status to a "SOD-dead" status (i.e., these two categories are mutually-exclusive). These are raw counts and have not been weighted by differences in the relative abundance of each species.

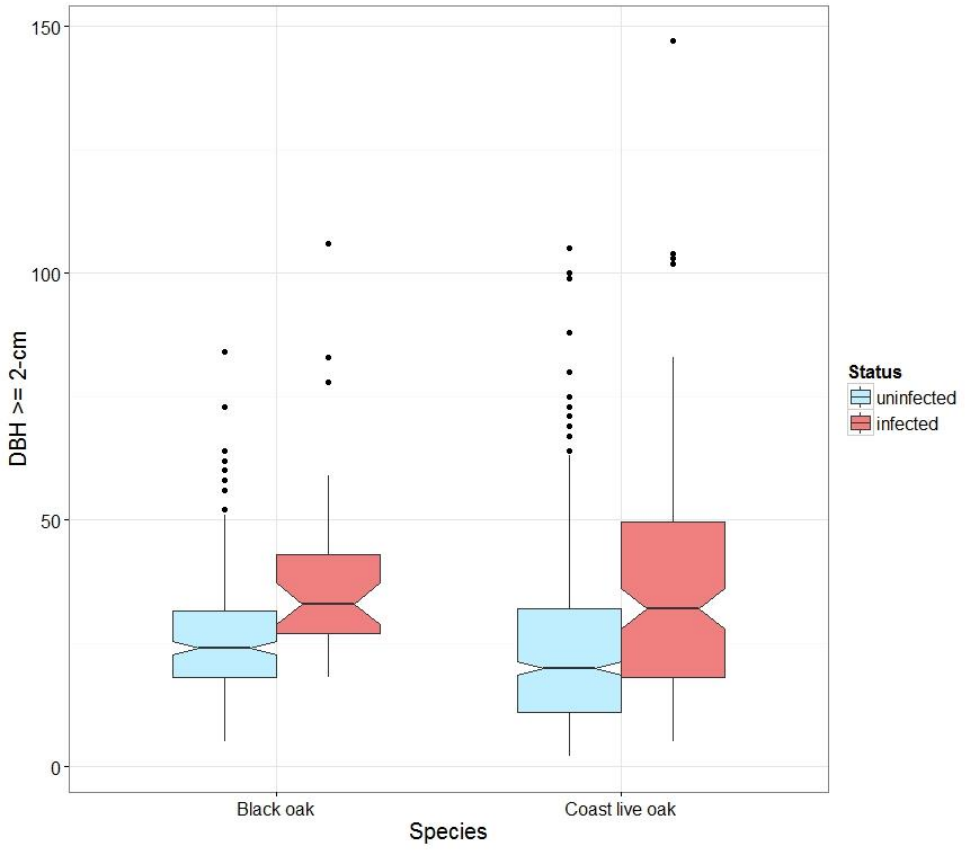

Figure 3.3. Boxplot showing the relationship between *P. ramorum* infection status and DBH for individual stems of black oak and coast live oak. Heavy line shows the median, notches extend to ±1.58 interquartile range/√n to indicate roughly a 95% confidence interval for the difference in two medians, and hinges (edges of box) encompass quartiles. Whiskers extend to extremes of data (outliers shown as circles). If the notches of two plots do not overlap this is strong evidence that the two medians differ (Chambers et al. 1983).

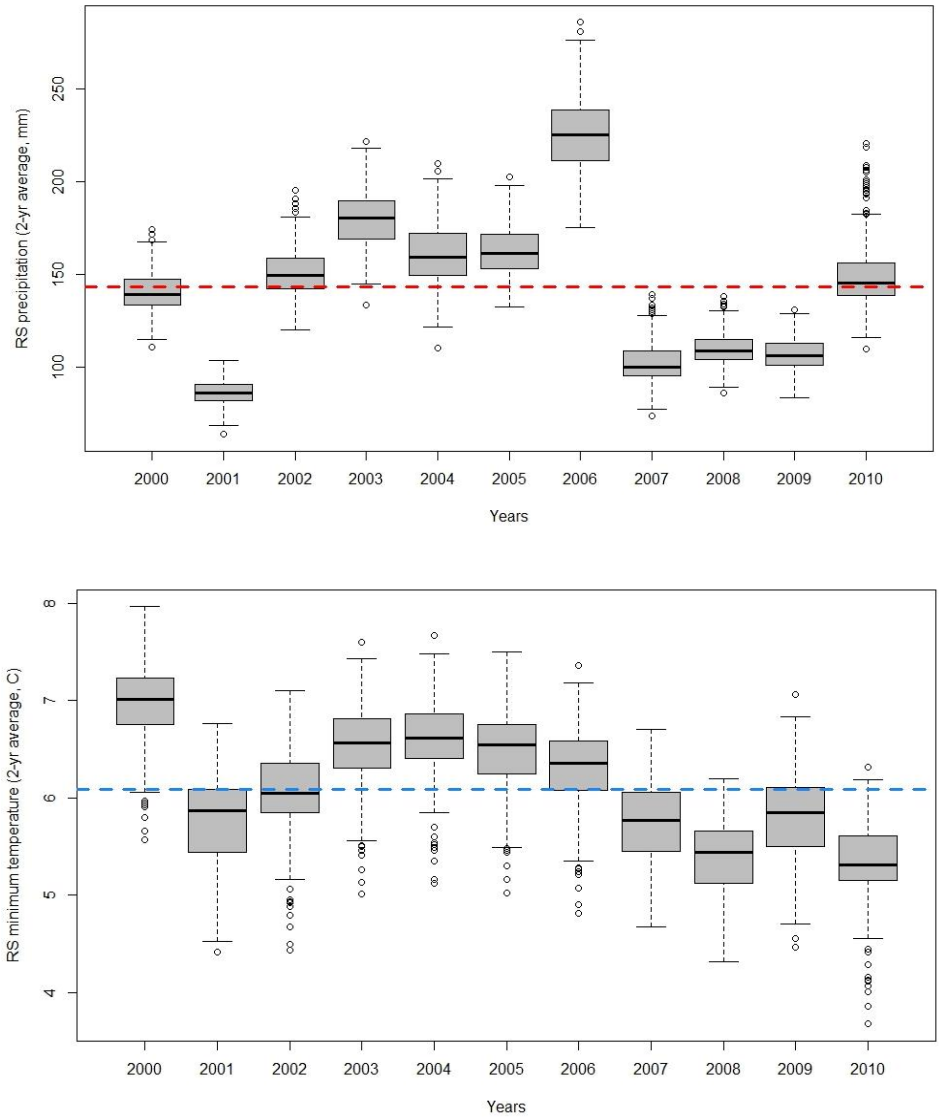

Figure 3.4. Box plots showing annual variation in (a) average cumulative rainfall (mm) and (b) average minimum temperature during the current year's rainy season across all plots. Dashed horizontal lines display the mean value across all years shown. Although the survival analysis models were analyzed using data from 2004–10, we show previous year conditions to provide a more comprehensive view of climatic variability across the study area. Heavy line shows median, notches extend to ±1.58 interquartile range/√n to indicate roughly a 95% confidence interval for the difference in two medians, and hinges (edges of box) encompass quartiles. Whiskers extend to extremes of data (outliers shown as circles).

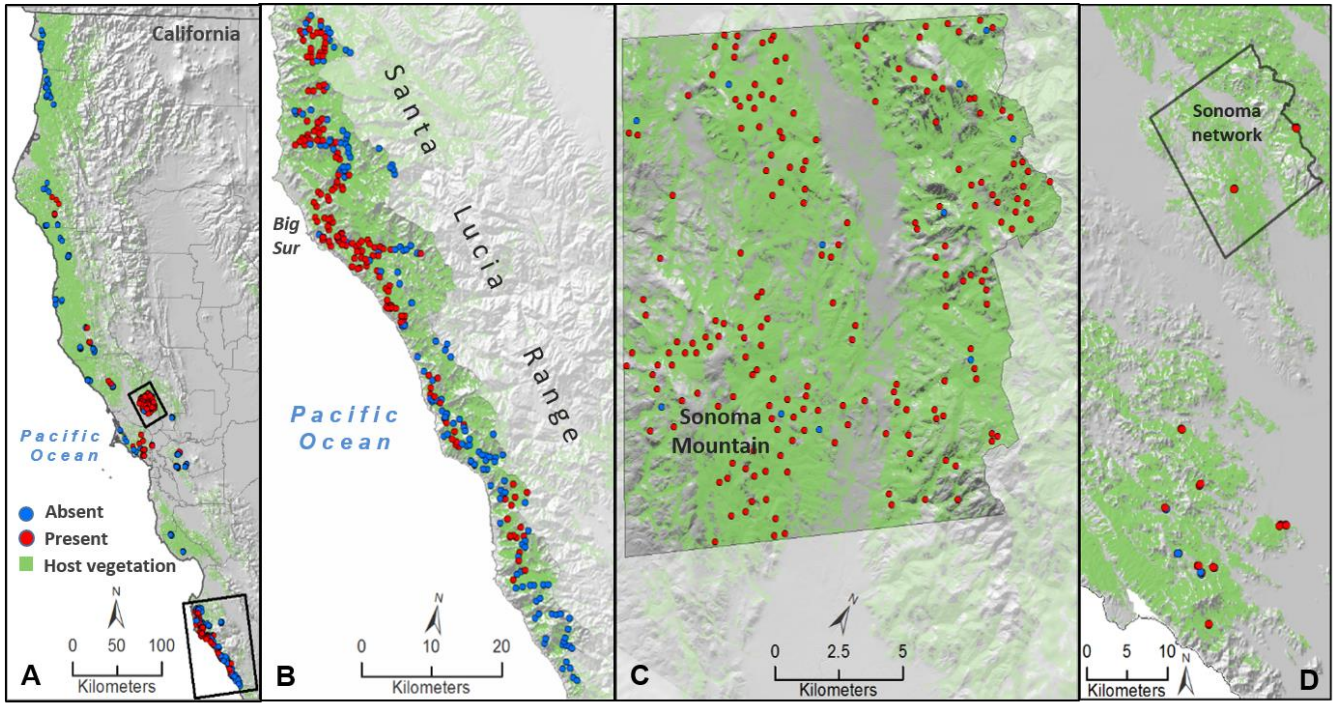

Figure 4.1. (A) A total of 815 plots from four long-term monitoring plot networks were assimilated to obtain spatial predictions of the number of host trees impacted by sudden oak death. Plots with and without confirmed *P. ramorum* detection are shown as red and blue circles. A total of 318 plots forming part of the "North Coast" network were used in this study, stretching from the northernmost plots shown near the California/Oregon border down to the Big Sur ecoregion. (B) The "Big Sur" network (n=264 plots) is distributed across a 79, 356 ha region extending 100 km along the Pacific slope of the Santa Lucia range. (C) The "Sonoma" plot network (n=198 plots), which is located further inland, is distributed across a 275 km^2 region in eastern Sonoma County. (D) We used a subset of plots (n=35) from the "Phytosphere" network, which extends from the San Francisco Bay Area upwards into the Sonoma plot network area.

Figure 4.2. The total number of trees and those impacted by *P. ramorum* varies by host species and plot network. The ‘all” category includes the number of alive and dead trees regardless of infection status. Because bay laurel does not die from sudden oak death, the “diseased” category includes only alive, infected trees. In contrast, the remaining three canker host species can die following pathogen infection, and the number of disease-impacted trees for these species was calculated using two methods: conservative and liberal (see methods section for more information). Individual bay laurel trees were not monitored in the Phytosphere plot network.

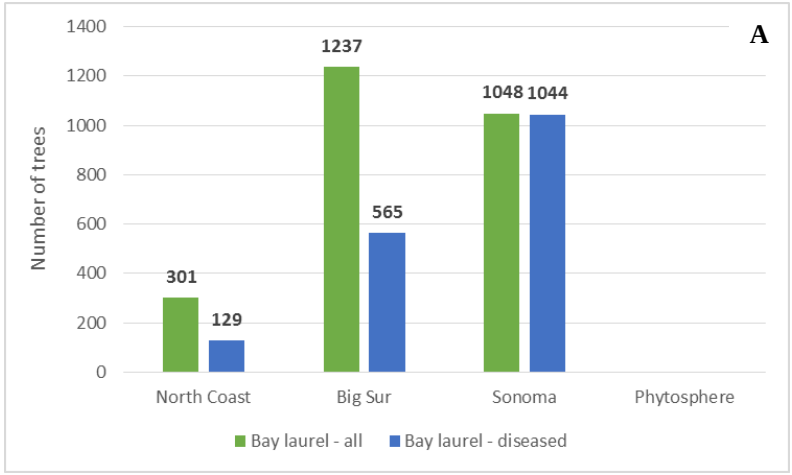
A
Number of trees
1400
1200
1000
800
600
400
200
0
301
129
1237
565
1048
1044
North Coast
Big Sur
Sonoma
Phytosphere
Bay laurel - all
Bay laurel - diseased

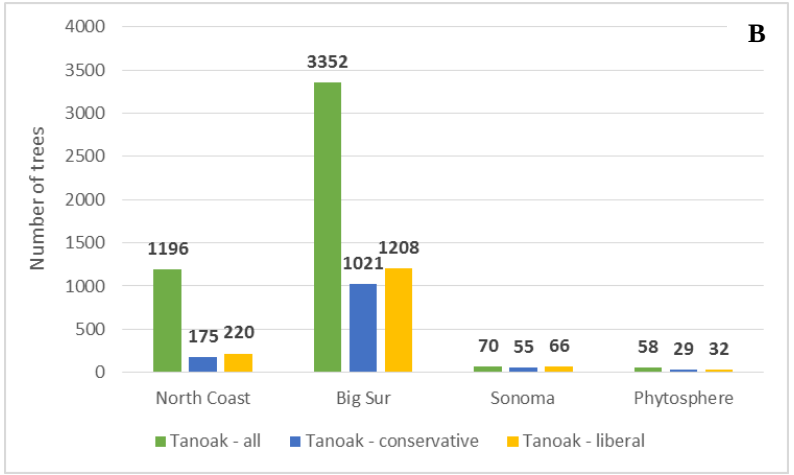
B
Number of trees
4000
3500
3000
2500
2000
1500
1000
500
0
1196
175
220
3352
1021
1208
70
55
66
58
29
32
North Coast
Big Sur
Sonoma
Phytosphere
Tanoak - all
Tanoak - conservative
Tanoak - liberal

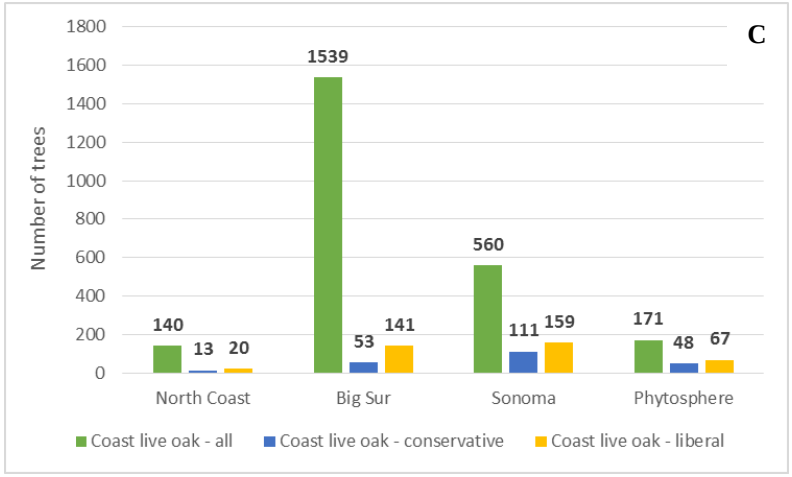
C
Number of trees
1800
1600
1400
1200
1000
800
600
400
200
0
140
13
20
1539
53
141
560
111
159
171
48
67
North Coast
Big Sur
Sonoma
Phytosphere
Coast live oak - all
Coast live oak - conservative
Coast live oak - liberal

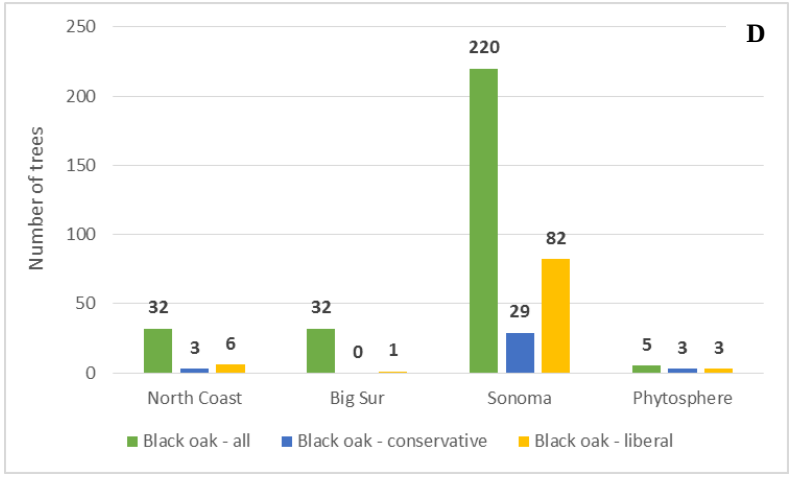
D
Number of trees
250
200
150
100
50
0
32
3
6
32
0
1
220
29
82
5
3
3
North Coast
Big Sur
Sonoma
Phytosphere
Black oak - all
Black oak - conservative
Black oak - liberal

Figure 4.3. Spatial predictions of the density of *P. ramorum* disease-impacted hosts (trees ha^{-1}) across each species geographic range, obtained using the liberal method of calculating plot-level disease prevalence. (A) There are 15 CA counties and one OR county that are known at this time to be infested with *P. ramorum* (shown in yellow). The geographic range of *P. ramorum* (shown in red) is based upon an assimilation of data sources on all known site locations harboring the pathogen (see 'Dispersal Constraints' section). The combined geographic range of all four key host species is shown in green. Spatial predictions of the four host species (B-E) were summarized by US-EPA Level III ecoregions (A= Coast Range; B= Klamath Mountains, C= California Chaparral and Oak Woodlands) in accordance with maps produced in Lamsal et al. (2011). The color ramp in each spatial prediction map represents 2.5 standard deviations from the mean; to the right of the color ramp are the minimum and maximum number of disease-impacted trees per hectare for each host species.

Figure 4.3. (continued)

(A)

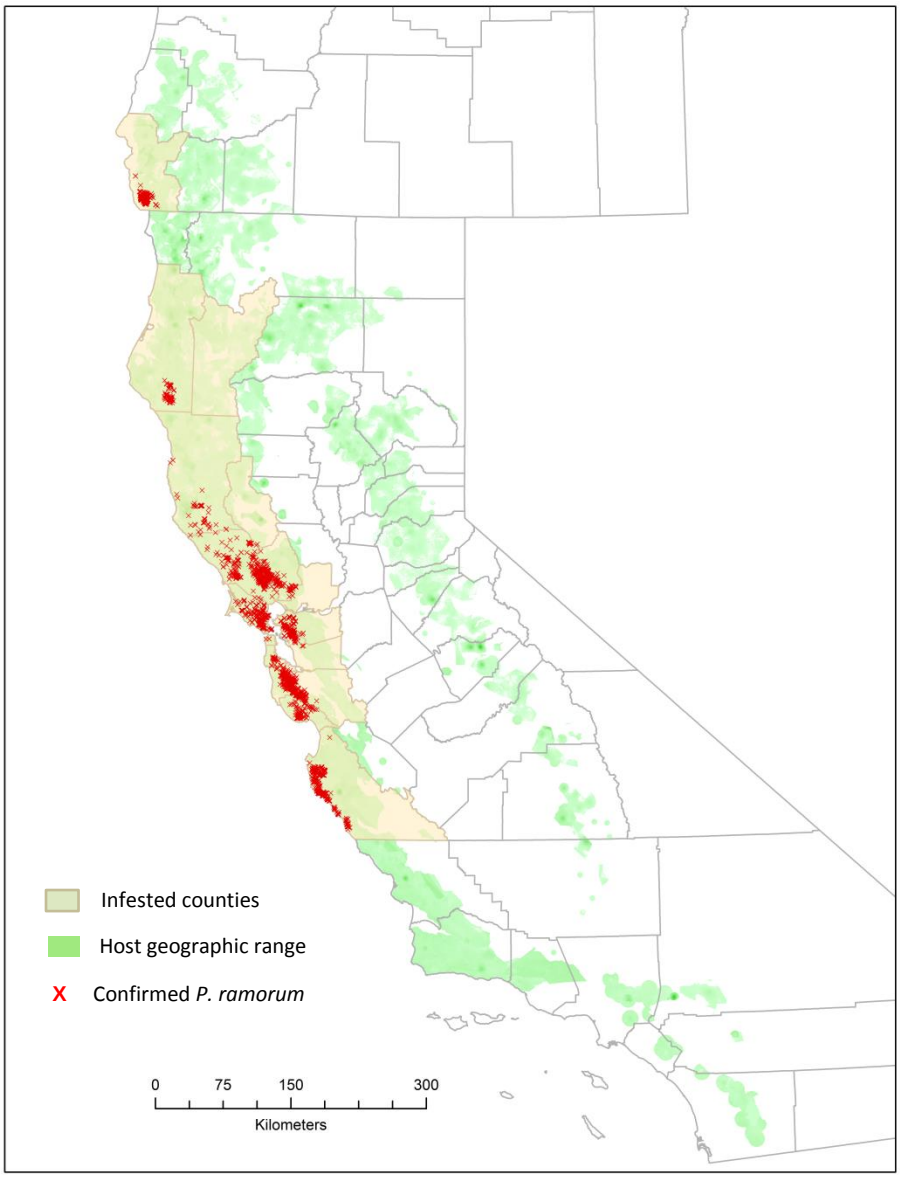

Figure 4.3. (continued)

(B)

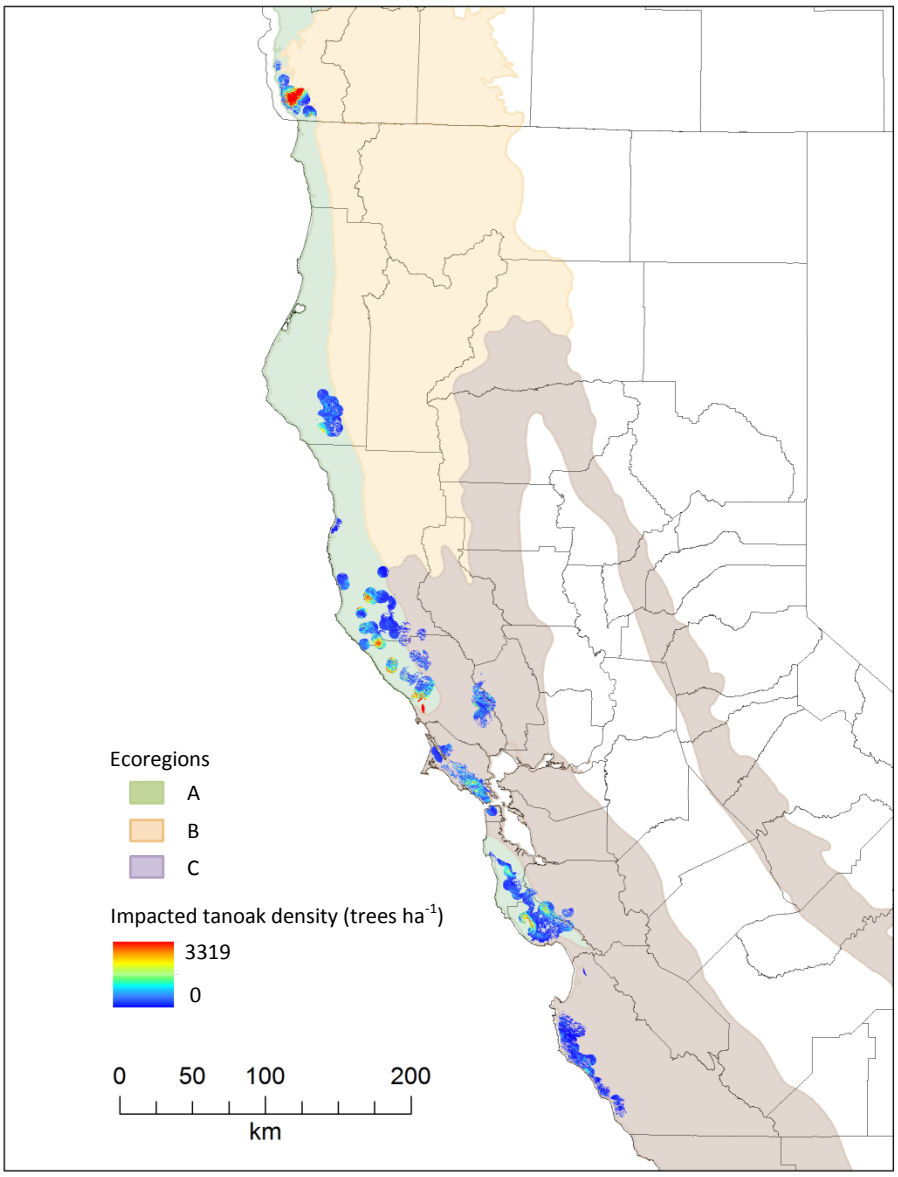

Figure 4.3. (continued)

(C)

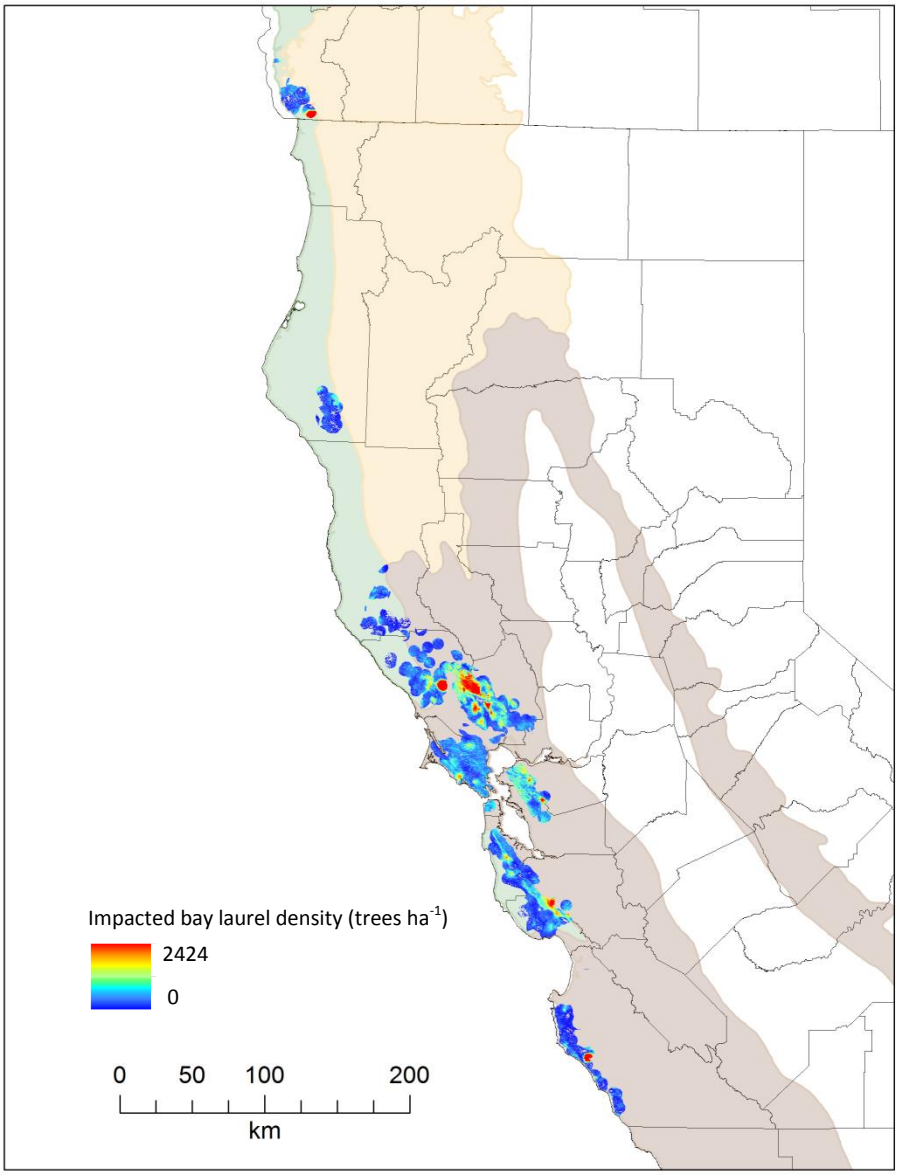

Figure 4.3. (continued)

(D)

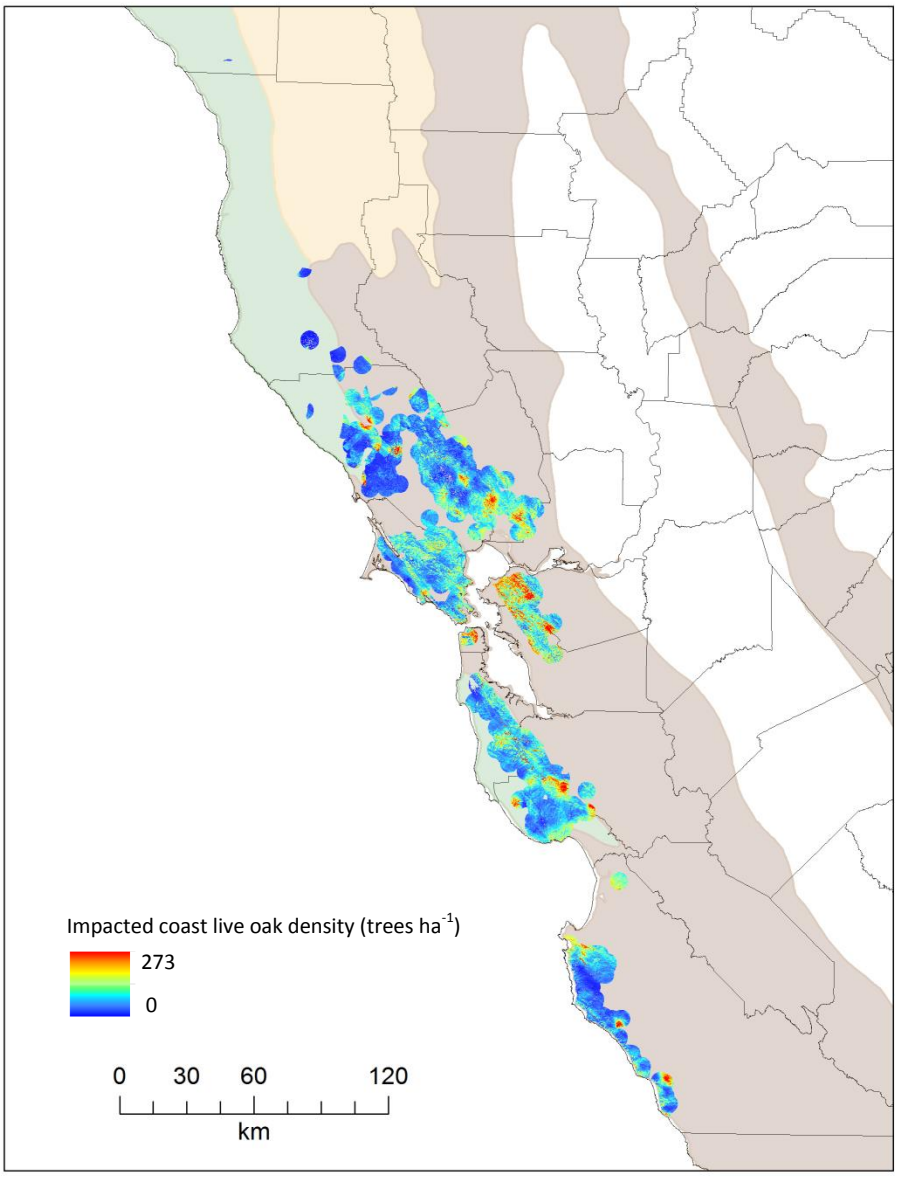

Figure 4.3. (continued)

(E)

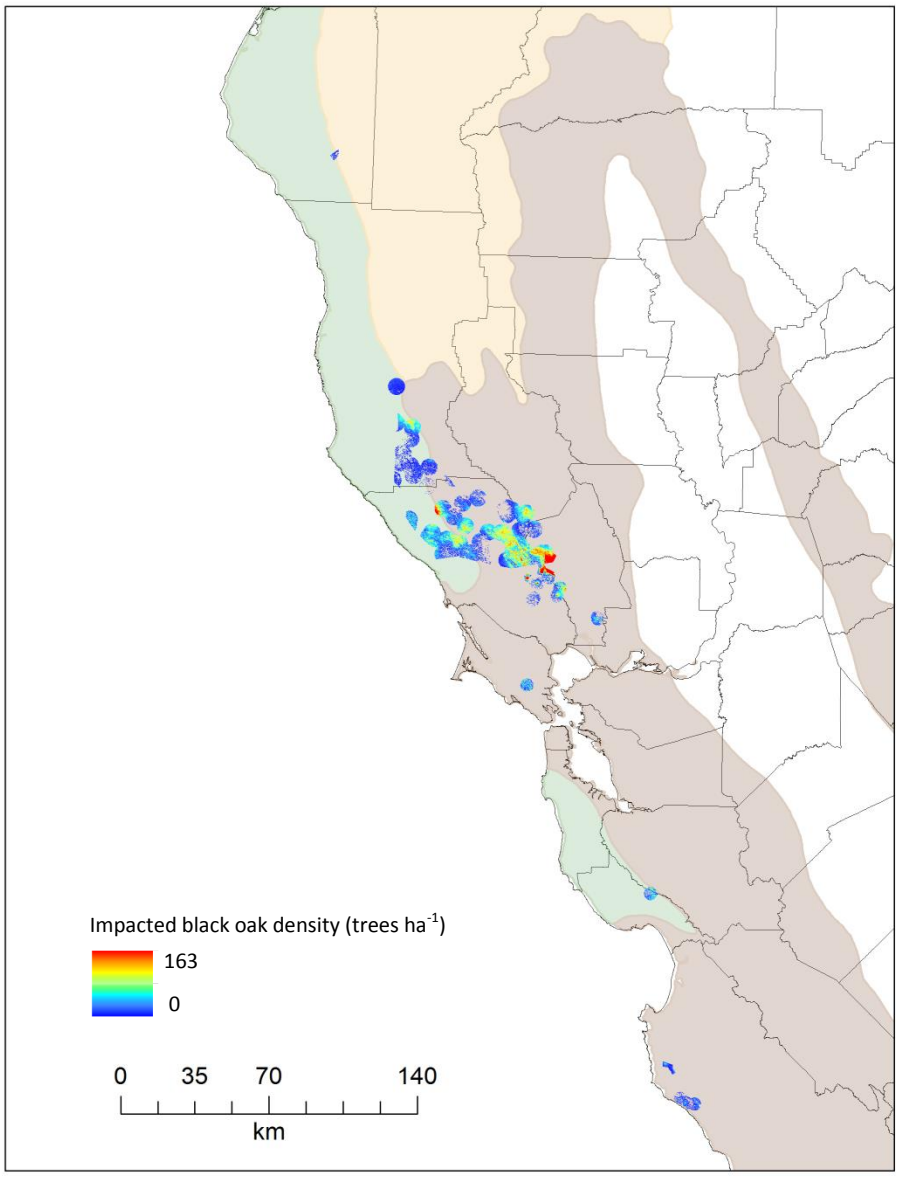

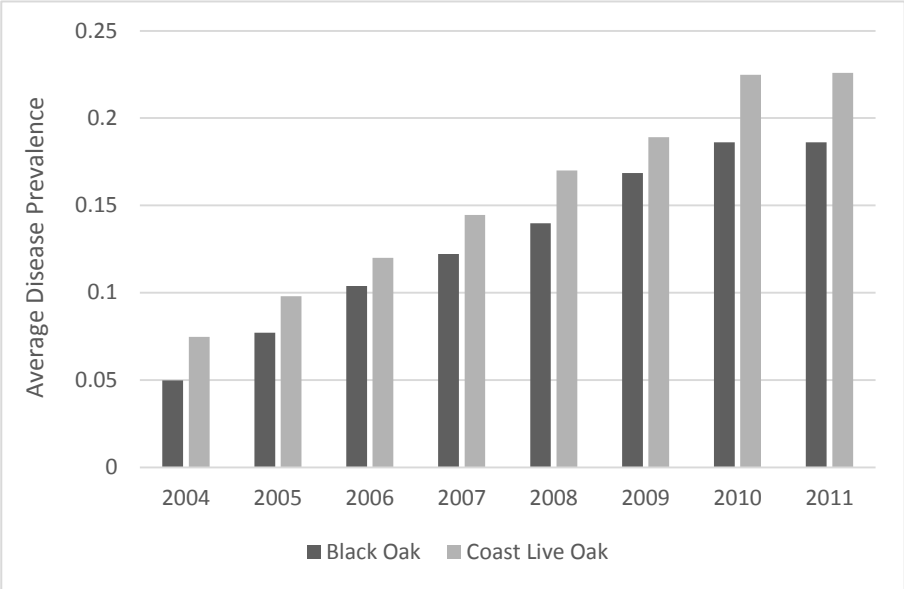

Figure 4.4. Average disease prevalence in coast live oak and black oak increased steadily from 2004–10 across the Sonoma plot network (n=164 plots). Although disease impacts did not discernibly increase from 2010 to 2011 at the individual tree level (i.e., there was only a single coast live oak tree found newly infected in 2011), survey data from the 2011 field season revealed a total of 23 new oak infections (19 on coast live oak and 4 on black oak) found at the stem level. These newly detected infections did not change overall disease prevalence because they either (i) corresponded to a newly infected stem forming part of a previously-infected multi-stem oak tree (n=6), or (ii) were not the first canker appearance detected on a single-stem tree (n=17). Disease prevalence was calculated using the conservative method here, whereby infection events were based solely upon empirical plot survey data of annual oak monitoring.

SUPPLEMENTARY MATERIALS

Table S2.1 The following 18 known host species were included in our diversity-disease risk analysis for the *P. ramorum* pathosystem throughout Big Sur, California. These 10,152 plants were sampled across 278 field plots (500 m^2). The two most competent foliar hosts are denoted by asterisks. Note that not all known host species were found to be infected by *P. ramorum* during our surveys during 2006-2007.

SCIENTIFIC NAME	COMMON NAME	SAMPLE SIZE	NUMBER INFECTED
Acer macrophyllum	Big leaf maple	45	0
Aesculus californica	California buckeye	5	1
Arbutus menziesii	Madrone	836	0
Arctostaphylos species	Manzanita	103	0
Heteromeles arbutifolia	Toyon	243	1
Notholithocarpus densiflorus	Tanoak*	3163	1280
Lonicera hispidula	Honeysuckle	30	0
Pseudotsuga menziesii	Douglas Fir	51	0
Quercus agrifolia	Coast live oak	766	49
Quercus chrysolepis	Canyon live oak	469	0
Quercus kelloggii	Black oak	30	0
Quercus parvula var. *shrevei*	Shreve's oak	978	31
Rhamnus californica	Coffeeberry	218	10
Rosa gymnocarpa	Wood rose	1	0
Sequoia sempervirens	Coast redwood	1281	9
Toxicodendron diversilobium	Poison oak	162	0
Umbellularia californica	California bay laurel*	1660	1000
Vaccinium ovatum	Huckleberry	111	4

Table S2.2 Summary statistics of the eight predictor variables used in our diversity-disease risk analysis for the *P. ramorum* pathosystem throughout Big Sur, California. Each variable was obtained for all 278 field plots (500 m^2) used in our analysis.

Covariate	Acronym	Units of Measurement	Mean	Standard Deviation	Range
Species richness	SR	--	4.73	2.03	1–12
Shannon-Weiner diversity index	H′	--	1.01	0.43	0.00–2.10
Bay laurel density	BAY	# of trees/ all trees in plot	5.95	10.24	0–92
Tanoak density	TOAK	# of trees/ all trees in plot	11.34	18.22	0–99
Forest community type	FOREST TYPE	--	*	*	*
Sampling year	YEAR	--	*	*	*
Average precipitation	PPT	mm	126.44	24.98	70.84–192.35
Potential solar insolation	PSI	watts/m^2	0.72	0.18	0.19–1.00
Host habitat (within 200-m buffer)	FOREST.200M	m^2	93,788	30,118	2,658–12,5581

* ‘Forest community type’ and ‘sampling year’ are indicator variables. There were 162 plots located in mixed evergreen forests and 116 plots in redwood-tanoak forests. For year, there were 174 plots sampled in 2006 and 104 plots in 2007.

Table S2.3 Model parameter estimates (i.e., marginal posterior means) and deviance information criterion (DIC) for diversity-disease risk analyses in the *P. ramorum* pathosystem throughout Big Sur, California. Variables were obtained for all 278 field plots distributed across the Big Sur, California study area. See Appendix D for a list of all covariate acronyms.

Diversity measured as 'Species Richness':

	SR	**BAY**	**TOAK**	**YEAR**	**FOREST TYPE**	**PPT**	**FOREST.200M**	**PSI**	**DIC**	**Δ DIC**
Null model	--	--	--	--	--	--	--	--	*6330.21*	--
Basic GLM	-0.65	0.95	0.71	-0.23	-0.90	-0.67	0.36	-0.18	3597.83	2732.38
Zero-inflated GLM	-0.55	0.76	0.65	-0.28	-0.71	-0.29	0.19	-0.18	2193.65	4136.56
Zero-inflated ICAR GLMM	-0.83	1.22	0.96	-0.75	-0.83	-0.73	0.41	ns	1050.15	5280.06

Diversity measured as 'Shannon-Weiner diversity index, H′':

	SE	**BAY**	**TOAK**	**YEAR**	**FOREST TYPE**	**PPT**	**FOREST.200M**	**PSI**	**DIC**	**Δ DIC**
Null model	--	--	--	--	--	--	--	--	*6330.21*	--
Basic GLM	-0.49	0.87	0.61	-0.22	-0.85	-0.75	0.39	-0.19	3727.45	2602.76
Zero-inflated GLM	-0.35	0.70	0.62	-0.31	-0.66	-0.39	0.20	-0.17	2312.05	4018.16
Zero-inflated ICAR GLMM	-0.48	1.16	0.91	-0.73	-0.72	-0.74	0.39	ns	1061.02	5269.19

'ns'= non-significant

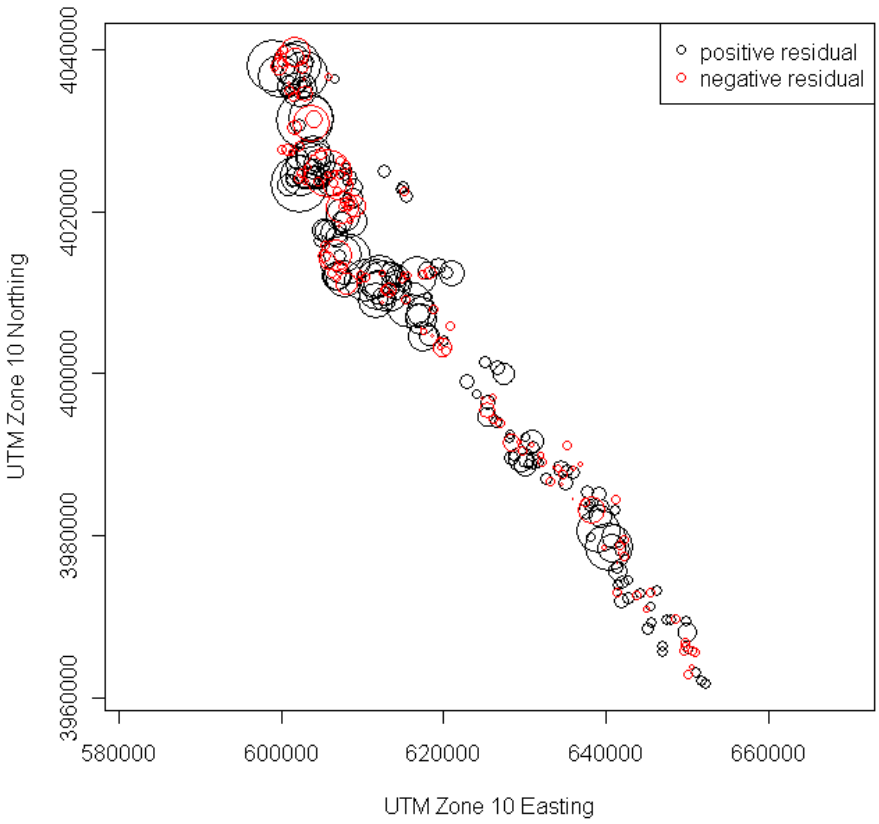

Figure S2.1 'Pseudo-residuals' (n=278 field plots) obtained from the zero-inflated GLM. Residuals are drawn proportional to their magnitude and are color-coded by sign. To obtain them for construction of our spatial proximity matrix, we fit the zero-inflated GLMM and included an observation level (i.e., the plot) i.i.d. random effect. This plot indicates potential latent spatial autocorrelation as the plots seem to cluster together by color and size.

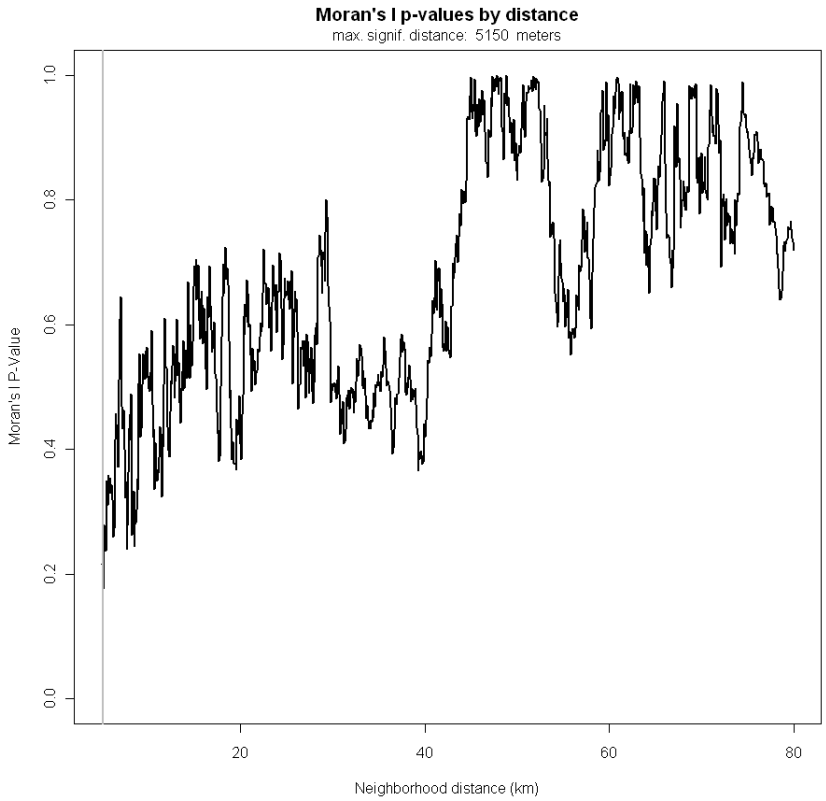

Figure S2.2 Moran's I p-values for assessing global spatial autocorrelation in our pseudo-residuals from the *Species Richness* model plotted against the inter-plot neighborhood distance (in km). The spatial proximity matrix was based on the distance that had the lowest p-value for Moran's I, which is marked by the vertical gray line (at 5,150-m). We assumed this distance was the dominant scale for autocorrelation that most needed to be accounted for in our model. To ensure that our model is a well-posed Markov random field, we limited the distance of spatial dependence to the cases where all study locations had at least one neighbor.

Figure S4.1. The best fitting variogram—out of a comparison among spherical, exponential and Gaussian models—for (A) coast live oak (lag size -7659.4-m, nugget -2.71, partial sill -0.72, major range -65,751-m); (B) tanoak (lag size -184.9-m, nugget -31.92, partial sill -67.48, major range -1291.48-m); (C) bay laurel (lag size -8298-m, partial sill -40.94, major range -70385-m); and (D) black oak (lag size -172-m, partial sill -0.69, major range -1540-m.

(A) Model: 2.71*Nugget+0.72*Gaussian(65751)

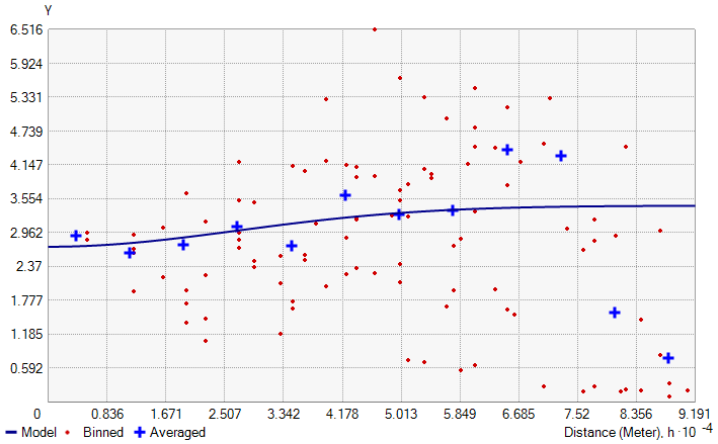

(B) Model: 31.92*Nugget+67.48*Gaussian(1291.5)

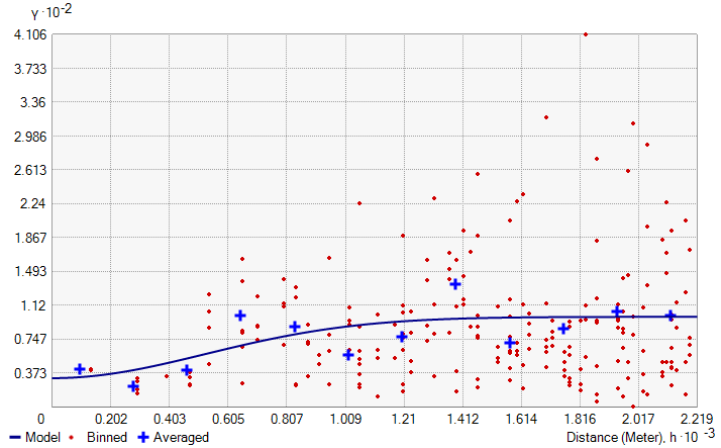

(C) Model: 10.48*Nugget+40.94*Gaussian(70385)

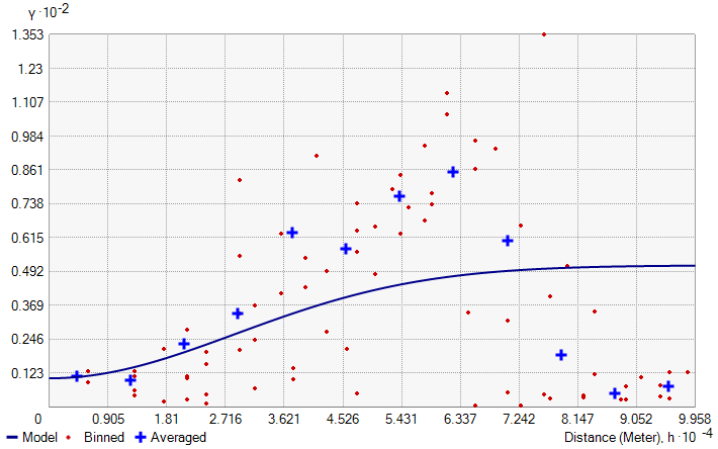

(D) Model: 0.46*Nugget+0.69*Gaussian(1540.4)